GDP-l-fucose synthase is a CD4+ T cell–specific autoantigen in DRB3*02:02 patients with multiple sclerosis

Planas, Raquel ; Santos, Radleigh ; Tomas-Ojer, Paula ; Cruciani, Carolina ; Lutterotti, Andreas ; Faigle, Wolfgang ; Schaeren-Wiemers, Nicole ; Espejo, Carmen ; Eixarch, Herena ; Pinilla, Clemencia ; Martin, Roland ; Sospedra, Mireia

Abstract: Multiple sclerosis is an immune-mediated autoimmune disease of the central nervous system that develops in genetically susceptible individuals and likely requires environmental triggers. The autoantigens and molecular mimics triggering the autoimmune response in multiple sclerosis remain incompletely understood. By using a brain-infiltrating CD4<jats:sup>+</jats:sup> T cell clone that is clonally expanded in multiple sclerosis brain lesions and a systematic approach for the identification of its target antigens, positional scanning peptide libraries in combination with biometrical analysis, we have identified guanosine diphosphate (GDP)–<jats:sc>l</jats:sc>-fucose synthase as an autoantigen that is recognized by cerebrospinal fluid–infiltrating CD4<jats:sup>+</jats:sup> T cells from HLA-DRB3*–positive patients. Significant associations were found between reactivity to GDP-<jats:sc>l</jats:sc>-fucose synthase peptides and DRB3*02:02 expression, along with reactivity against an immunodominant myelin basic protein peptide. These results, coupled with the cross-recognition of homologous peptides from gut microbiota, suggest a possible role of this antigen as an inducer or driver of pathogenic autoimmune responses in multiple sclerosis.

DOI: https://doi.org/10.1126/scitranslmed.aat4301

GDP-L-Fucose Synthase As A Novel CD4$^+$ T Cell-Specific Autoantigen in DRB3*02:02 Multiple Sclerosis Patients

Authors: Raquel Planas[1], Radleigh Santos[2], Paula Tomas-Ojer[1], Carolina Cruciani[1], Andreas Lutterotti[1], Wolfgang Faigle[1], Nicole Schaeren-Wiemers[3], Carmen Espejo[4], Herena Eixarch[4], Clemencia Pinilla[2], Roland Martin[1], Mireia Sospedra[1*]

Affiliations:

1 Neuroimmunology and MS Research (nims), Department of Neurology, University Zurich, Frauenklinikstrasse 26, 8091 Zürich, Switzerland

2 Torrey Pines Institute for Molecular Studies, 11350 SW Village Parkway Port St. Lucie, FL 34987, USA.

3 Department of Biomedicine, University Hospital Basel, Hebelstrasse 20, 4031 Basel, Switzerland

4 Servei de Neurologia-Neuroimmunologia, Centre d'Esclerosi Múltiple de Catalunya, Vall d'Hebron Institut de Recerca, Hospital Universitari Vall d'Hebron, 08035 Barcelona, Spain; Universitat Autònoma de Barcelona, 08193 Bellaterra, Cerdanyola del Vallès, Spain.

*Corresponding author:
Mireia Sospedra, PhD
Neuroimmunology and MS Research (nims)
Department of Neurology
University Hospital Zürich
Frauenklinikstrasse 26
8091 Zürich
Switzerland
Tel. +41442553905
Fax. +41442558864
e-mail: Mireia.SospedraRamos@usz.ch

One Sentence Summary: Using a brain-infiltrating T cell clone that is clonally expanded in multiple sclerosis brain lesions and positional scanning peptide libraries in combination with biometrical analysis, we have identified GDP-L-fucose synthase as a putative autoantigen that is recognized by cerebrospinal fluid-infiltrating CD4$^+$ T cells from HLA-DRB3*-positive patients.

ABSTRACT

Multiple sclerosis is a $CD4^+$ T cell-mediated autoimmune disease of the central nervous system that develops in genetically susceptible individuals and likely requires environmental triggers. The autoantigen/s and molecular mimic/s triggering the autoimmune response in multiple sclerosis remain incompletely understood. By using a brain-infiltrating T cell clone that is clonally expanded in multiple sclerosis brain lesions and an unbiased approach for the identification of its target antigens, positional scanning peptide libraries in combination with biometrical analysis, we have identified GDP-L-fucose synthase as a novel autoantigen that is recognized by cerebrospinal fluid-infiltrating $CD4^+$ T cells from HLA-DRB3*-positive patients. Significant associations were found between reactivity to GDP-L-fucose synthase peptides and DRB3*02:02 expression, along with reactivity against an immunodominant myelin basic protein peptide. These results, coupled with the cross-recognition of homologous peptides from gut microbiota, suggest a possible role of this antigen as inducer or driver of pathogenic autoimmune responses in MS.

INTRODUCTION

Multiple sclerosis (MS) is considered a demyelinating autoimmune disease of the central nervous system (*1-4*). The inflammatory infiltrate in demyelinating brain lesions, the intrathecal production of oligoclonal immunoglobulin G, the genetic trait consisting of multiple immune-related genes (*5, 6*), the positive effect of immunotherapies targeting B and T cells, and the similarities with the animal model experimental autoimmune encephalomyelitis, all support that MS is an immune-mediated disease. The dominance of $CD8^+$ T cells in MS brain lesions and the predisposition conferred by the HLA-A*03:01 allele and protection by HLA-A*0201 (*6, 7*) as well as evidence in experimental animal models (*8*) hint at a relevant role of these cells in MS pathogenesis. However, the fact that the HLA-DR15 haplotype is by far the strongest genetic risk factor associated with MS and that immunization with myelin components induces relapsing or chronic demyelinating disease models, which can be transferred by myelin-specific $CD4^+$ T cells to naive animals, underscore that autoreactive $CD4^+$ T cells play a central role in MS pathogenesis (*1*). Although myelin protein/peptides are considered relevant autoantigens in MS (*9*), the full spectrum of target antigen(s) driving the immune response in this disease has yet to be defined.

The etiology of MS involves both a complex genetic trait with more than 100 quantitative trait loci (*5, 6*) and several environmental risk factors including vitamin D, smoking (*10*), viral infections (*11*) and gut microbiota (*12*). Several studies have reported distinct fecal microbial community profiles in MS patients compared to healthy controls (*13-16*), which might affect autoimmune responses by regulating permeability of the blood brain barrier (BBB), by modulating the maturation, activation and function of immune cells (*12, 15-17*), or by controlling the maturation and function of microglia (*18*) and astroglia (*19*). In order to be able to cross the BBB and infiltrate the brain, autoreactive T cells first have to be activated outside the CNS. Cross-reactivity between autoantigens and peptides from pathogens or gut microbiota, i.e. molecular mimicry, has been considered a putative trigger of the autoimmune reaction in MS.

The identification of autoantigen/s and molecular mimic/s targeted by pathogenic $CD4^+$ T cells in MS may improve our understanding of disease mechanisms, help in diagnostic classification of MS patients and enable the development of antigen-specific immunotherapies (*20*). In the past, the search for candidate autoantigen/s in MS has concentrated on myelin components based on the fact that demyelination is a hallmark of MS brain lesions. Furthermore, immunological research in MS patients focused on studying myelin-specific T cells from the peripheral blood, since the target tissue, i.e. brain and spinal cord, is rarely available for immunological studies. Autoimmune diseases like primary biliary cirrhosis can be exquisitely

organ- or tissue-specific, and nevertheless T cell autoreactivity be directed against ubiquitous autoantigens such as pyruvate dehydrogenase (*21*). Thus, the focus on myelin-specific $CD4^+$ T cells and on cells circulating in the peripheral blood has had limitations in the search for candidate autoantigen/s and molecular mimic/s in MS. Non-myelin target antigens should therefore also be considered in MS. To overcome these limitations, we (a) applied the unbiased identification of stimulatory peptides using positional scanning peptide libraries (*22, 23*) and biometrical analysis (*24, 25*), and (b) concentrated on putatively disease-relevant T cells that infiltrated brain lesions and were clonally expanded locally. We focused on T cell clone (TCC) 21.1, a $CD4^+$ TCC that was identified in active pattern II demyelinating brain lesions from a secondary progressive (SP) MS patient using deep T cell receptor (TCR) β-chain sequencing and that was isolated from autologous cerebrospinal fluid (CSF)-infiltrating cells as previously described (*26*). The release of Th2 cytokines and the ability to help B cells (*26*) supports a pathogenic role of this TCC in pattern II demyelination that is mediated by antibodies and complement (*27*). Using the above methodological approach, we have identified GDP-L-fucose synthase as the main specificity of TCC21.1. Reactivity against this protein as well as against myelin and putative molecular mimic/s has then been examined more broadly in CSF-infiltrating $CD4^+$ T cells from MS patients and led to the identification of a novel target autoantigen in MS.

RESULTS

Peptide mixtures to identify the specificity of a brain-infiltrating TCC

TCC21.1 is a $CD4^+$ TCC isolated from CSF-infiltrating cells and clonally expanded in two active white matter demyelinating MS lesions (LI and LIII) from a SPMS patient (1154SA) with pattern II demyelination (*26*). TCC21.1 releases Th2 cytokines and helps proliferation and antibody production by autologous B cells upon unspecific activation. TCR α- and β-chain sequences of TCC21.1 are: TRAV12-2, TRAJ42*01, CDR3α CAVNEGSQGNLIF and TRBV11-2*01, TRBJ1-2*01, TRBD1*01, CDR3β CASSGRGPSYGYT, respectively. In order to study the peptides recognized by this TCC of unknown specificity using a decapeptide positional scanning library, we first identified the HLA class II molecule used by TCC21.1 to recognize the peptide mixtures (*28*). Since patient 1154SA was homozygous for the DR15 haplotype, we tested TCC21.1 initially only with the mixtures with amino acids (AAs) defined at position 5, presented by EBV immortalized BLS B cells (BCL) transfected with different single autologous HLA DR/DQ molecules (DRA*01:01/DRB5*01:01, DRA*01:01/DRB1*15:01 and DQA1*01:02/DQB1*06:02). As readout of T cell activation we used GM-CSF production (*29*), since TCC21.1 releases this cytokine after unspecific stimulation with anti-CD3 and PMA (*26*). Only mixtures presented by BCL expressing DRB1*15:01 class II molecules were stimulatory (Fig. 1A). We then tested TCC21.1 with the complete decapeptide positional scanning library (200 mixtures), presented by BCL expressing DRB1*15:01 class II molecules. GM-CSF release in response to the complete library is shown in Fig. 1B (black histograms). Next, we generated a biometrical analysis scoring matrix by assigning numerical values to the stimulatory potential of each of the 20 defined AAs in each of the ten positions of the decapeptide library as previously described (*24*). Here, the values were calculated as the log base 10 of the median GM-CSF (pg/ml) secretion of three independent experiments in the presence of mixtures, minus the secretion in the absence of mixtures (Fig. 1C). Based on a model of independent contribution of individual AAs to peptide antigen recognition, the predicted stimulatory score of a given peptide is the sum of the matrix values of each AA contained in the peptide at each position (*24*). This scoring approach was applied to rank, according to their stimulatory score that is predictive of their stimulatory potency, all natural overlapping 10-mers peptides of the protein sequences within the UniProt human protein database (*30*). Based upon these predicted values, we synthesized and tested at 5 μg/ml the 50 predicted human natural peptides with highest scores (Table S1). Unexpectedly, none of the peptides was clearly stimulatory (Fig. 1D). The predictive capacity of the above approach combining positional scanning library and biometrical analysis was lower for this TCC than for others in previous studies (*25*).

To further explore this unusual discrepancy between the mixture activities and the lower than expected activity of the peptides described above, we first noted that TCC21.1 also released

high levels of IL-10 after unspecific stimulation with anti-CD3 and PMA (*26*). TCC21.1 was then tested with the complete decapeptide positional scanning library using IL-10 production as readout (Fig.1B, white histograms). A similar but not identical response pattern was obtained with both readouts. The most stimulatory mixtures with both approaches are shown in Fig. 1C. Interestingly, these mixtures have identical defined AAs in consecutive positions, suggesting a possible recognition of one AA motif in multiple frames. To confirm this observation, a set of 22 dual-defined mixtures (i.e. positional scanning mixtures with two defined positions) was designed, synthesized, and tested (Fig. 1E); the results confirmed the presence of a unique recognition motif (LHSXFEV) with different flanking residues (Fig. 1F). In order to apply this recognition motif in the two frames to the original GM-CSF-derived matrix and perform biometrical analysis, we used the harmonic mean model (HM) (*31*) to integrate the stimulatory responses of some of the dual defined mixtures (Fig. 1E, Frame 1/2-HM mixtures) into the original matrix (Fig. S1). Using the new "harmonic boost" frame 1 and frame 2 matrices, all natural overlapping 10-mers peptides in the protein sequences within the UniProt human database were scored and ranked as before. The 50 predicted natural peptides with highest scores for both matrices were synthesized and tested for GM-CSF release (Table S1). These two matrices allowed us the identification of three clearly stimulatory peptides (Fig. 1G). The two most stimulatory peptides, NVLHSAFEVG predicted with harmonic boost frame 1 and DNVLHSAFEV predicted with harmonic boost frame 2, belong to GDP-L-fucose synthase encoded by the TSTA3 gene, and overlap by 9 AAs. The third stimulatory peptide (KLLLHSGVEN) was predicted with harmonic boost frame 2 and belongs to a transmembrane protein (FLJ37396).

GDP-L-fucose synthase as the main autoantigen for a brain-infiltrating TCC

In order to identify autoantigens recognized by TCC21.1 in the two autologous brain lesions within which TCC21.1 was known to be clonally expanded (LI and III (*26*)), the harmonic boost frame 1 and frame 2 matrices were then used to score and rank, according to their stimulatory score, all natural overlapping 10-mer peptides in the protein sequences within a brain-protein sub-database created with RNASeq-based transcriptome data from these two lesions (GSE60943). Of the 40 predicted natural brain peptides with highest scores for the frame 1 matrix, 38 peptides were already predicted from the unbiased UniProt human database. For frame 2 matrix, the top 40 peptides were previously predicted (Table S1). The two new peptides for frame 1 were synthesized and tested. NVLHSAFEVG (GDP-L-fucose synthase 96-105) and DNVLHSAFEV (95-104) were the only peptides from proteins transcribed in autologous brain lesions found to stimulate TCC21.1 (Table S1).

Transcript level, expressed as reads per kilo base of exon model per million mapped reads (RPKM), of GDP-L-fucose synthase in the autologous brain LI and LIII is shown in Table 1.

Transcript values for other brain-specific genes are also shown as quality control of the samples and as reference for genes expressed at high (myelin basic protein (MBP), myelin proteolipid protein 1 (PLP1)), and medium (myelin-associated glycoprotein (MAG), myelin-associated oligodendrocyte basic protein (MOBP) and oligodendrocyte myelin glycoprotein (OMG)) level.

Seventeen GDP-L-fucose synthase peptides were identified in white and grey matter brain tissue from other MS patients and non-MS controls by proteomic analysis. The peptide sequences are listed in Table 1 as well as the peptide spectrum matches (PSM) in the different samples. The percentage of the GDP-L-fucose synthase AA sequence covered by identified peptides was 56%. Analysis of other brain-specific proteins as reference is also included (Table 1 and Table S3).

Characterization of GDP-L-fucose synthase recognition by a brain-infiltrating TCC

As mentioned above, the two GDP-L-fucose synthase peptides recognized by TCC21.1 overlap by 9 AAs. We synthesized and tested on DRB1*15:01-expressing BCL nine additional 10-mer peptides overlapping by 9 AAs and identified an additional peptide, VLHSAFEVGA (97-106), which induced GM-CSF release (Fig. 2A). Peptide NVLHSAFEVG (96-105) gave the optimal response with an EC50 of 0.2 μg/ml (Fig. 2B) and was presented by DRB1*15:01 and DQB1*0602 molecules (Fig. 2C). As we demonstrated previously, the cross-reactivity and cross-restriction of TCC21.1 might facilitate its activation (*32, 33*). The common AAs of the three stimulatory GDP-L-fucose synthase peptides are VLHSAFEV (97-104). Single alanine (A) substitutions of these three overlapping peptides revealed that the substitution of H99 and S100 abrogated the T cell responses, suggesting that they are the primary AA involved in TCR or HLA interaction. The substitution of V97, L98, F102 or E103 for A in the most active peptide NVLHSAFEVG (96-105) resulted in peptides with some stimulatory activity, in contrast to the two other overlapping peptides in which their substitution resulted in non-stimulatory peptides. Thus the residues V97, L98, F102 and E103 appear to be secondary TCR or HLA contacts (Fig. 2D).

Next, we characterized the response of TCC21.1 to GDP-L-fucose synthase peptides presented by autologous irradiated peripheral blood mononuclear cells (PBMCs) and BCL. GDP-L-fucose synthase peptides presented by the two types of APCs were able to induce proliferation, although PBMCs were more efficient (Fig. 2E). We also analyzed the functional phenotype of this response (Fig. 2E). TCC21.1 displayed a Th2 phenotype, releasing mainly Th2 cytokines and lower levels of IL-22 and IL-10. Unexpectedly, when peptides were presented by autologous BCL, they induced higher levels of IFNγ. In addition, TCC21.1 also released GM-CSF and IL-3 in response to GDP-L-fucose synthase peptides (Fig. 2F). The release of these two cytokines seems to be a specific feature of this TCC compared with other Th1, Th1* or

Th1/2 TCCs that our laboratory had generated from patients with different conditions. Intracellular cytokine staining confirmed the Th2 functional phenotype of TCC21.1 in response to GDP-L-fucose synthase (96-105) (Fig. 2G). More than 60% of TCC21.1 cells were IL-4$^+$ after stimulation with GDP-L-fucose synthase (96-105), while only around 12% were IFNγ^+. Around 60% of the cells were GM-CSF$^+$ and 47.7% of these also IL-4$^+$. Further characterization of TCC21.1 demonstrated expression of CD28 and the chemokine receptor CRTh2 (Fig. 2H).

Recognition of GDP-L-fucose synthase by CSF-infiltrating CD4$^+$ T cells from patient 1154SA

Sixty-two 15-mer peptides overlapping by 10 AAs and covering the entire GDP-L-fucose synthase protein (Table S2) were synthesized and tested for their ability to induce TCC21.1 proliferation when presented by autologous PBMCs. Seven immunodominant/encephalitogenic myelin peptides (*34*), CEF (cytomegalovirus, EBV, influenza virus and tetanus toxoid) peptide pool and control beads were tested in parallel (Table S2 and Fig. 3A). TCC21.1 only recognized two overlapping GDP-L-fucose synthase peptides, 91-105 and 96-110, containing the three stimulatory decapeptides (95-104, 96-105 and 97-106) that we identified previously. Bulk CSF-infiltrating CD4$^+$ T cells after short and long phytohaemagglutinin (PHA) expansion (see M&M) were tested with the GDP-L-fucose synthase-, myelin- and CEF peptides (Fig. 3A). Long- but not short-PHA-expanded CSF-infiltrating CD4$^+$ T cells proliferated in response to three GDP-L-fucose synthase peptides suggesting a low frequency of specific TCCs in the initial CSF infiltrate and a preferential expansion with enrichment of some TCCs, including TCC21.1, during the long PHA expansion. Proliferation of long-PHA-expanded CSF-infiltrating CD4$^+$ T cells to peptides 91-105 and 96-110 was mainly mediated by TCC21.1 since Vb21+ (that included TCC21.1) but not Vb21- CSF-infiltrating CD4$^+$ T cells proliferated in response to this peptide (Fig. 3B). Interestingly, the third GDP-L-fucose synthase peptide recognized by long-PHA-expanded CSF-infiltrating CD4$^+$ T cells (191-205) was not recognized by TCC21.1 (Fig. 3A). We generated a T cell line (TCL) from these proliferating cells (TCL39, Fig. 3C), and its TCR sequencing confirmed the existence of three TCCs other than TCC21.1. Although we have not been able to identify the TCC responsible for GDP-L-fucose-specific response, it is interesting to note that two of these TCCs were clonally expanded in active brain lesion III and ranked in positions 51 and 56 regarding their frequency (Fig. 3D (*26*)). Functional phenotype analysis of responses to peptides 91-105 and 191-205 showed a Th2 response for peptide 91-105, confirming activation of TCC21.1, but a Th1/Th2 response for peptide 191-205 supporting activation of other TCCs (Fig. 3E). Bulk CSF-infiltrating CD4$^+$ T cells did not recognize either the myelin peptides or the CEF peptide pool.

Recognition of GDP-L-fucose synthase by CSF-infiltrating CD4$^+$ T cells from CIS/MS patients.

In order to find out how frequently specific recognition of GDP-L-fucose synthase occurs in CSF-infiltrating $CD4^+$ T cells in CIS/MS patients, we developed a new protocol to expand fresh CSF-infiltrating $CD4^+$ T cells to high numbers in a single round to minimize variations in the original T cell repertoire (see M&M). Resting PHA-expanded CSF-infiltrating $CD4^+$ T cells from 31 CIS/MS patients were tested in quadruplicate with the 62 overlapping GDP-L-fucose synthase peptides presented by autologous irradiated PBMCs, as well as with the seven myelin peptides, CEF peptide pool and control beads. All SIs (except control beads) were pooled and SI values less than one were treated as having unit value. Cluster k-means analysis was performed to determine the optimal cut-off to differentiate responsive SI values from non-responsive in this patient population. K-means clustering resulted in a cut-off value of 1.455 to differentiate positive responses from negative. Subsequently, for each patient, all peptides having a median SI (of the quadruplicate wells) greater than 1.455 were identified as positive responses (Table S4A). Notably, a follow-up study of the negative control well SI values using Monte-Carlo bootstrapping indicated that the 1.455 cut-off showed a 0.26% false positive rate when applied to simulated medians of quadruplicate negative values.

Next, patient scores were constructed by calculating the sum of each responsive peptide median SI, weighted by the number of total patients that responded to that peptide. In this way, both the SI values themselves for each peptide, as well as the relative immunogenicity of each peptide, were factored in. Three-cluster k-means analysis was performed on base 10 patient scores and clearly grouped patients into three categories: “nonresponders”, “moderate responders”, and “high responders” (Table S4A). Nineteen patients (61.3%) were therefore characterized as nonresponders to GDP-L-fucose synthase (Fig. S2A), six (19.35%) as moderate, and six (19.35%) as high responders (Fig.4A). No significant differences between the three groups were found for CEF responses or for the positive or negative controls (Fig. S2B). Immunodominant peptides were defined as peptides able to induce positive responses in at least three patients. The 14 GDP-L-fucose peptides achieving this criterion are shown in Figure 4B. Functional analysis of the strongest responses to some immunodominant peptides revealed a Th1 phenotype with mainly production of IFNγ (Fig. 4C).

T cell responses to immunodominant GDP-L-fucose synthase peptides are associated with reactivity against MBP 83-99

In order to judge better the reactivity of CSF-infiltrating $CD4^+$ T cells in CIS/MS patients against GDP-L-fucose synthase peptides, we compared it with reactivity against the seven immunodominant/encephalitogenic myelin peptides, which had previously been shown to be the targets of high avidity T cells in MS (*34*) (Fig.5A). Four out of six (67%) of the high responder patients to GDP-L-fucose synthase also responded to myelin peptides, while only one of the six (17%) moderate responders and two of the 19 (11%) nonresponders did (Fig.5A). This

association is significant (p=0.0138, Fisher's exact test). When comparing the recognition of immunodominant GDP-L-fucose synthase peptides and specific myelin peptides (Fig.5B), we found a significant association between recognition of peptide MBP 83-99 and three immunodominant GDP-L-fucose synthase peptides (1-15 – p=0.0122, 156-170 – p=0.0122, and 256-270 – p=0.0481, Fisher's exact tests with Bonferroni-Holm correction) (Fig.5B).

T cell response to GDP-L-fucose synthase is associated with DRB3* alleles

Table 2 summarizes demographical and clinical characteristics of the CIS/MS patients and their designation as nonresponders, moderate responders, or high responders to GDP-L-fucose synthase peptides. No significant differences between groups could be identified regarding disease course or clinical presentation, gender, age, CSF IgG index or number of CSF-infiltrating cells. HLA class II typing is also summarized in Table 2. Interestingly, all six of the high responder patients are DRB3*02:02, while only one of the six (17%) moderate responders and four of the 19 (21%) nonresponders express this class II molecule. This association is significant (p=0.0006, Fisher's exact test). Further, when looking only at the difference between moderate responders and nonresponders, an additional significant association was observed; three of the six (50%) moderate responders are DRB3*01:01 while only one of the 19 (5%) nonresponders is (p=0.0312, Fisher's exact test). The predicted binding affinities of positive peptides to DRB3*01:01 and DRB3*02:02 are summarized in Table S4B.

Cross-recognition of human and bacterial GDP-L-fucose synthase peptides by $CD4^+$ CSF-infiltrating T cells

GDP-L-fucose synthase is a cytosolic enzyme that converts GDP-4-keto-6-deoxy-D-mannose into GDP-L-fucose that then is used to fucosylate oligosaccharides (*35*) including sugars and glycoproteins on mucosal intestinal cells. Gut microbiota use a mammalian-like pathway of fucosylation to colonize the mammalian intestine (*36*). GDP-L-fucose synthase is an evolutionarily conserved protein (*37*). In order to search for molecular mimics that might induce or perpetuate GDP-L-fucose synthase-specific T cells, we therefore compared the protein sequence of human GDP-L-fucose synthase with several bacterial GDP-L-fucose synthase sequences. We focused on bacterial species that have been reported to be altered in gut microbiota of MS patients and for which GDP-L-fucose synthase sequences were available, further on bacterial species present in gut microbiota without association with MS, and also some pathogens not present in gut (Table S5). Sequence comparison of the four main immunodominant peptides is shown in Table S6A. The most immunodominant human GDP-L-fucose synthase peptide, 161-175, showed the highest homology with bacterial sequences, and particularly with those associated with MS, with which it shares at least 40% homology. Eight 15-mer bacterial peptides with at least 40% homology with the human 161-175 peptide and

shared by different bacteria species were synthesized as 15- and 10-mer (overlapping in 5 AAs) peptides (Table S6B). Reactivity of CSF-infiltrating $CD4^+$ T cells against these bacterial peptides was tested in eight CIS/MS patients. Six of these patients were patients from our previous cohort from whom autologous PBMCs were available (748UR, 1005ME, 1129RE, 1173DI, 718MA and 776JE). Five of them (748UR, 1129RE, 1173DI, 718MA and 776JE) had a positive response to human peptide 161-175, while patient 1005ME did not respond to this peptide and was included as control (Fig. 4A). Two additional patients (1440AM and 1489HE), from whom autologous PBMCs were not sufficient to test all GDP-L-fucose synthase peptides and who were not included in the previous cohort, were also identified as high responders to GDP-L-fucose synthase peptides, including peptide 161-175, after testing with a selection of six immunodominant peptides (Fig. S3A). Both patients were also DRB3* (Fig. S3B). 1489HE was DRB3*02:02 and 1440AM expressed DRB3*03:01 with high homology with DRB3*02:02 (*38*). $CD4^+$ CSF-infiltrating T cells from four of these patients (1489HE, 1173DI, 748UR and 776JE) proliferated in response to different bacterial peptides (Fig. 6). Interestingly, the four patients showed reactivity against peptides 3 and 4, which show the highest degree of homology (53,3%) with the human peptide (Fig. 6). Blast (NCBI) analysis of these bacterial peptides (Fig. S3C) revealed that peptide 3 was shared by bacteria from the genera Akkermansia and Prevotella, which both have been reported to be altered in MS patients (*14*). Peptide 4 is also shared by different bacterial genera present in gut microbiota and belonging to the phylum Bacteroidetes, the second most abundant phylum, after Firmicutes, in gut microbiota.

DISCUSSION

Assuming that MS is a $CD4^+$ T cell-mediated autoimmune disease it is crucial to elucidate the target antigens responsible for inducing $CD4^+$ T cell activation to understand MS pathogenesis. In addition, it is a prerequisite for developing antigen-specific tolerization strategies. Using positional scanning peptide libraries in combination with biometric analysis, we have identified GDP-L-fucose synthase as the main specificity of TCC21.1, a brain-infiltrating and clonally expanded TCC from a SPMS patient with pattern II demyelination (*26*). In pattern II lesions, demyelination is mediated by deposits of antibody and complement in addition to macrophages and T cells (*27*). TCC21.1, in addition to be clonally expanded in active MS lesions, was able to release Th2 cytokines and help B cells after unspecific activation, characteristics that strongly support its putative pathogenic role in pattern II demyelination. Here, we confirmed a clear Th2 functional phenotype of TCC21.1 in response to GDP-L-fucose synthase peptides presented by autologous PBMCs and the expression of the chemokine receptor CRTh2, a marker of human Th2 cells. Furthermore, in response to GDP-L-fucose synthase peptides, TCC21.1 also released GM-CSF, which is considered relevant in MS pathogenesis (*39, 40*), and IL-3, reported to promote Th2 responses (*41, 42*). Reactivity against GDP-L-fucose synthase peptides was also identified in bulk CSF-infiltrating $CD4^+$ T cells from the same patient after long but not short PHA expansion. TCC21.1 and at least one other GDP-L-fucose synthase-specific $CD4^+$ TCC were responsible for this response further supporting a putative role of GDP-L-fucose synthase as autoantigen. The inability to detect GDP-L-fucose synthase-specific CSF-infiltrating $CD4^+$ T cells after short PHA expansion suggests a low frequency of these cells in the CSF. The fact that TCC21.1 and most likely also the TCC specific for peptide 191-205 were clonally expanded in the most active lesion III (*26*) suggests that these TCCs might be retained in the brain parenchyma and recirculate through the CSF compartment to a limited extent. The long PHA expansion that we performed to obtain sufficient cell numbers to isolate brain-infiltrating clonally expanded TCCs (*26*) resulted in enrichment of some TCCs that allowed us to identify at least one additional CSF-infiltrating TCC specific for GDP-L-fucose synthase.

The identification of TCC21.1 specificity using positional scanning libraries was less efficient than in previous studies (*23, 25*) due to recognition by this TCC of peptides with identical binding/contact motif but variable flanking C- and N-terminal AA. MHC-class II molecules have open binding grooves and are able to present peptides with a highly variable length rendering TCR binding very flexible (*43*). However, at present it is unclear why the recognition of a TCR motif in different frames influenced the results for TCC21.1 more so than other TCCs. Further development of quantitative approaches to both detect and account for frame shifting within scoring matrices based on the results of TCC21.1 are currently in development. The number of stimulatory peptides identified for TCC21.1 was unusually low compared with previous studies

(*23, 25*). The limited cross-reactivity of TCC21.1 might underlie the special features of this TCC recognition profile of the decapeptide positional scanning library.

Analysis of bulk CSF-infiltrating $CD4^+$ T cells from other CIS/MS patients after a single PHA expansion demonstrated reactivity against GDP-L-fucose synthase in 40% of patients. Fourteen immunodominant peptides were identified that unexpectedly induced a Th1 response excluding a firm association between GDP-L-fucose synthase reactivity and pattern II demyelination. Interestingly, a significant association between recognition of GDP-L-fucose synthase and myelin has been found between the immunodominant GDP-L-fucose synthase peptides 1-15, 156-170 and 256-270 and the myelin peptide MBP 83-99, and all patients reacting to both GDP-L-fucose synthase peptides and MBP 83-99 were high responders. The putative cross-recognition of these peptides by CSF-infiltrating $CD4^+$ T cells might play a relevant role in MS pathogenesis, since $CD4^+$ T cells specific for MBP 83-99 not only are able to induce a demyelinating disease similar to MS in experimental animal models, but also to exacerbate the human disease (*44-48*). Further studies are needed to determine whether single TCCs are able to cross-recognize MBP 83-99 and GDP-L-fucose synthase peptides, whether the recognition of one of these peptides facilitates the release of the other and the novo activation of new autoreactive T cells, a phenomenon known as epitope spreading (*49*), or whether these responses co-develop from as yet unknown reasons.

HLA typing of the CIS/MS patients demonstrated reactivity against GDP-L-fucose synthase in DRB3*-positive patients and particularly strong reactivity in those expressing DRB3*02:02. The HLA DRB1*03 and the DRB3* haplotype most likely appeared via gene duplication of a common DRB1* gene in that locus, and in consequence DRB3* has been considered a secondary redundant locus (*50*). However, the ability of DRB3* molecules to present a distinct pattern of peptides and the existence of DRB3*-restricted T cells in peripheral blood have been demonstrated (*51*). Here, we found that the GDP-L-fucose synthase peptide 51-65, the only peptide stimulatory in all high responder DRB3*02:02 patients, showed the highest predicted binding affinity to this class II molecule, suggesting DRB3*02:02-restricted T cell recognition of this peptide. The DRB3*02:02 allele has been associated with MS in Korean children (*52*) and also with neuromyelitis optica (NMO) (*53*). Interestingly, DRB3*02:02 was over-represented in a cohort of NMO patients, in whom aquaporin 4-specific T cells cross-recognized a peptide from *Clostridium perfringens*, a normal component of gut microbiota (*54*).

The cytosolic enzyme GDP-L-fucose synthase converts GDP-4-keto-6-deoxy-D-mannose into GDP-L-fucose, which is then used by fucosyltransferases to fucosylate all oligosaccharides (*35*). Synthesis of GDP-L-fucose from free L-fucose represents a minor route. In mammals, fucosylated glycans play important roles in many biological processes including blood transfusion reactions, host-microbe interactions, and cancer pathogenesis (*55, 56*). Fucosylated

glycans are highly expressed in brain tissue, and quantitative glycan profiling of human CNS myelin demonstrated an unusually rich variety of Lewis-type antigen containing fucosylated glycans compared with other tissues (*57*). Brain fucosylated glycans have been implicated in the molecular mechanisms that underlie neuronal development, survival and function (*55, 58-60*) as well as in modulating immune responses. The encephalitogenic MOG is decorated with fucosylated glycans that support recognition by DC-SIGN on microglia and DCs. This recognition results in a tolerogenic signal characterized by IL-10 secretion and decreased T cell proliferation, while reduced fucosylation results in immunogenic signals (*57*). Reduction of brain fucosylated glycans as a consequence of T cell reactivity against GDP-L-fucose synthase might directly affect neurons and facilitate MS development by inducing a pro-inflammatory immune response. Fucosylated glycans are highly expressed also in gut tissue, where they play a crucial role in the host-microbe interaction (*61*). Fucosylation is less common in prokaryotic organisms, and it seems to be involved in adhesion, colonization, and regulation of the host immune response. In addition, a putative role of fucosylated glycans as mechanism to mimic the host and evade the immune system has been suggested in these organisms (*56*). Such a mechanism might be very beneficial for pathogens colonizing highly fucosylated tissues like the gut. In this context, the putative cross-reactivity of human and gut microbial GDP-L-fucose synthase peptides may represent a new role of gut microbiota in MS pathogenesis. Supporting this hypothesis, we demonstrated that CSF-infiltrating $CD4^+$ T cells from four CIS/MS patients that were reactive against the human GDP-L-fucose synthase peptide 161-175 also recognized two gut microbial GDP-L-fucose synthase peptides from bacterial genera that have been associated with MS (*13-16, 62-65*) and that in addition showed the highest homology with the human peptide. However, since demonstration of cross-reactivity at single TCC level is missing, further investigation is required to clarify the putative involvement of gut-microbiota via this mechanism in MS pathogenesis. Recently, molecular mimicry between a specific β-cell autoantigen and a bacteroides integrase peptide has been demonstrated in mice. Diabetogenic CD8+ T cells specific of the pancreatic peptide were able to cross-recognize the microbiota derived peptide and suppress colitis (*66*).

In conclusion, using positional scanning peptide libraries and biometrical analysis we identified GDP-L-fucose synthase as the main specificity of a brain-infiltrating clonally expanded TCC most likely involved in MS pathogenesis. This putative autoantigen is widely recognized by CSF-infiltrating $CD4^+$ T cells from DRB3*-positive MS patients. The significant correlation between myelin and GDP-L-fucose synthase reactivity in DRB3*02:02 patients as well as the putative cross-recognition of homologous peptides from gut microbiota, support a role of this antigen as potential inducer or driver of relevant immune responses in MS. Further studies are needed to confirm the existence of DRB3*02:02-restricted TCCs able to cross-recognize myelin,

human and bacterial GDP-L-fucose synthase peptides that might provide the basis for a role of molecular mimicry in the development of MS.

MATERIAL AND METHODS

Patient Material

Patient 1154SA: CSF-derived mononuclear cells and PBMCs were obtained from a SPMS patient with pattern II demyelinating lesions as previously described (*26*). HLA-class I and II types of this patient were: A*32:01, A*33:01, B*14:02, B*51:01, DRB1*15:01, DRB5* 01:01, DQB1*06:02 and DQA1*01:02.

CSF from diagnostic lumbar puncture and paired peripheral blood were collected from 31 untreated MS patients: 8 patients with clinically isolated syndrome (CIS), 20 patients with relapsing-remitting (RR) MS and 3 patients with SPMS. Demographical and clinical characteristics of the patients are summarized in Table 2. Patients were recruited from the inims outpatient clinic and day hospital at the University Medical Center Hamburg-Eppendorf and the nims section, Neurology Clinic, University Hospital Zurich. MS diagnosis was based on the revised McDonald criteria (*67*). All CIS patients had CSF-specific oligoclonal bands detected by isoelectric focusing (IEF). Patients, who had not received steroids at least 4 weeks prior to enrolment or any immunomodulatory or immunosuppressive agent during the last 3 months, were considered untreated and included in the study. Fresh CSF cells from these patients were expanded *in vitro* (see below). PBMCs were freshly isolated from EDTA-containing blood tubes by Ficoll density gradient centrifugation (PAA, Pasching, Austria) and cryopreserved.

The Ethik Kommission der Ärztekammer Hamburg, protocol No. 2758 and the Cantonal Ethical Committee of Zurich, EC-No. of the research project 2013-0001, approved the study procedures. Informed consent was obtained from all patients or relatives.

Brain autopsy tissue from 13 MS patients (7 SPMS, 5 primary progressive (PP) MS and 1 primary relapsing (PR) MS) and 7 non-MS controls were obtained from the UK Multiple Sclerosis Tissue Bank (UK Multicentre Research Ethics Committee, MREC/02/2/39). Demographical and clinical characteristics of MS patients and non-MS controls are summarized in Table S7.

Transcriptomic and Proteomic Analysis

Transcriptomic analysis of brain lesions was performed as previously described (*26*). The data discussed in this paper was deposited in NCBI's Gene Expression Omnibus and are accessible through GEO Series accession number GSE60943.

For proteomic analysis, pressure-assisted protein extraction was performed with a barocycler (2320EXT, BioSciences, Inc, South Easton, MA) (*68*). Reduction and alkylation was applied on the homogenate before samples were digested with Lys-C and trypsin. Peptides were desalted on solid phase extraction columns (C18 Finisterre, Wicom Germany), vacuum dried, re-

dissolved and measured (Nanodrop 1000, spectrophotometer (Thermo Scientific, Wilmington, DE, USA). Resulting peptides were purified and separated by hydrophilic interaction chromatography (HILIC, Agilent LC1200 equipped with a column Polyamin II 250 x 3.0 mm 120 Å, 5μm) before they were injected on a nano liquid chromatography system Easy-nLC linked to an Orbitrap Fusion instrument (Thermo Fisher). Data analysis was performed with MASCOT software using a human UniProtKB/Swiss-Prot protein database (March 22, 2016 with 40912 entries). Search parameters were 0.05 Da fragment mass tolerance and 10ppm precursor mass, minimal number of peptides 2, and FDR (false discovery rate) of 0.1%, allowing 2 mis-cleavages on trypsin fragments. Carbamidomethylation at cysteine was set as a fixed modification, and oxidation of methionine, n-terminal acetylation as variable modifications.

Positional Scanning Peptide Libraries and Individual Peptides

A synthetic N-acetylated, C-amide L-amino acid (AA) decapeptide combinatorial library in a positional scanning format (200 mixtures) and twenty-two dual defined mixtures were prepared as previously described (*69*). Individual peptides (Table S1 and S2) were synthesized by Peptides and Elephants GmbH (Potsdam, Germany).

Cells and culture conditions

Bulk CSF-derived mononuclear cells from patient 1154SA were expanded as previously reported (*26*). Briefly, 2000 cells per well were seeded in 96-well U-bottom microtiter plates together with 2 x 10^5 allogeneic irradiated PBMC (45 Gy), 1 µg/ml of PHA-L (Sigma, St Louis, MO) and IL-2 supernatant (500 U/ml) (IL-2 hybridoma kindly provided by Dr. Sallusto, Institute for Research in Biomedicine, Bellinzona, Switzerland). Medium consisted of IMDM (PAA) containing 100 U/ml penicillin/streptomycin (PAA), 50 µg/ml gentamicin (BioWhittaker, Cambrex), 2 mM L-glutamine (Gibco, Invitrogen, Carlsbad, CA) and 5% heat-decomplemented human serum (PAA). Additional IL-2 was added every 3-4 days. After two weeks, cells were pooled (short expansion) or expanded by eight rounds of restimulation. In each round, 2000 PHA-pre-expanded cells per well were seeded in 96-well U-bottom microtiter plates together with 2 x 10^5 allogeneic irradiated PBMC, PHA-L and IL-2. IL-2 was added every 3-4 days. After 16 weeks, eight rounds of two weeks, cells were pooled (long expansion). CSF-infiltrating $CD4^+$ T cells were positively selected from short and long PHA-expanded bulk CSF-derived cells using anti-CD4 magnetic beads (CD4 Micro Beads human MACS, Miltenyi Biotec Inc, CA, USA) and restimulated once again with PHA-L, IL-2 and allogeneic irradiated PBMC.

TCC21.1 was established from CSF-infiltrating cells as previously described (*26*). TCL-39 was generated from CSF-derived $CD4^+$ T cells (long PHA expansion) that responded to GDP-L-fucose synthase peptide 191-205. Positive wells underwent five rounds of restimulation with PHA and allogeneic irradiated PBMCs and IL-2. Additional IL-2 was added every 3-4 days.

The approach used to expand CSF-derived CD4+ T cells from the 31 CIS/MS patients was an adaptation from a method previously reported (*70*). Fresh bulk CSF-derived mononuclear cells were mixed with 5 x 10^6 allogeneic irradiated PBMCs and $CD4^+$ T cells were positively selected with anti-CD4 magnetic beads. $CD4^+$ fractions were then seeded at 1500 cells per well in 96-well U-bottom microtiter plates together with 1.5 x 10^5 allogeneic irradiated PBMC, 1 µg/ml of PHA-L and IL-2 supernatant. Medium consisted of RPMI 1640 without Hepes (Pan-Biotech, Aidenbach, Germany) supplemented with 2 mM glutamine (Pan-Biotech), 1% (vol/vol) nonessential amino acids (Gibco), 1% (vol/vol) sodium pyruvate (Gibco), 50 µg/ml penicillin-streptomycin (Corning, NY, USA), 0.00001% β-Mercaptoethanol (Gibco) and 5% human serum (Blood Bank Basel). Additional IL-2 was added every 4 days. Growing wells were transferred to 48 well plates and finally to 75 cm^3 flask until cells were fully rested (20-25 days). Cells were highly expanded in a single round of stimulation.

An autologous B cell line (BCL) from patient 1154SA was generated by Epstein–Barr virus (EBV)-transformation. Bare lymphocyte syndrome (BLS) cells transfected with single HLA class II molecules, DR2a (DRA1*01:01, DRB5*01:01), DR2b (DRA1*01:01, DRB1*15:01) and DQw6 (DQA1*01:02, DQB1*06:02) were kindly provided by Dr. Nepom and Dr. Kwok (University of Washington, Seattle).

T cell stimulation

TCC responses to single/dual defined peptide mixtures or individual decapeptides were tested by seeding in duplicate 2 x 10^4 T cells and 5 x 10^4 irradiated BLS cell lines or autologous BCL or 1 x 10^5 irradiated PBMC (as indicated) with or without combinatorial peptide mixtures or individual decapeptides. 2.5 µg/ml PHA and 10^{-7} M PMA (Sigma), 1 µg/ml of surface-coated anti-CD3 (OKT3, Ortho Biotech Products, Raritan, NJ) and 0.5 µg/ml of soluble anti-CD28 (Biolegend, San Diego, CA), and a T Cell Activation Kit (anti-CD3, anti-CD28, anti-CD2 beads) (Miltenyi Biotec) served as positive controls as indicated.

The response of PHA-expanded CSF-infiltrating $CD4^+$ T cells to GDP-L-fucose synthase, myelin and CEF peptides (Table S2) was tested by seeding in quadruplicate 6 x 10^4 T cells and 2 x 10^5 irradiated autologous PBMCs with or without peptides. For EdU experiments BLS DRB1*15:01 were used as APCs. T Cell Activation Kit was used as positive control.

Cytokine measurement

Cytokines in the supernatant of stimulated and unstimulated TCC21.1 or expanded CSF-infiltrating T cells were measured after 48 h of culture using the Human T Helper Cytokine Panel LEGENDplex bead-based immunoassay (Biolegend), GM-CSF ELISA (BD Biosciences, Franklin Lakes, NJ) and IL-3 ELISA (Biolegend) according to the manufacturer´s instructions. The amount of each cytokine released by TCC21.1 or expanded CSF-infiltrating T cells to

specific or unspecific stimuli was normalized by subtracting the amount of the corresponding cytokine released by T cells in absence of stimulus (negative control). For cytokines defining functional phenotypes, i.e. IFNγ for Th1, IL-4 for Th2, IL-17A and -F for Th17, IL-9 for Th9 and IL-22 for Th22, a threshold for positivity was defined based on published data (*33, 71-73*) to facilitate functional classification of TCC21.1.

For intracellular cytokine staining, TCC21.1 was analyzed 48 h after stimulation. After 5 h in presence of GolgiStop protein transport inhibitor (BD Biosciences), T cells were labeled with Live/Dead® Aqua (Invitrogen). Following fixation and permeabilization with Cytofix/Cytoperm (BD Biosciences), cells were stained with antibodies against CD4 (APC-Cy7, Biolegend), IFN-γ (FITC, Biolegend), IL-4 (PE, BD Bioscience), GM-CSF (APC, Biolegend) and IL-3 (PE, Biolegend) in PBS containing saponin and BSA, and analyzed by flow cytometry.

Proliferative Responses

Proliferation was measured 72 h after stimulation by 3H-thymidine (Hartmann Analytic, Braunschweig, Germany) incorporation in a scintillation counter (Wallac 1450, PerkinElmer, Rodgau-Jürgesheim, Germany). The stimulatory index (SI) was calculated as follows: SI = Median (replicates cpm peptide) / Median (replicates cpm without peptide).

Proliferation was also measured using a Click-iTTM EdU Flow Cytometry Assay Kit (APC, Molecular Probes, Invitrogen) following manufacturer's instructions. Cells were stained with the following antibodies anti-CD3 (PE-Cy-7, e-Bioscience, San Diego, CA) and anti-TRBV-21 (FITC, Beckman Coulter, Brea, CA) and analyzed by flow cytometry.

Surface receptor expression

Resting TCC21.1 was stained with antibodies against CD4 (PE-Texas Red, Thermo Fischer, Waltham, MA), TRBV21 (FITC, Beckman Coulter), CD28 (PE-Cy7, BioLegend), CCR4 (APC, BioLegend), CCR6 (BV785, BioLegend) and CRTh2 (PE, BioLegend) and analyzed by flow cytometry.

Flow Cytometric Analysis

Sample acquisition was conducted using a LSR Fortessa Flow Cytometer (BD Biosciences) with Diva software, and data were analyzed with FlowJo (Tree Star, Ashland, OR).

RT-PCR and Sequencing of TCR Rearrangements

RNA extraction, reverse transcription and TCRα/β-chain (TRA/BV) sequencing of TCC21.1 and TCL-39 was assessed as previously reported (*26*). TCR gene designations are in accord with IMGT nomenclature (ImMunoGeneTics, www.IMGT.org).

HLA

Individuals were typed for HLA-class I and II molecules at Histogenetics LLC, NY, USA. Isolation of DNA from whole blood with a final concentration of 15 ng/µl was performed with a standard DNA isolation protocol using a Triton lysis buffer and Proteinase K treatment. The samples were typed for HLA class I (A* and B*) and HLA class II (DRB1*, DRB3*, DRB4*, DRB5*, DQA1* and DQB1*) using high-resolution HLA sequence-based typing (SBT).

The MHC class II binding predictions were made using the IEDB analysis resource Consensus tool (*74, 75*).

Statistical analysis

Three-cluster k-means analysis was performed on patient scores to group patients into three categories. Associations between response levels of peptides, patients, and HLA status were all performed using Fisher's Exact Test with Bonferroni-Holm correction applied as appropriate, with 5% significance.

SUPPLEMENTARY MATERIALS

Supplementary Figures

Figure S1. Integration of stimulatory responses from testing dual-defined mixtures into the original scoring matrix

Figure S2. Response of CSF-infiltrating CD4+ T cells

Figure S3. New CIS/MS patients and phylogeny of bacterial species sharing GDP-L-fucose synthase peptides

Supplementary Tables

Table S1. Summary of human decapeptides predicted with the biometrical approach, synthesized and tested for stimulatory capacity

Table S2. GDP-L-fucose synthase, myelin and CEF Peptides

Table S3. Peptides from brain proteins identified by proteomic analysis in brain tissue.

Table S4. Patient classification and HLA binding

Table S5. Bacteria selected for GDP-L-fucose synthase comparison

Table S6. Sequence homology between human and bacterial GDP-L-fucose synthase peptides

Table S7. Demographical and clinical characteristics of MS patients and non-MS controls

REFERENCES

1. **M. Sospedra, R. Martin, Immunology of multiple sclerosis. *Annual review of immunology* 23, 683-747 (2005).**
2. **A. Nylander, D. A. Hafler, Multiple sclerosis. *The Journal of clinical investigation* 122, 1180-1188 (2012).**
3. **C. A. Dendrou, L. Fugger, M. A. Friese, Immunopathology of multiple sclerosis. *Nature reviews. Immunology* 15, 545-558 (2015).**
4. **C. Baecher-Allan, B. J. Kaskow, H. L. Weiner, Multiple Sclerosis: Mechanisms and Immunotherapy. *Neuron* 97, 742-768 (2018).**
5. **C. International Multiple Sclerosis Genetics, A. H. Beecham, N. A. Patsopoulos, D. K. Xifara, M. F. Davis, A. Kemppinen, C. Cotsapas, T. S. Shah, C. Spencer, D. Booth, A. Goris, A. Oturai, J. Saarela, B. Fontaine, B. Hemmer, C. Martin, F. Zipp, S. D'Alfonso, F. Martinelli-Boneschi, B. Taylor, H. F. Harbo, I. Kockum, J. Hillert, T. Olsson, M. Ban, J. R. Oksenberg, R. Hintzen, L. F. Barcellos, C. Wellcome Trust Case Control, I. B. D. G. C. International, C. Agliardi, L. Alfredsson, M. Alizadeh, C. Anderson, R. Andrews, H. B. Sondergaard, A. Baker, G. Band, S. E. Baranzini, N. Barizzone, J. Barrett, C. Bellenguez, L. Bergamaschi, L. Bernardinelli, A. Berthele, V. Biberacher, T. M. Binder, H. Blackburn, I. L. Bomfim, P. Brambilla, S. Broadley, B. Brochet, L. Brundin, D. Buck, H. Butzkueven, S. J. Caillier, W. Camu, W. Carpentier, P. Cavalla, E. G. Celius, I. Coman, G. Comi, L. Corrado, L. Cosemans, I. Cournu-Rebeix, B. A. Cree, D. Cusi, V. Damotte, G. Defer, S. R. Delgado, P. Deloukas, A. di Sapio, A. T. Dilthey, P. Donnelly, B. Dubois, M. Duddy, S. Edkins, I. Elovaara, F. Esposito, N. Evangelou, B. Fiddes, J. Field, A. Franke, C. Freeman, I. Y. Frohlich, D. Galimberti, C. Gieger, P. A. Gourraud, C. Graetz, A. Graham, V. Grummel, C. Guaschino, A. Hadjixenofontos, H. Hakonarson, C. Halfpenny, G. Hall, P. Hall, A. Hamsten, J. Harley, T. Harrower, C. Hawkins, G. Hellenthal, C. Hillier, J. Hobart, M. Hoshi, S. E. Hunt, M. Jagodic, I. Jelcic, A. Jochim, B. Kendall, A. Kermode, T. Kilpatrick, K. Koivisto, I. Konidari, T. Korn, H. Kronsbein, C. Langford, M. Larsson, M. Lathrop, C. Lebrun-Frenay, J. Lechner-Scott, M. H. Lee, M. A. Leone, V. Leppa, G. Liberatore, B. A. Lie, C. M. Lill, M. Linden, J. Link, F. Luessi, J. Lycke, F. Macciardi, S. Mannisto, C. P. Manrique, R. Martin, V. Martinelli, D. Mason, G. Mazibrada, C. McCabe, I. L. Mero, J. Mescheriakova, L. Moutsianas, K. M. Myhr, G. Nagels, R. Nicholas, P. Nilsson, F. Piehl, M. Pirinen, S. E. Price, H. Quach, M. Reunanen, W. Robberecht, N. P. Robertson, M. Rodegher, D. Rog, M. Salvetti, N. C. Schnetz-Boutaud, F. Sellebjerg, R. C. Selter, C. Schaefer, S. Shaunak, L. Shen, S. Shields, V. Siffrin, M. Slee, P. S. Sorensen, M. Sorosina, M. Sospedra, A. Spurkland, A. Strange, E. Sundqvist, V. Thijs, J. Thorpe, A. Ticca, P. Tienari, C. van Duijn, E. M. Visser, S. Vucic, H. Westerlind, J. S. Wiley, A. Wilkins, J. F. Wilson, J. Winkelmann, J. Zajicek, E. Zindler, J. L. Haines, M. A. Pericak-Vance, A. J. Ivinson, G. Stewart, D. Hafler, S. L. Hauser, A. Compston, G. McVean, P. De Jager, S. J. Sawcer, J. L. McCauley, Analysis of immune-related loci identifies 48 new susceptibility variants for multiple sclerosis. *Nature genetics* 45, 1353-1360 (2013).**
6. **C. International Multiple Sclerosis Genetics, C. Wellcome Trust Case Control, S. Sawcer, G. Hellenthal, M. Pirinen, C. C. Spencer, N. A. Patsopoulos, L. Moutsianas, A. Dilthey, Z. Su, C. Freeman, S. E. Hunt, S. Edkins, E. Gray, D. R. Booth, S. C. Potter, A. Goris, G. Band, A. B. Oturai, A. Strange, J. Saarela, C. Bellenguez, B. Fontaine, M. Gillman, B. Hemmer, R. Gwilliam, F. Zipp, A.**

Jayakumar, R. Martin, S. Leslie, S. Hawkins, E. Giannoulatou, S. D'Alfonso, H. Blackburn, F. Martinelli Boneschi, J. Liddle, H. F. Harbo, M. L. Perez, A. Spurkland, M. J. Waller, M. P. Mycko, M. Ricketts, M. Comabella, N. Hammond, I. Kockum, O. T. McCann, M. Ban, P. Whittaker, A. Kemppinen, P. Weston, C. Hawkins, S. Widaa, J. Zajicek, S. Dronov, N. Robertson, S. J. Bumpstead, L. F. Barcellos, R. Ravindrarajah, R. Abraham, L. Alfredsson, K. Ardlie, C. Aubin, A. Baker, K. Baker, S. E. Baranzini, L. Bergamaschi, R. Bergamaschi, A. Bernstein, A. Berthele, M. Boggild, J. P. Bradfield, D. Brassat, S. A. Broadley, D. Buck, H. Butzkueven, R. Capra, W. M. Carroll, P. Cavalla, E. G. Celius, S. Cepok, R. Chiavacci, F. Clerget-Darpoux, K. Clysters, G. Comi, M. Cossburn, I. Cournu-Rebeix, M. B. Cox, W. Cozen, B. A. Cree, A. H. Cross, D. Cusi, M. J. Daly, E. Davis, P. I. de Bakker, M. Debouverie, B. D'Hooghe M, K. Dixon, R. Dobosi, B. Dubois, D. Ellinghaus, I. Elovaara, F. Esposito, C. Fontenille, S. Foote, A. Franke, D. Galimberti, A. Ghezzi, J. Glessner, R. Gomez, O. Gout, C. Graham, S. F. Grant, F. R. Guerini, H. Hakonarson, P. Hall, A. Hamsten, H. P. Hartung, R. N. Heard, S. Heath, J. Hobart, M. Hoshi, C. Infante-Duarte, G. Ingram, W. Ingram, T. Islam, M. Jagodic, M. Kabesch, A. G. Kermode, T. J. Kilpatrick, C. Kim, N. Klopp, K. Koivisto, M. Larsson, M. Lathrop, J. S. Lechner-Scott, M. A. Leone, V. Leppa, U. Liljedahl, I. L. Bomfim, R. R. Lincoln, J. Link, J. Liu, A. R. Lorentzen, S. Lupoli, F. Macciardi, T. Mack, M. Marriott, V. Martinelli, D. Mason, J. L. McCauley, F. Mentch, I. L. Mero, T. Mihalova, X. Montalban, J. Mottershead, K. M. Myhr, P. Naldi, W. Ollier, A. Page, A. Palotie, J. Pelletier, L. Piccio, T. Pickersgill, F. Piehl, S. Pobywajlo, H. L. Quach, P. P. Ramsay, M. Reunanen, R. Reynolds, J. D. Rioux, M. Rodegher, S. Roesner, J. P. Rubio, I. M. Ruckert, M. Salvetti, E. Salvi, A. Santaniello, C. A. Schaefer, S. Schreiber, C. Schulze, R. J. Scott, F. Sellebjerg, K. W. Selmaj, D. Sexton, L. Shen, B. Simms-Acuna, S. Skidmore, P. M. Sleiman, C. Smestad, P. S. Sorensen, H. B. Sondergaard, J. Stankovich, R. C. Strange, A. M. Sulonen, E. Sundqvist, A. C. Syvanen, F. Taddeo, B. Taylor, J. M. Blackwell, P. Tienari, E. Bramon, A. Tourbah, M. A. Brown, E. Tronczynska, J. P. Casas, N. Tubridy, A. Corvin, J. Vickery, J. Jankowski, P. Villoslada, H. S. Markus, K. Wang, C. G. Mathew, J. Wason, C. N. Palmer, H. E. Wichmann, R. Plomin, E. Willoughby, A. Rautanen, J. Winkelmann, M. Wittig, R. C. Trembath, J. Yaouanq, A. C. Viswanathan, H. Zhang, N. W. Wood, R. Zuvich, P. Deloukas, C. Langford, A. Duncanson, J. R. Oksenberg, M. A. Pericak-Vance, J. L. Haines, T. Olsson, J. Hillert, A. J. Ivinson, P. L. De Jager, L. Peltonen, G. J. Stewart, D. A. Hafler, S. L. Hauser, G. McVean, P. Donnelly, A. Compston, Genetic risk and a primary role for cell-mediated immune mechanisms in multiple sclerosis. *Nature* 476, 214-219 (2011).

7. **A. Fogdell-Hahn, A. Ligers, M. Gronning, J. Hillert, O. Olerup, Multiple sclerosis: a modifying influence of HLA class I genes in an HLA class II associated autoimmune disease. *Tissue antigens* 55, 140-148 (2000).**
8. **M. A. Friese, K. B. Jakobsen, L. Friis, R. Etzensperger, M. J. Craner, R. M. McMahon, L. T. Jensen, V. Huygelen, E. Y. Jones, J. I. Bell, L. Fugger, Opposing effects of HLA class I molecules in tuning autoreactive CD8+ T cells in multiple sclerosis. *Nature medicine* 14, 1227-1235 (2008).**
9. **R. Hohlfeld, K. Dornmair, E. Meinl, H. Wekerle, The search for the target antigens of multiple sclerosis, part 1: autoreactive CD4+ T lymphocytes as pathogenic effectors and therapeutic targets. *The Lancet. Neurology* 15, 198-209 (2016).**

10. **A. Ascherio, K. L. Munger, Environmental risk factors for multiple sclerosis. Part II: Noninfectious factors. *Annals of neurology* 61, 504-513 (2007).**
11. **A. Ascherio, K. L. Munger, J. D. Lunemann, The initiation and prevention of multiple sclerosis. *Nature reviews. Neurology* 8, 602-612 (2012).**
12. **H. Wekerle, Brain Autoimmunity and Intestinal Microbiota: 100 Trillion Game Changers. *Trends in immunology*, (2017).**
13. **J. Chen, N. Chia, K. R. Kalari, J. Z. Yao, M. Novotna, M. M. Soldan, D. H. Luckey, E. V. Marietta, P. R. Jeraldo, X. Chen, B. G. Weinshenker, M. Rodriguez, O. H. Kantarci, H. Nelson, J. A. Murray, A. K. Mangalam, Multiple sclerosis patients have a distinct gut microbiota compared to healthy controls. *Scientific reports* 6, 28484 (2016).**
14. **S. Jangi, R. Gandhi, L. M. Cox, N. Li, F. von Glehn, R. Yan, B. Patel, M. A. Mazzola, S. Liu, B. L. Glanz, S. Cook, S. Tankou, F. Stuart, K. Melo, P. Nejad, K. Smith, B. D. Topcuolu, J. Holden, P. Kivisakk, T. Chitnis, P. L. De Jager, F. J. Quintana, G. K. Gerber, L. Bry, H. L. Weiner, Alterations of the human gut microbiome in multiple sclerosis. *Nature communications* 7, 12015 (2016).**
15. **K. Berer, L. A. Gerdes, E. Cekanaviciute, X. Jia, L. Xiao, Z. Xia, C. Liu, L. Klotz, U. Stauffer, S. E. Baranzini, T. Kumpfel, R. Hohlfeld, G. Krishnamoorthy, H. Wekerle, Gut microbiota from multiple sclerosis patients enables spontaneous autoimmune encephalomyelitis in mice. *Proceedings of the National Academy of Sciences of the United States of America* 114, 10719-10724 (2017).**
16. **E. Cekanaviciute, B. B. Yoo, T. F. Runia, J. W. Debelius, S. Singh, C. A. Nelson, R. Kanner, Y. Bencosme, Y. K. Lee, S. L. Hauser, E. Crabtree-Hartman, I. K. Sand, M. Gacias, Y. Zhu, P. Casaccia, B. A. C. Cree, R. Knight, S. K. Mazmanian, S. E. Baranzini, Gut bacteria from multiple sclerosis patients modulate human T cells and exacerbate symptoms in mouse models. *Proceedings of the National Academy of Sciences of the United States of America* 114, 10713-10718 (2017).**
17. **T. C. Fung, C. A. Olson, E. Y. Hsiao, Interactions between the microbiota, immune and nervous systems in health and disease. *Nature neuroscience* 20, 145-155 (2017).**
18. **D. Erny, A. L. Hrabe de Angelis, D. Jaitin, P. Wieghofer, O. Staszewski, E. David, H. Keren-Shaul, T. Mahlakoiv, K. Jakobshagen, T. Buch, V. Schwierzeck, O. Utermohlen, E. Chun, W. S. Garrett, K. D. McCoy, A. Diefenbach, P. Staeheli, B. Stecher, I. Amit, M. Prinz, Host microbiota constantly control maturation and function of microglia in the CNS. *Nature neuroscience* 18, 965-977 (2015).**
19. **V. Rothhammer, I. D. Mascanfroni, L. Bunse, M. C. Takenaka, J. E. Kenison, L. Mayo, C. C. Chao, B. Patel, R. Yan, M. Blain, J. I. Alvarez, H. Kebir, N. Anandasabapathy, G. Izquierdo, S. Jung, N. Obholzer, N. Pochet, C. B. Clish, M. Prinz, A. Prat, J. Antel, F. J. Quintana, Type I interferons and microbial metabolites of tryptophan modulate astrocyte activity and central nervous system inflammation via the aryl hydrocarbon receptor. *Nature medicine* 22, 586-597 (2016).**
20. **A. Lutterotti, M. Sospedra, R. Martin, Antigen-specific therapies in MS - Current concepts and novel approaches. *Journal of the neurological sciences* 274, 18-22 (2008).**
21. **S. Shimoda, M. Nakamura, H. Ishibashi, K. Hayashida, Y. Niho, HLA DRB4 0101-restricted immunodominant T cell autoepitope of pyruvate dehydrogenase complex in primary biliary cirrhosis: evidence of molecular mimicry in human**

autoimmune diseases. *The Journal of experimental medicine* 181, 1835-1845 (1995).

22. C. Pinilla, J. R. Appel, P. Blanc, R. A. Houghten, Rapid identification of high affinity peptide ligands using positional scanning synthetic peptide combinatorial libraries. *BioTechniques* 13, 901-905 (1992).
23. B. Hemmer, B. Gran, Y. Zhao, A. Marques, J. Pascal, A. Tzou, T. Kondo, I. Cortese, B. Bielekova, S. E. Straus, H. F. McFarland, R. Houghten, R. Simon, C. Pinilla, R. Martin, Identification of candidate T-cell epitopes and molecular mimics in chronic Lyme disease. *Nature medicine* 5, 1375-1382 (1999).
24. Y. Zhao, B. Gran, C. Pinilla, S. Markovic-Plese, B. Hemmer, A. Tzou, L. W. Whitney, W. E. Biddison, R. Martin, R. Simon, Combinatorial peptide libraries and biometric score matrices permit the quantitative analysis of specific and degenerate interactions between clonotypic TCR and MHC peptide ligands. *Journal of immunology* 167, 2130-2141 (2001).
25. M. Sospedra, Y. Zhao, H. zur Hausen, P. A. Muraro, C. Hamashin, E. M. de Villiers, C. Pinilla, R. Martin, Recognition of conserved amino acid motifs of common viruses and its role in autoimmunity. *PLoS Pathog* 1, e41 (2005).
26. R. Planas, I. Metz, Y. Ortiz, N. Vilarrasa, I. Jelcic, G. Salinas-Riester, C. Heesen, W. Bruck, R. Martin, M. Sospedra, Central role of Th2/Tc2 lymphocytes in pattern II multiple sclerosis lesions. *Annals of clinical and translational neurology* 2, 875-893 (2015).
27. C. Lucchinetti, W. Bruck, J. Parisi, B. Scheithauer, M. Rodriguez, H. Lassmann, Heterogeneity of multiple sclerosis lesions: implications for the pathogenesis of demyelination. *Annals of neurology* 47, 707-717 (2000).
28. M. Sospedra, Y. Zhao, M. Giulianotti, R. Simon, C. Pinilla, R. Martin, Combining positional scanning peptide libraries, HLA-DR transfectants and bioinformatics to dissect the epitope spectrum of HLA class II cross-restricted CD4+ T cell clones. *J Immunol Methods* 353, 93-101 (2010).
29. V. Judkowski, A. Bunying, F. Ge, J. R. Appel, K. Law, A. Sharma, C. Raja-Gabaglia, P. Norori, R. G. Santos, M. A. Giulianotti, M. K. Slifka, D. C. Douek, B. S. Graham, C. Pinilla, GM-CSF production allows the identification of immunoprevalent antigens recognized by human CD4+ T cells following smallpox vaccination. *PloS one* 6, e24091 (2011).
30. C. The UniProt, UniProt: the universal protein knowledgebase. *Nucleic acids research* 45, D158-D169 (2017).
31. R. G. Santos, M. A. Giulianotti, C. T. Dooley, C. Pinilla, J. R. Appel, R. A. Houghten, Use and implications of the harmonic mean model on mixtures for basic research and drug discovery. *ACS Comb Sci* 13, 337-344 (2011).
32. M. Sospedra, P. A. Muraro, I. Stefanova, Y. Zhao, K. Chung, Y. Li, M. Giulianotti, R. Simon, R. Mariuzza, C. Pinilla, R. Martin, Redundancy in antigen-presenting function of the HLA-DR and -DQ molecules in the multiple sclerosis-associated HLA-DR2 haplotype. *Journal of immunology* 176, 1951-1961 (2006).
33. S. Yousef, R. Planas, K. Chakroun, S. Hoffmeister-Ullerich, T. M. Binder, T. H. Eiermann, R. Martin, M. Sospedra, TCR bias and HLA cross-restriction are strategies of human brain-infiltrating JC virus-specific CD4+ T cells during viral infection. *Journal of immunology* 189, 3618-3630 (2012).
34. B. Bielekova, M. H. Sung, N. Kadom, R. Simon, H. McFarland, R. Martin, Expansion and functional relevance of high-avidity myelin-specific CD4+ T cells in multiple sclerosis. *Journal of immunology* 172, 3893-3904 (2004).

35. **H. Zhou, L. Sun, J. Li, C. Xu, F. Yu, Y. Liu, C. Ji, J. He, The crystal structure of human GDP-L-fucose synthase. *Acta biochimica et biophysica Sinica* 45, 720-725 (2013).**
36. **M. J. Coyne, B. Reinap, M. M. Lee, L. E. Comstock, Human symbionts use a host-like pathway for surface fucosylation. *Science* 307, 1778-1781 (2005).**
37. **W. S. Somers, M. L. Stahl, F. X. Sullivan, GDP-fucose synthetase from Escherichia coli: structure of a unique member of the short-chain dehydrogenase/reductase family that catalyzes two distinct reactions at the same active site. *Structure* 6, 1601-1612 (1998).**
38. **S. Dai, F. Crawford, P. Marrack, J. W. Kappler, The structure of HLA-DR52c: comparison to other HLA-DRB3 alleles. *Proceedings of the National Academy of Sciences of the United States of America* 105, 11893-11897 (2008).**
39. **M. El-Behi, B. Ciric, H. Dai, Y. Yan, M. Cullimore, F. Safavi, G. X. Zhang, B. N. Dittel, A. Rostami, The encephalitogenicity of T(H)17 cells is dependent on IL-1- and IL-23-induced production of the cytokine GM-CSF. *Nature immunology* 12, 568-575 (2011).**
40. **L. Codarri, G. Gyulveszi, V. Tosevski, L. Hesske, A. Fontana, L. Magnenat, T. Suter, B. Becher, RORgammat drives production of the cytokine GM-CSF in helper T cells, which is essential for the effector phase of autoimmune neuroinflammation. *Nature immunology* 12, 560-567 (2011).**
41. **Y. Dan, Y. Katakura, A. Ametani, S. Kaminogawa, Y. Asano, IL-3 augments TCR-mediated responses of type 2 CD4 T cells. *Journal of immunology* 156, 27-34 (1996).**
42. **S. Ebner, S. Hofer, V. A. Nguyen, C. Furhapter, M. Herold, P. Fritsch, C. Heufler, N. Romani, A novel role for IL-3: human monocytes cultured in the presence of IL-3 and IL-4 differentiate into dendritic cells that produce less IL-12 and shift Th cell responses toward a Th2 cytokine pattern. *Journal of immunology* 168, 6199-6207 (2002).**
43. **C. J. Holland, D. K. Cole, A. Godkin, Re-Directing CD4(+) T Cell Responses with the Flanking Residues of MHC Class II-Bound Peptides: The Core is Not Enough. *Front Immunol* 4, 172 (2013).**
44. **B. Bielekova, B. Goodwin, N. Richert, I. Cortese, T. Kondo, G. Afshar, B. Gran, J. Eaton, J. Antel, J. A. Frank, H. F. McFarland, R. Martin, Encephalitogenic potential of the myelin basic protein peptide (amino acids 83-99) in multiple sclerosis: results of a phase II clinical trial with an altered peptide ligand. *Nature medicine* 6, 1167-1175 (2000).**
45. **K. Ota, M. Matsui, E. L. Milford, G. A. Mackin, H. L. Weiner, D. A. Hafler, T-cell recognition of an immunodominant myelin basic protein epitope in multiple sclerosis. *Nature* 346, 183-187 (1990).**
46. **M. Pette, K. Fujita, B. Kitze, J. N. Whitaker, E. Albert, L. Kappos, H. Wekerle, Myelin basic protein-specific T lymphocyte lines from MS patients and healthy individuals. *Neurology* 40, 1770-1776 (1990).**
47. **R. Martin, D. Jaraquemada, M. Flerlage, J. Richert, J. Whitaker, E. O. Long, D. E. McFarlin, H. F. McFarland, Fine specificity and HLA restriction of myelin basic protein-specific cytotoxic T cell lines from multiple sclerosis patients and healthy individuals. *Journal of immunology* 145, 540-548 (1990).**
48. **R. Martin, M. D. Howell, D. Jaraquemada, M. Flerlage, J. Richert, S. Brostoff, E. O. Long, D. E. McFarlin, H. F. McFarland, A myelin basic protein peptide is recognized by cytotoxic T cells in the context of four HLA-DR types associated**

with multiple sclerosis. *The Journal of experimental medicine* 173, 19-24 (1991).

49. **J. E. Libbey, M. F. Cusick, R. S. Fujinami, Role of pathogens in multiple sclerosis. *International reviews of immunology* 33, 266-283 (2014).**
50. **T. F. Bergstrom, R. Erlandsson, H. Engkvist, A. Josefsson, H. A. Erlich, U. Gyllensten, Phylogenetic history of hominoid DRB loci and alleles inferred from intron sequences. *Immunological reviews* 167, 351-365 (1999).**
51. **R. Faner, E. James, L. Huston, R. Pujol-Borrel, W. W. Kwok, M. Juan, Reassessing the role of HLA-DRB3 T-cell responses: evidence for significant expression and complementary antigen presentation. *European journal of immunology* 40, 91-102 (2010).**
52. **H. H. Oh, S. H. Kwon, C. W. Kim, B. H. Choe, C. W. Ko, H. D. Jung, J. S. Suh, J. H. Lee, Molecular analysis of HLA class II-associated susceptibility to neuroinflammatory diseases in Korean children. *Journal of Korean medical science* 19, 426-430 (2004).**
53. **D. G. Brum, A. A. Barreira, A. C. dos Santos, D. R. Kaimen-Maciel, M. Matiello, R. M. Costa, N. H. Deghaide, L. S. Costa, P. Louzada-Junior, P. R. Diniz, E. R. Comini-Frota, C. T. Mendes-Junior, E. A. Donadi, HLA-DRB association in neuromyelitis optica is different from that observed in multiple sclerosis. *Multiple sclerosis* 16, 21-29 (2010).**
54. **M. Varrin-Doyer, C. M. Spencer, U. Schulze-Topphoff, P. A. Nelson, R. M. Stroud, B. A. Cree, S. S. Zamvil, Aquaporin 4-specific T cells in neuromyelitis optica exhibit a Th17 bias and recognize Clostridium ABC transporter. *Annals of neurology* 72, 53-64 (2012).**
55. **D. J. Becker, J. B. Lowe, Fucose: biosynthesis and biological function in mammals. *Glycobiology* 13, 41R-53R (2003).**
56. **B. Ma, J. L. Simala-Grant, D. E. Taylor, Fucosylation in prokaryotes and eukaryotes. *Glycobiology* 16, 158R-184R (2006).**
57. **J. J. Garcia-Vallejo, J. M. Ilarregui, H. Kalay, S. Chamorro, N. Koning, W. W. Unger, M. Ambrosini, V. Montserrat, R. J. Fernandes, S. C. Bruijns, J. R. van Weering, N. J. Paauw, T. O'Toole, J. van Horssen, P. van der Valk, K. Nazmi, J. G. Bolscher, J. Bajramovic, C. D. Dijkstra, B. A. t Hart, Y. van Kooyk, CNS myelin induces regulatory functions of DC-SIGN-expressing, antigen-presenting cells via cognate interaction with MOG. *The Journal of experimental medicine* 211, 1465-1483 (2014).**
58. **D. Lutz, G. Loers, R. Kleene, I. Oezen, H. Kataria, N. Katagihallimath, I. Braren, G. Harauz, M. Schachner, Myelin basic protein cleaves cell adhesion molecule L1 and promotes neuritogenesis and cell survival. *The Journal of biological chemistry* 289, 13503-13518 (2014).**
59. **H. E. Murrey, C. I. Gama, S. A. Kalovidouris, W. I. Luo, E. M. Driggers, B. Porton, L. C. Hsieh-Wilson, Protein fucosylation regulates synapsin Ia/Ib expression and neuronal morphology in primary hippocampal neurons. *Proceedings of the National Academy of Sciences of the United States of America* 103, 21-26 (2006).**
60. **S. Yaji, H. Manya, N. Nakagawa, H. Takematsu, T. Endo, R. Kannagi, T. Yoshihara, M. Asano, S. Oka, Major glycan structure underlying expression of the Lewis X epitope in the developing brain is O-mannose-linked glycans on phosphacan/RPTPbeta. *Glycobiology* 25, 376-385 (2015).**

61. **Y. Goto, S. Uematsu, H. Kiyono, Epithelial glycosylation in gut homeostasis and inflammation. *Nature immunology* 17, 1244-1251 (2016).**
62. **S. Miyake, S. Kim, W. Suda, K. Oshima, M. Nakamura, T. Matsuoka, N. Chihara, A. Tomita, W. Sato, S. W. Kim, H. Morita, M. Hattori, T. Yamamura, Dysbiosis in the Gut Microbiota of Patients with Multiple Sclerosis, with a Striking Depletion of Species Belonging to Clostridia XIVa and IV Clusters. *PloS one* 10, e0137429 (2015).**
63. **H. Tremlett, D. W. Fadrosh, A. A. Faruqi, F. Zhu, J. Hart, S. Roalstad, J. Graves, S. Lynch, E. Waubant, U. S. N. o. P. M. Centers, Gut microbiota in early pediatric multiple sclerosis: a case-control study. *European journal of neurology* 23, 1308-1321 (2016).**
64. **K. R. Rumah, J. Linden, V. A. Fischetti, T. Vartanian, Isolation of Clostridium perfringens type B in an individual at first clinical presentation of multiple sclerosis provides clues for environmental triggers of the disease. *PloS one* 8, e76359 (2013).**
65. **J. Ochoa-Reparaz, D. W. Mielcarz, L. E. Ditrio, A. R. Burroughs, S. Begum-Haque, S. Dasgupta, D. L. Kasper, L. H. Kasper, Central nervous system demyelinating disease protection by the human commensal Bacteroides fragilis depends on polysaccharide A expression. *Journal of immunology* 185, 4101-4108 (2010).**
66. **R. Hebbandi Nanjundappa, F. Ronchi, J. Wang, X. Clemente-Casares, J. Yamanouchi, C. Sokke Umeshappa, Y. Yang, J. Blanco, H. Bassolas-Molina, A. Salas, H. Khan, R. M. Slattery, M. Wyss, C. Mooser, A. J. Macpherson, L. K. Sycuro, P. Serra, D. M. McKay, K. D. McCoy, P. Santamaria, A Gut Microbial Mimic that Hijacks Diabetogenic Autoreactivity to Suppress Colitis. *Cell* 171, 655-667 e617 (2017).**
67. **C. H. Polman, S. C. Reingold, B. Banwell, M. Clanet, J. A. Cohen, M. Filippi, K. Fujihara, E. Havrdova, M. Hutchinson, L. Kappos, F. D. Lublin, X. Montalban, P. O'Connor, M. Sandberg-Wollheim, A. J. Thompson, E. Waubant, B. Weinshenker, J. S. Wolinsky, Diagnostic criteria for multiple sclerosis: 2010 revisions to the McDonald criteria. *Annals of neurology* 69, 292-302 (2011).**
68. **T. Guo, P. Kouvonen, C. C. Koh, L. C. Gillet, W. E. Wolski, H. L. Rost, G. Rosenberger, B. C. Collins, L. C. Blum, S. Gillessen, M. Joerger, W. Jochum, R. Aebersold, Rapid mass spectrometric conversion of tissue biopsy samples into permanent quantitative digital proteome maps. *Nature medicine* 21, 407-413 (2015).**
69. **C. Pinilla, J. R. Appel, R. A. Houghten, Investigation of antigen-antibody interactions using a soluble, non-support-bound synthetic decapeptide library composed of four trillion (4 x 10(12) sequences. *The Biochemical journal* 301 (Pt 3), 847-853 (1994).**
70. **R. Geiger, T. Duhen, A. Lanzavecchia, F. Sallusto, Human naive and memory CD4+ T cell repertoires specific for naturally processed antigens analyzed using libraries of amplified T cells. *The Journal of experimental medicine* 206, 1525-1534 (2009).**
71. **R. Noster, R. Riedel, M. F. Mashreghi, H. Radbruch, L. Harms, C. Haftmann, H. D. Chang, A. Radbruch, C. E. Zielinski, IL-17 and GM-CSF expression are antagonistically regulated by human T helper cells. *Science translational medicine* 6, 241ra280 (2014).**
72. **S. Trifari, C. D. Kaplan, E. H. Tran, N. K. Crellin, H. Spits, Identification of a human helper T cell population that has abundant production of interleukin**

22 and is distinct from T(H)-17, T(H)1 and T(H)2 cells. *Nature immunology* 10, 864-871 (2009).

73. C. Schlapbach, A. Gehad, C. Yang, R. Watanabe, E. Guenova, J. E. Teague, L. Campbell, N. Yawalkar, T. S. Kupper, R. A. Clark, Human TH9 cells are skin-tropic and have autocrine and paracrine proinflammatory capacity. *Science translational medicine* 6, 219ra218 (2014).

74. P. Wang, J. Sidney, C. Dow, B. Mothe, A. Sette, B. Peters, A systematic assessment of MHC class II peptide binding predictions and evaluation of a consensus approach. *PLoS computational biology* 4, e1000048 (2008).

75. P. Wang, J. Sidney, Y. Kim, A. Sette, O. Lund, M. Nielsen, B. Peters, Peptide binding predictions for HLA DR, DP and DQ molecules. *BMC bioinformatics* 11, 568 (2010).

Acknowledgements: We thank Dr. G. Nepom and Dr. B. Kwok (University of Washington, Seattle) for BLS tranfectants and Dr. F. Sallusto (Institute for Research in Biomedicine, Bellinzona, Switzerland) for IL-2 hybridoma. We wish to acknowledge Dr. A. Willing and the inims outpatient clinic and day hospital at the University Medical Center Hamburg-Eppendorf and the clinical staff of nims, Neurology Clinic, University Hospital Zurich for clinical samples. **Funding:** This work was supported by DFG Clinical Research Group, KFO 228/1, DFG Center Grant - SFB 841 and SNF: 310030_146945. European Research Council Advanced Grant (340733) (RM), Clinical Research Priority Program MS ($CRPP^{MS}$) of the University Zurich (RM and MS), Swiss National Science Foundation (Sinergia UnmetMS) (RM and MS) and the Swiss MS Society (RM). RP was supported by UZH FK-13-046. UK Multiple Sclerosis Tissue Bank was supported by the Multiple Sclerosis Society of Great Britain and Northern Ireland (registered charity 207495). This work was supported in part by Multiple Sclerosis National Research Institute (RS and CP). **Author contributions:** M.S. designed and supervised the study and wrote the manuscript. R.M. participated in study design and reviewed the manuscript. R.P. performed the experiments with T cells. R.S. and C.P. provided the peptide libraries and participated in the design and analysis of the results. P.T.O. and C.C. help in the expansion of the CSF-infiltrating cells. A.L. supervised the provision of clinical samples. W.F. and N.S.W. performed the proteomic analysis of the brain. C.E. and H.E. discussed and analyzed data and gave conceptual advice. All authors discussed the results and commented on the manuscript. **Competing interests:** All authors declare that they have no competing financial interests in the context of this work. A patent to use GDP-L-Fucose Synthase in the treatment, diagnosis and/or prevention of multiple sclerosis (MS) is being filed. **Data and materials availability:** Peptide libraries are available under a material transfer agreement with Torrey Pines Institute for Molecular Studies.

FIGURE LEGENDS

Figure 1. Single and dual-defined decapeptide positional scanning mixtures in combination with biometric analysis to identify the specifity of TCC21.1. A GM-CSF production by TCC21.1 in response to 20 combinatorial peptide mixtures with AAs defined at position 5 and presented by BLS cells expressing only DRB1*15:01, DRB5*01:01 or DQB1*06:02 class II molecules. X-axes, single-letter AA code; Y-axes, cytokine production. **B.** GM-CSF (black histograms) and IL-10 (white histograms) production by TCC21.1 in response to a complete decapeptide positional scanning library (200 mixtures) presented by BLS cells expressing only DRB1*15:01. **C.** Score matrix designed with the log10 median of GM-CSF production of three independent experiments. Dark grey cells correspond to values equal or higher than 2 and light grey cells to values between 1.5 and 2. Bold borders show mixtures selected for dual defined mixtures, continuous borders based on GM-CSF results and dotted borders on IL-10 results. **D.** GM-CSF production by TCC21.1 in response to the 50 peptides with highest scores predicted using the GM-CSF based score matrix. **E.** GM-CSF production by TCC21.1 in response to 22 dual-defined mixtures. In green, mixtures with defined AAs of the TCR motif in frame 1 and in blue in frame 2. Stimulatory responses of mixtures shown with darker colors (Frame 1/2-HM) were integrated into the original matrix using the harmonic mean model. **F.** TCR motif and dual-defined mixture activity values selected based on the harmonic mean model and incorporated into the original matrix, Frame 1-HM in green and Frame 2-HM in blue. **G.** GM-CSF production by TCC21.1 in response to the 50 peptides with higher scores predicted using harmonic boost frame 1 and 2 score matrices. Complete decapeptide library, dual defined mixtures and individual decapeptides were presented by BLS cells expressing DRB1*15:01. Mixtures were tested at 200 μg/ml and individual decapeptides at 5 μg/ml. Histograms show mean ± standard error mean (SEM) and dot plots mean of three independent experiments. Cytokine released is always expressed as pg/ml released by TCC21.1 in response to stimuli minus pg/ml released in absence of stimulus (negative control).

Figure 2. Characterization of TCC21.1 response to GDP-L-fucose synthase peptides. A. GM-CSF production by TCC21.1 in response to eleven decapeptides overlapping by nine AA and tested at 0.5 and 5 μg/ml. **B-C.** GM-CSF dose response of TCC21.1 to GDP-L-fucose synthase peptide (96-105) presented by BLS cells expressing DRA*01:01/DRB1*15:01, DRA*01:01/DRB5*01:01 or DQA1*01:02/DQB1*06:02 class II molecules. **D.** GM-CSF production by TCC21.1 in response to 13 alanine scan peptides presented by BLS cells expressing DRA*01:01/DRB1*15:01. Alanine substitution is shown in grey. **E-F.** Proliferative

responses (white histograms) and production of cytokines (black histograms) by TCC21.1 in response to GDP-L-fucose synthase peptides presented by autologous PBMCs/BCL and unspecific stimulus. **F**. Proliferative response (white histograms) and GM-CSF and IL-3 production (black histograms) by TCC21.1 and other TCCs with different functional phenotype in response to the corresponding specific peptides presented by autologous PBMCs, for TCC21.1 also autologous BCL, and to unspecific stimuli. Cytokine released is always expressed as pg/ml released by TCC21.1 in response to stimuli minus pg/ml released in absence of stimulus (negative control). All results show the mean ± SEM. Dotted lines show a putative threshold for positivity: SI=2 in proliferation histograms and the amount of IFNγ, IL-4, IL-17, IL-9 and IL-22 released by T cells with Th1, Th2, Th17, Th9 Th22 functional phenotype respectively. **G.** Representative flow cytometry analysis of intracellular IL-4, IFN-γ, GM-CSF and IL-3 production by TCC21.1 in response to GDP-L-fucose synthase peptide (96-105) and PMA/Ionomycin. Numbers represent the percentage of positive cells. **H.** Histograms representing the mean fluorescence intensity of CD28, CCR4, CCR6 and CRTh2 on the surface of resting TCC21.1 (black lines) in comparison to the isotype control staining (gray shaded).

Figure 3. Recognition of GDP-L-fucose synthase peptides by TCC21.1 and CSF-infiltrating CD4$^+$ T cells from patient 1154SA. A. Proliferative responses expressed as SI of TCC21.1 and CSF-infiltrating CD4$^+$ T cells after short- and long PHA expansion, to GDP-L-fucose synthase-, myelin- and CEF peptides presented by autologous PBMCs as well as to control beads. TCC21.1 graph shows the mean SI ± SEM, while in the CSF graphs each dot represents one well. Positive peptides are shown in black. **B.** Proliferation of long expanded CSF-infiltrating CD4$^+$ T to GDP-L-fucose synthase peptide (91-105), CEF pool and PHA using as APCs BLS DRA*01:01/DRB1*15:01 and assessed by EdU incorporation. Numbers represent the percentage of EdU-positive cells. **C.** Proliferative responses expressed as stimulation indexes (SI) of positive wells to GDP-L-fucose synthase peptide (191-205) for generation of TCL-39. **D.** TCRBV sequencing of TCCs present in TCL-39. **E.** Production of cytokines of long expanded CSF-infiltrating CD4$^+$ T to GDP-L-fucose synthase peptides 91-105 and 191-205 presented by autologous PBMCs as well as to control beads. Cytokine released is expressed as pg/ml released by stimulated cells minus pg/ml released in absence of stimulus (negative control). Results show the mean ± SEM.

Figure 4. Recognition of GDP-L-fucose synthase peptides by CSF-infiltrating CD4$^+$ T cells from moderate and high responder CIS/MS patients. A. Proliferative responses expressed as stimulation indexes (SI) of CSF-infiltrating CD4$^+$ T cells (single round of PHA expansion) to

GDP-L-fucose synthase and CEF peptides presented by autologous PBMCs as well as to control beads. Each dot represents one well, and median SIs are shown as solid lines. Positive peptides (black dots and red line) are peptides with median of all SIs > 1.455 (dotted red line). All peptides have been tested in four wells, except for peptides 156-170 and/or 161-175 in 748UR, 1129RE, 1005ME, 1173DI, 718MA and 776JE, which were tested also for bacterial peptides by seeding 8 wells. **B.** Number of CIS/MS patients with CSF-infiltrating $CD4^+$ T cells that responded to GDP-L-fucose synthase peptides. Immunodominant peptides that were positive in at least three patients are shown in red. Solid red are high responder and light red moderate responder patients. **C.** Production of cytokines of CSF-infiltrating $CD4^+$ T cells from three patients to GDP-L-fucose synthase immunodominant peptides presented by autologous PBMCs.

Figure 5. Recognition of myelin peptides by CSF-infiltrating $CD4^+$ T cells from CIS/MS patients. A. Proliferative responses expressed as stimulation indexes (SI) of CSF-infiltrating $CD4^+$ T cells (single round of PHA expansion) to myelin peptides presented by autologous PBMCs. Each dot represents one well, and median SIs are shown as solid lines. Positive peptides (black wells and red line) are peptides with median of all SIs > 1.455 (dotted red line). **B.** Checkerboard graph illustrating GDP-L-fucose synthase immunodominant (red) and myelin (blue) peptides recognized by each CIS/MS patient. Solid colors are GDP-L-fucose synthase and myelin peptides showing significant correlation between them. P values for Fisher's exact tests with Bonferroni-Holm correction are shown.

Figure 6. Recognition of bacterial GDP-L-fucose synthase peptides by CSF-infiltrating $CD4^+$ T cells from CIS/MS patients. Proliferative responses expressed as stimulation indexes (SI) of CSF-infiltrating $CD4^+$ T cells (single round of PHA expansion) to eight bacterial GDP-L-fucose synthase peptides, sharing with the human homologous peptide at least six of the 15 amino acids (blue), presented by autologous PBMCs. Each dot represents one well and median SIs are shown as solid lines. Positive peptides (black wells and red line) are peptides with median of all SIs > 2 (dotted red line).

Table 1. GDP-L-fucose synthase transcripts and peptides identified in brain tissue.

		Transcriptome						Proteome (PSM[3])					Distinct	Protein
	Gene	RPKM[1]			UniProt			MS		Non-MS			peptides	coverage
Protein	ID	LI[2]	LII	LIII	ID	Peptide sequence	Residues	WM	GM	WM	GM	Total	#	%
GDP-L-fucose synthase	**TSTA3**	**2.17**	**2.02**	**2.67**	**Q13630**	ILVTGGSGLVGK	10 - 21	12	12	12	12	48	**17**	**56.0**
						VVADGAGLPGEDWVFVSSK	26 - 44	12	12	12	12	48		
						DADLTDTAQTR	45 - 55	12	12	12	12	48		
						VQPTHVIHLAAMVGGLFR	61 - 78	-	9	9	9	27		
						YNLDFWR	82 - 88	12	12	12	12	48		
						YNLDFWRK	82 - 89	-	-	-	1	1		
						NVHMNDNVLHSAFEVGAR	90 - 107	-	13	13	13	39		
						NVHMNDNVLHSAFEVGARK	90 - 108	-	-	-	3	3		
						VVSCLSTCIFPDK	109 - 121	-	-	-	3	3		
						MIDVQNR	149 - 155	-	2	-	2	4		
						RMIDVQNR	148 - 155	-	-	2	2	4		
						SSGSALTVWGTGNPR	200 - 214	3	-	-	-	3		
						SSGSALTVWGTGNPRR	200 - 215	-	-	1	-	1		
						TTYPIDETMIHNGPPHNSNFGYSYAK	222 - 247	-	-	3	-	3		
						EYNEVEPIILSVGEEDEVSIK	233 - 253	-	3	-	-	3		
						TYLPDFR	291 - 297	12	12	12	12	48		
						LRTYLPDFR	289 - 297	-	-	-	2	2		
								63	**87**	**88**	**95**	**333**		
Myelin basic protein	MBP	37.20	28.97	59.21	P02686			993	871	985	865	3714	80	79.6
Myelin proteolipid protein	PLP1	458.31	341.43	431.91	P60201			148	153	129	157	587	13	30.6
Myelin-oligodendrocyte glycoprotein	MOG	-	-	-	Q16653			216	199	222	216	853	28	49.8
Myelin-associated glycoprotein	MAG	16.29	10.83	26.84	P20916			243	232	221	243	939	34	36.9
Myelin-associated oligodendrocyte basic protein	MOBP	14.48	11.16	19.82	Q13875			20	12	27	14	73	6	26.2
Oligodendrocyte myelin glycoprotein	OMG	5.21	5.07	3.26	P23515			144	155	136	155	590	13	28.8
2',3'-cyclic-nucleotide 3'-phosphodiesterase	CNP	-	-	-	P09543			1168	985	1157	1060	4370	112	96.4

[1] RPKM, reads per kilobase of exon model per million mapped reads. [2] LI and LIII, active lesions in which TCC21.1 was clonally expanded. LII, inactive lesion in which TCC21.1 was not idenfied. [3] PSM, peptide spectrum matches. Proteome data correspond to white matter (WM) and grey matter (GM) from multiple sclerosis patients (MS, n=15) and non-MS controls (Non-MS, n=9). In bold are GDP-L-fucose synthase values.

Table 2. Demographical and clinical characteristics of CIS/MS patients and HLA-DR –DQ typing.

Patient				IgG	CSF	HLA											
ID	Disease	Sex	Age	Index	# cells/uL	DRB1*	DRB1*	DRB3*	DRB3*	DRB4*	DRB4*	DRB5*	DRB5*	DQA1*	DQA1*	DQB1*	DQB1*
UNRESPONDERS																	
66JO	RRMS	F	38	2.89	8	15:01	15:01					01:01	01:01	01:02	01:02	06:02	06:02
103HR	CIS	M	37	0.68	9	15:01	15:01					01:01	01:01	01:02	01:02	06:02	06:02
0204AM	RRMS	F	38	1.04	8	15:01	15:01					01:01	01:01	01:02	01:02	06:02	06:02
0247PE	SPMS	F	39	1.5	3	15:01	07:01			01:03		01:01		01:02	02:01	06:02	03:03
0381MA	SPMS	F	45	0.5	3	15:01	04:01			01:01		01:01		01:02	03:XX	06:02	03:02
0702AN	RRMS	M	45	0.73	5	15:01	01:03					01:01		01:02	05:01	03:01	06:02
0740RA	CIS	F	35	0.5	3	04:01	07:01			01:01	01:01			02:01	03:01	02:01	03:01
0936MA	RRMS	F	31	0.66	2	15:01	15:01					01:01	01:01	01:02	01:02	06:02	06:02
0973JO	RRMS	M	22	0.51	18	15:01	04:02			01:01		01:01		01:02	03:01	03:02	06:02
1125PA	RRMS	M	41	0.63	6	04:02	14:54		**02:02**	01:01				01:01	03:01	03:02	05:03
1292DI	RRMS	F	27	1.28	10	15:01	16:01					01:01	02:02	01:02	01:02	05:02	06:02
1300EV	RRMS	F	37	0.57	2	03:01	08:01		**02:02**					04:01	05:01	02:01	04:02
0897UR	RRMS	F	34	1.97	7	15:01	08:01					01:01		01:02	04:01	04:02	06:02
0127RO	CIS	M	30	1.38	27	15:01	08:01					01:01		01:02	04:01	04:02	06:02
1290JA	SPMS	M	27	0.5	8	15:01	04:04			01:01		01:01		03:02	06:02	01:02	03:XX
0800TH	RRMS	M	22	0.52	7	15:01	11:04		**02:02**			01:01		01:02	05:01	03:01	06:02
0830OL	CIS	F	36	0.56	4	15:01	11:01		**02:02**			01:01		01:02	05:01	03:01	06:02
0818MA	RRMS	M	37	0.67	3	03:01	04:07	01:01		01:01				03:01	05:01	02:01	03:01
1206CO	RRMS	F	37	1.37	5	15:01	04:01			01:01		01:01		01:02	03:01	03:02	06:02
MODERATE RESPONDERS																	
0780UR	RRMS	M	27	1.19	8	15:01	09:01			01:01		01:01		01:02	03:01	03:03	06:02
0866JE	RRMS	F	30	1.14	10	11:01	13:01	01:01	**02:02**					01:03	05:01	03:01	06:03
0748UR	RRMS	M	53	1.49	7	15:01	15:01					01:01	01:01	01:02	01:02	06:02	06:02
1346JU	RRMS	F	21	1.09	12	07:01	13:01	01:01		01:01				01:03	02:01	02:01	06:03
1081SA	CIS	F	49	0.71	23	01:01	08:03							01:01	06:01	03:01	05:01
0817JD	RRMS	M	28	0.53	6	15:01	03:01	01:01					01:01	01:02	05:01	02:01	06:02
HIGH RESPONDERS																	
1129RE	RRMS	M	32	0.92	3	07:01	11:03		**02:02**	01:03				02:01	05:01	03:01	03:03
1005ME	CIS	F	33	0.76	4	15:03	03:01		**02:02**			01:01		01:02	05:01	02:01	06:02
1173DI	RRMS	M	32	0.51	14	04:04	11:04		**02:02**	01:01				03:01	05:01	03:02	03:01
0718MA	RRMS	F	36	0.54	1	15:01	03:01		**02:02**			01:01		05:01	05:01	02:01	03:01
0816DA	CIS	F	52	1.14	12	15:01	13:01		**02:02**			01:01		01:03	01:02	06:02	06:03
0776JE	CIS	F	28	0.7	6	03:01	08:03		**02:02**					05:01	06:01	02:01	03:01

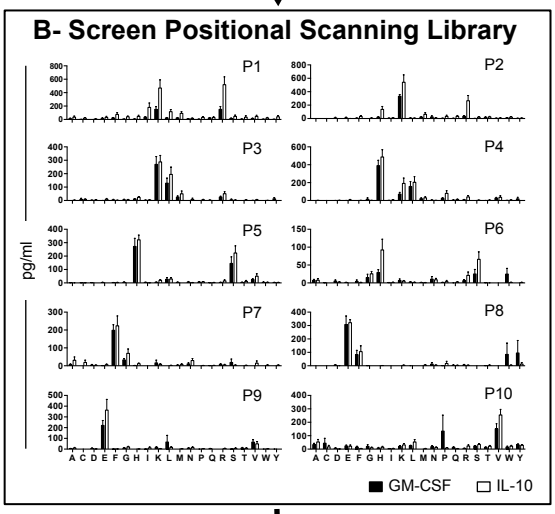

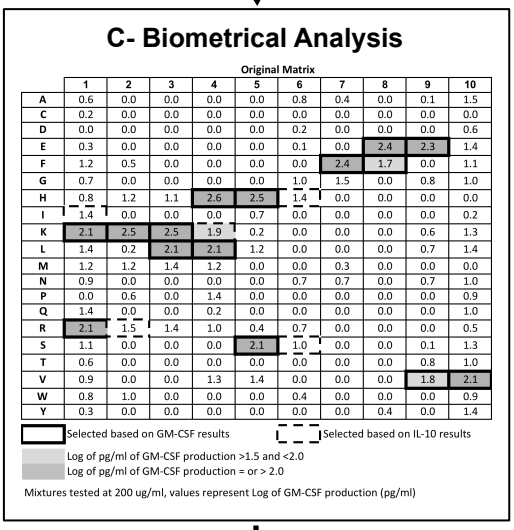

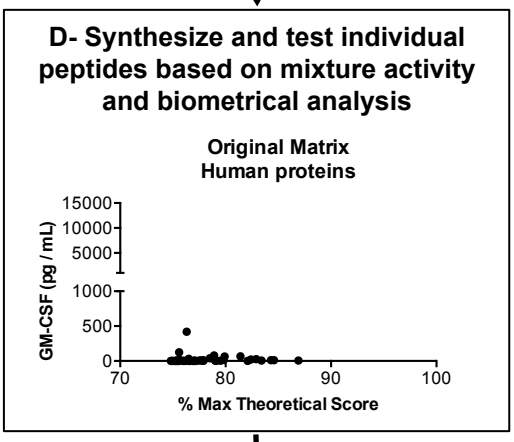

Individual activity insufficient to explain mixture activity

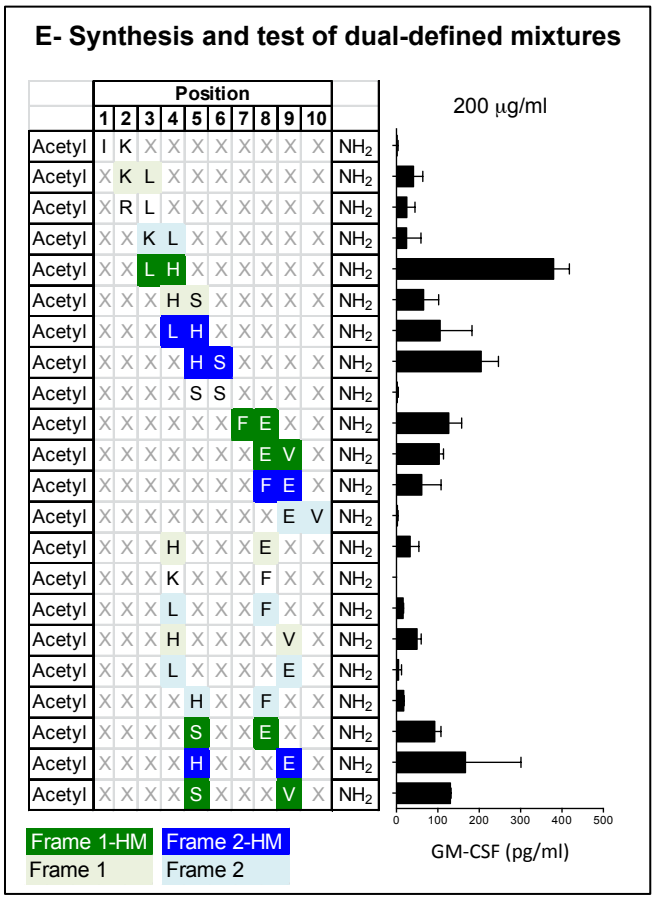

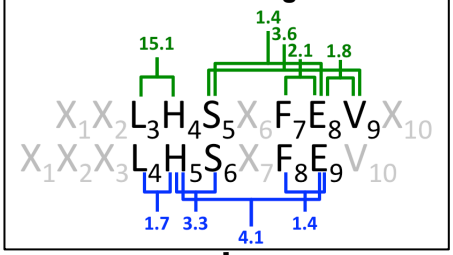

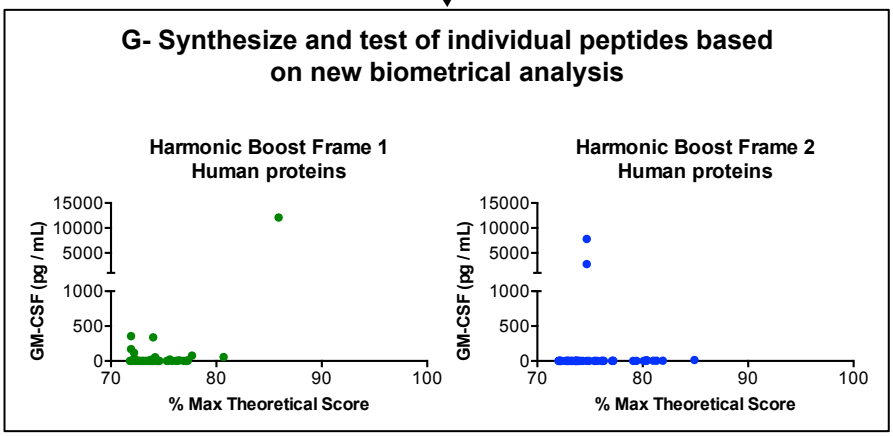

Individual activity now sufficient to explain mixture activity

Figure 1

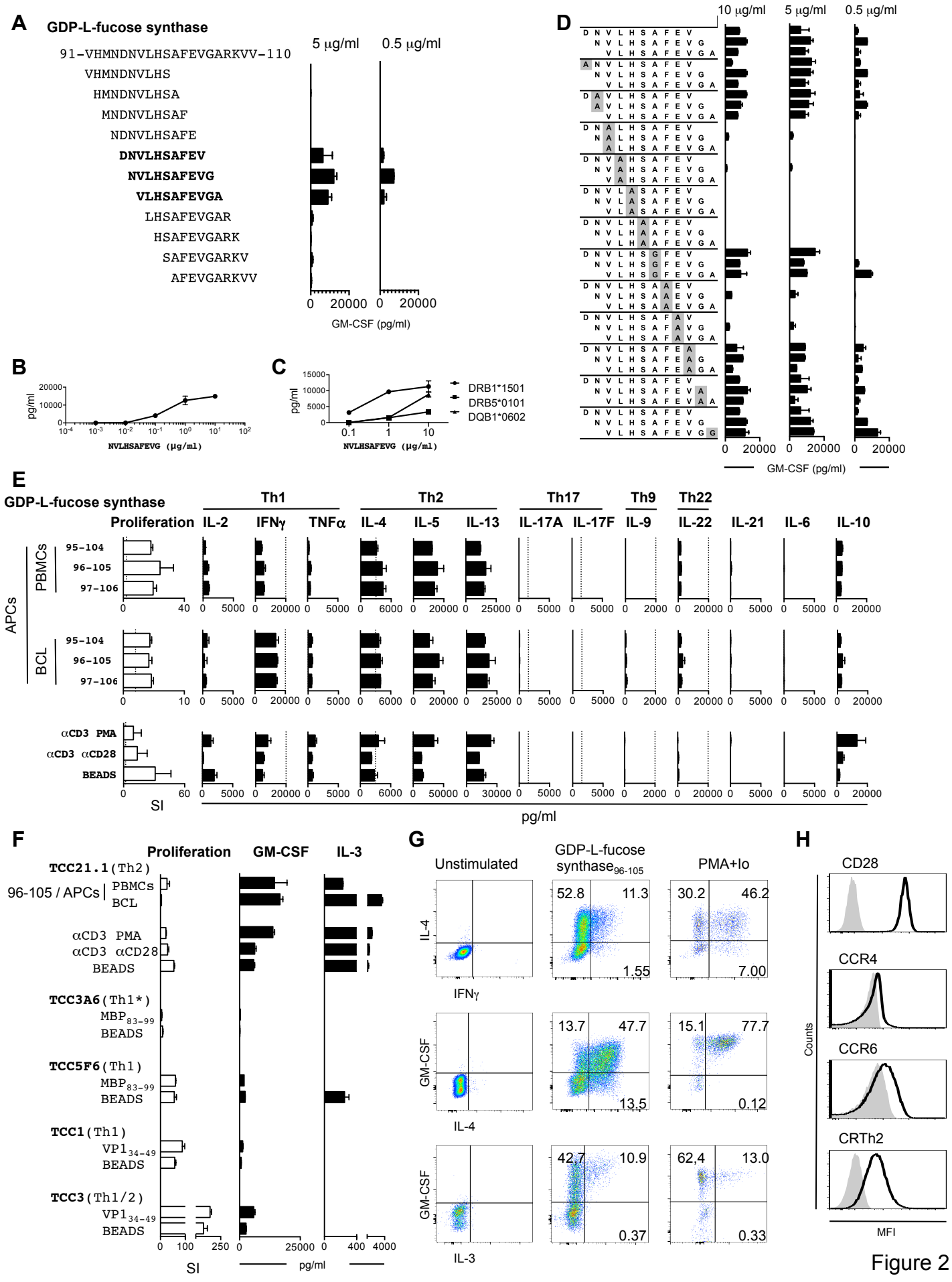
A
GDP-L-fucose synthase
91-VHMNDNVLHSAFEVGARKVV-110
VHMNDNVLHS
HMNDNVLHSA
MNDNVLHSAF
NDNVLHSAFE
DNVLHSAFEV
NVLHSAFEVG
VLHSAFEVGA
LHSAFEVGAR
HSAFEVGARK
SAFEVGARKV
AFEVGARKVV
5 μg/ml
0.5 μg/ml
GM-CSF (pg/ml)
B
pg/ml
NVLHSAFEVG (μg/ml)
C
DRB1*1501
DRB5*0101
DQB1*0602
D
10 μg/ml
5 μg/ml
0.5 μg/ml
GM-CSF (pg/ml)
E
GDP-L-fucose synthase
Th1
Th2
Th17
Th9
Th22
Proliferation
IL-2
IFNγ
TNFα
IL-4
IL-5
IL-13
IL-17A
IL-17F
IL-9
IL-22
IL-21
IL-6
IL-10
APCs
PBMCs
BCL
95-104
96-105
97-106
αCD3 PMA
αCD3 αCD28
BEADS
SI
pg/ml
F
Proliferation
GM-CSF
IL-3
TCC21.1(Th2)
96-105 / APCs
PBMCs
BCL
αCD3 PMA
αCD3 αCD28
BEADS
TCC3A6(Th1*)
MBP83-99
BEADS
TCC5F6(Th1)
MBP83-99
BEADS
TCC1(Th1)
VP134-49
BEADS
TCC3(Th1/2)
VP134-49
BEADS
SI
pg/ml
G
Unstimulated
GDP-L-fucose synthase96-105
PMA+Io
IL-4
IFNγ
GM-CSF
IL-4
GM-CSF
IL-3
52.8
11.3
1.55
30.2
46.2
7.00
13.7
47.7
13.5
15.1
77.7
0.12
42.7
10.9
0.37
62.4
13.0
0.33
H
CD28
CCR4
CCR6
CRTh2
Counts
MFI

Figure 2

Figure 3

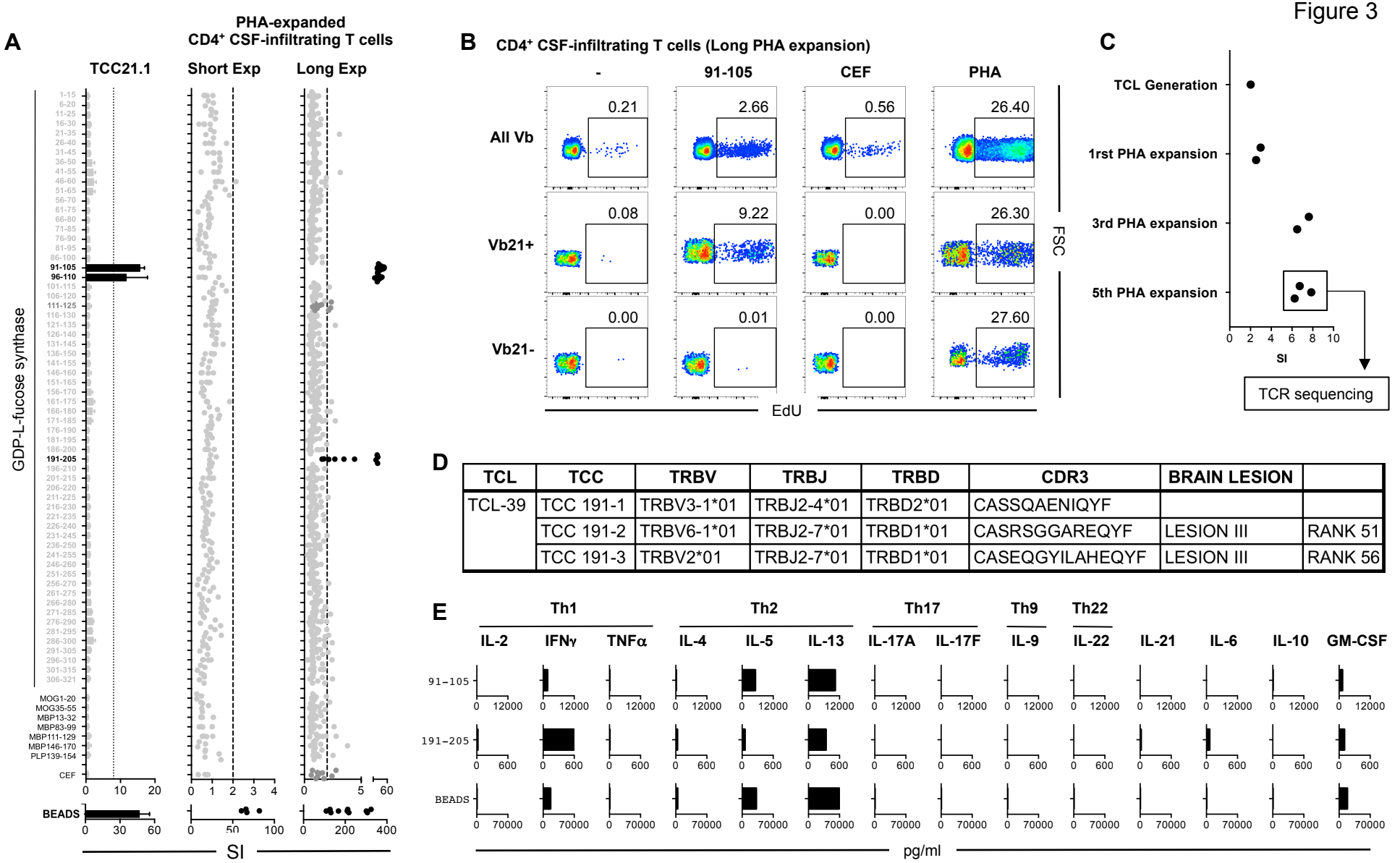

TCL	TCC	TRBV	TRBJ	TRBD	CDR3	BRAIN LESION	
TCL-39	TCC 191-1	TRBV3-1*01	TRBJ2-4*01	TRBD2*01	CASSQAENIQYF		
	TCC 191-2	TRBV6-1*01	TRBJ2-7*01	TRBD1*01	CASRSGGAREQYF	LESION III	RANK 51
	TCC 191-3	TRBV2*01	TRBJ2-7*01	TRBD1*01	CASEQGYILAHEQYF	LESION III	RANK 56

Figure 4

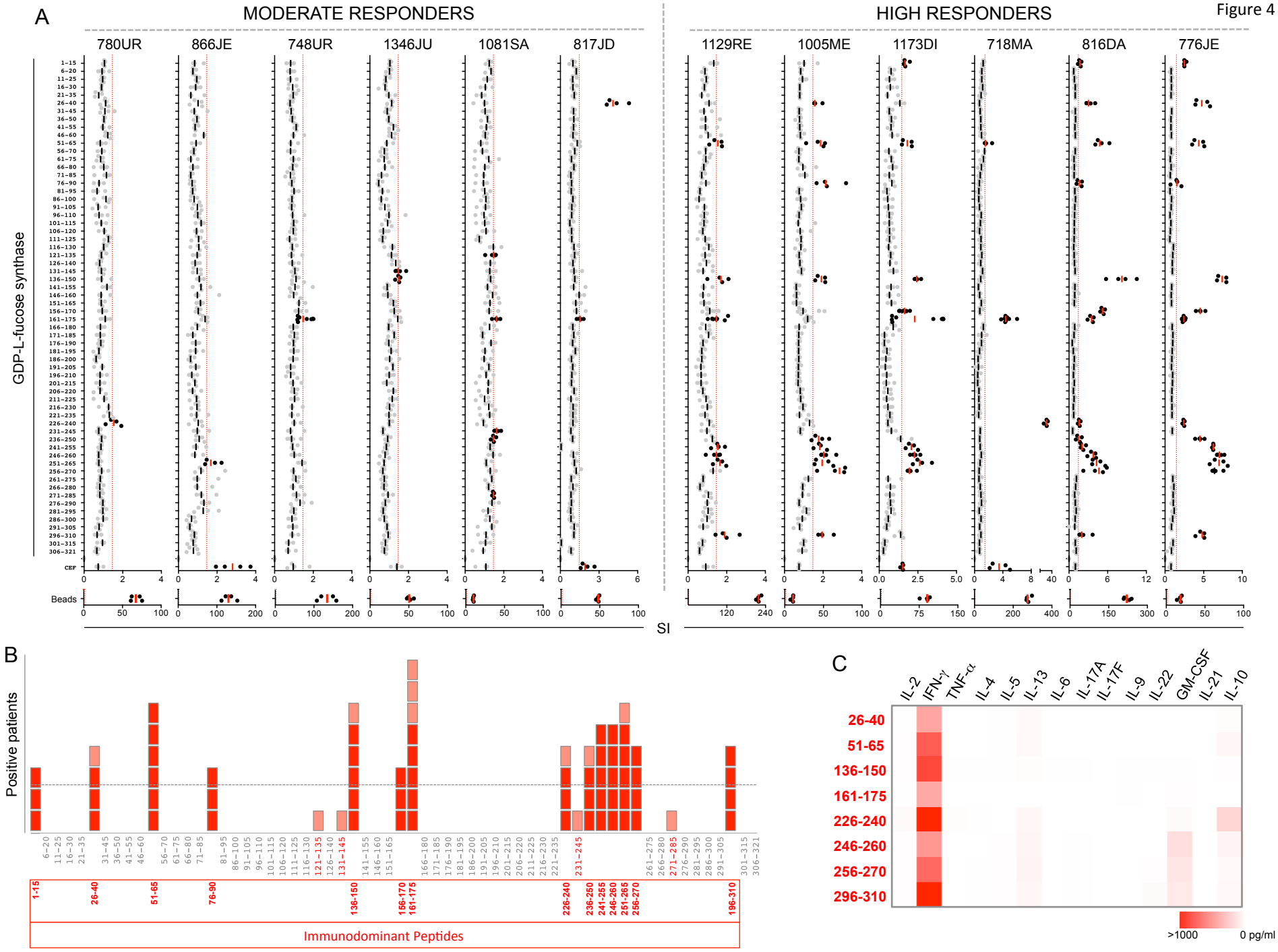
A
MODERATE RESPONDERS
HIGH RESPONDERS
780UR
866JE
748UR
1346JU
1081SA
817JD
1129RE
1005ME
1173DI
718MA
816DA
776JE
GDP-L-fucose synthase
CEF
Beads
SI
B
Positive patients
Immunodominant Peptides
1-15
26-40
51-65
76-90
136-150
156-170
161-175
226-240
236-250
241-255
246-260
251-265
256-270
196-310
C
IL-2
IFN-γ
TNF-α
IL-4
IL-5
IL-13
IL-6
IL-17A
IL-17F
IL-9
IL-22
GM-CSF
IL-21
IL-10
26-40
51-65
136-150
161-175
226-240
246-260
256-270
296-310
>1000
0 pg/ml

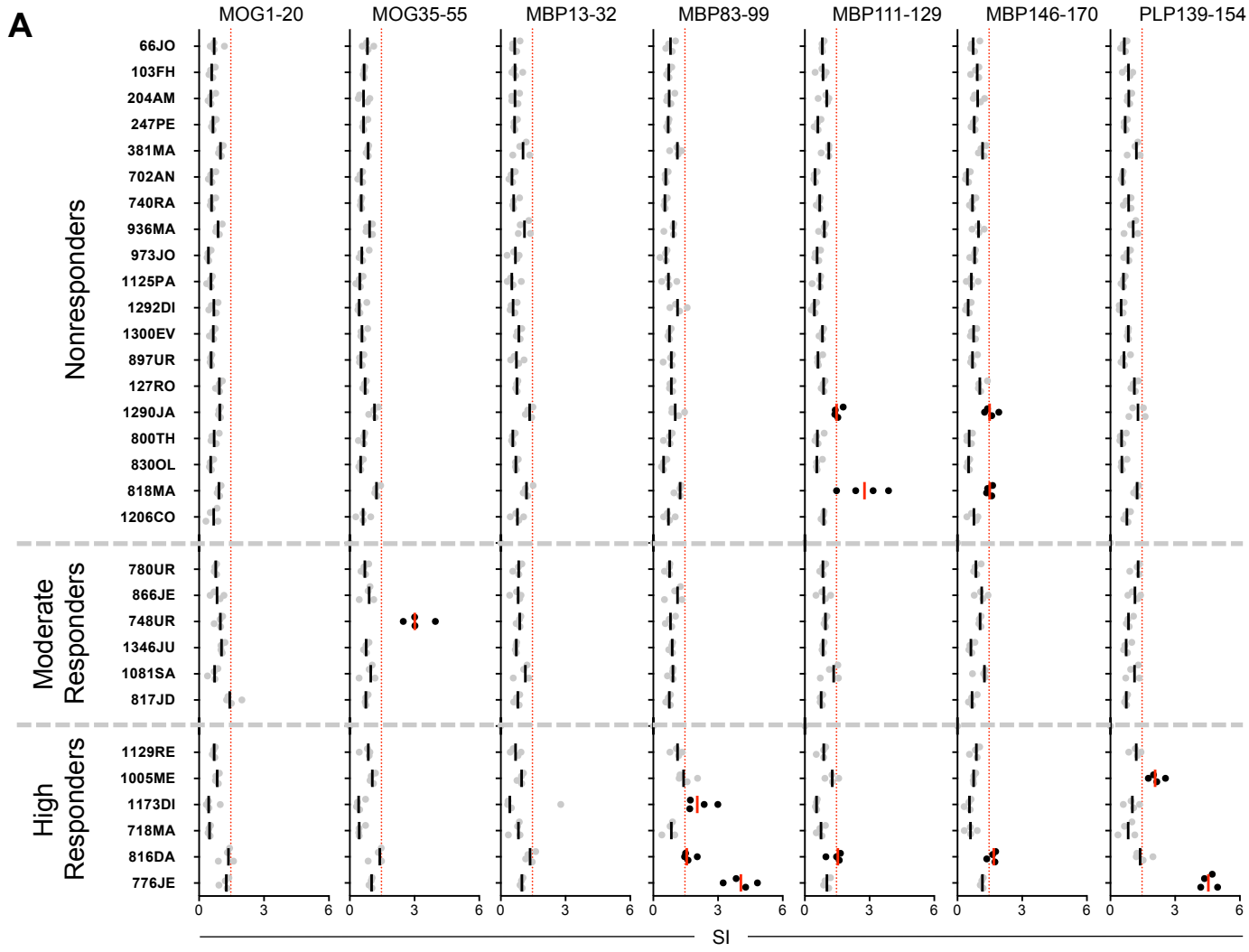

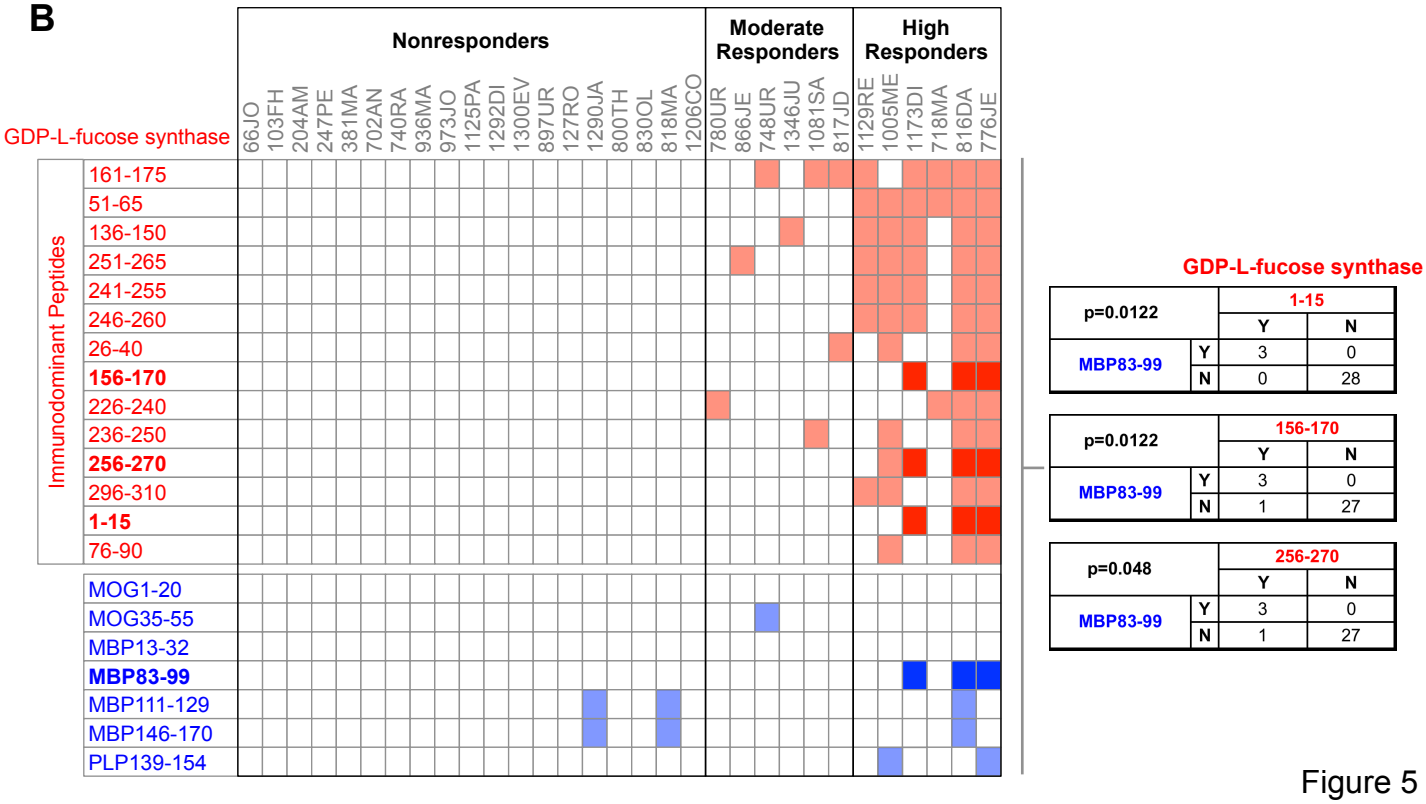

GDP-L-fucose synthase

p=0.0122		1-15	
		Y	N
MBP83-99	Y	3	0
	N	0	28

p=0.0122		156-170	
		Y	N
MBP83-99	Y	3	0
	N	1	27

p=0.048		256-270	
		Y	N
MBP83-99	Y	3	0
	N	1	27

Figure 5

Figure 6

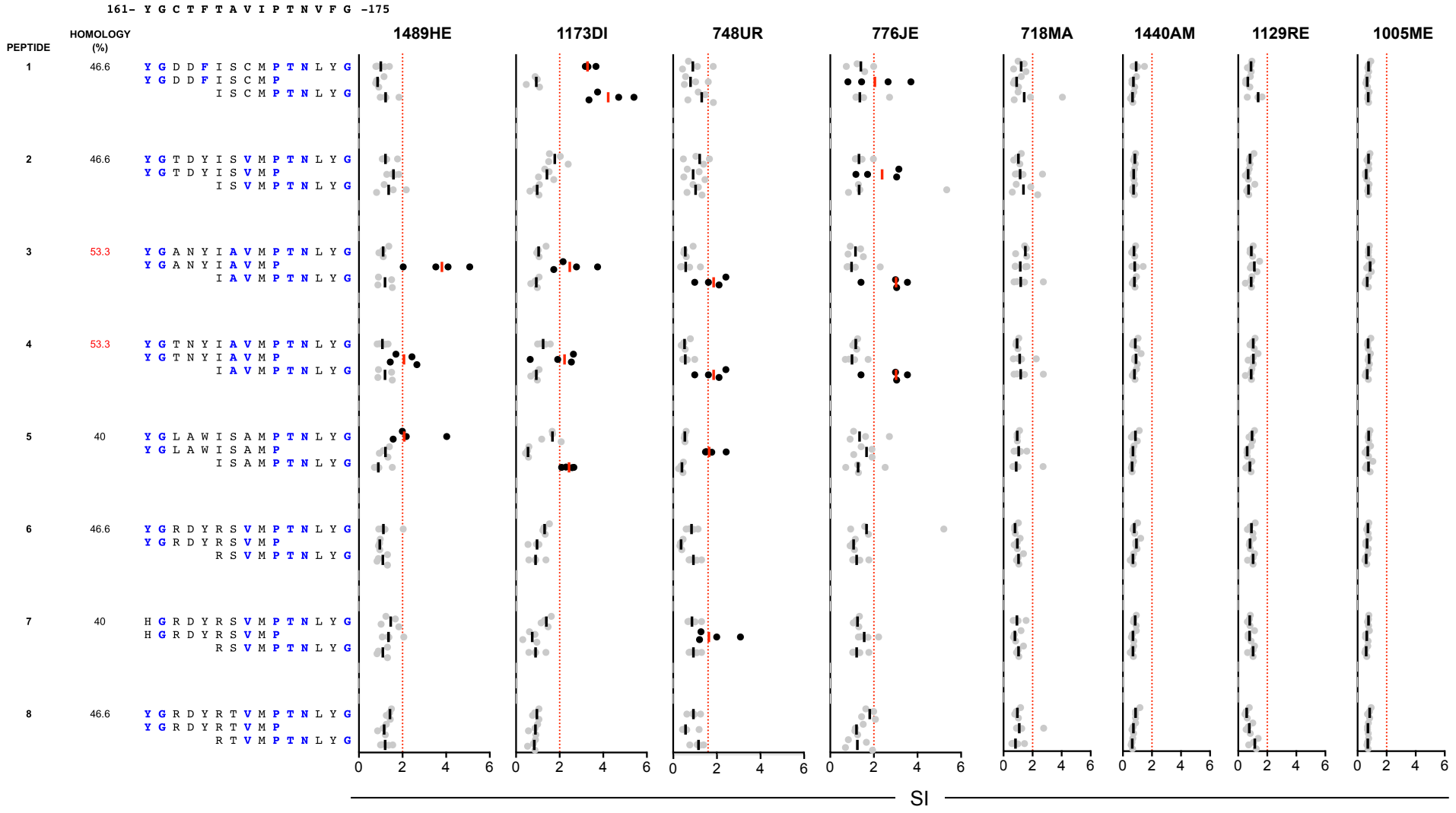
161- Y G C T F T A V I P T N V F G -175
PEPTIDE
HOMOLOGY (%)
1489HE
1173DI
748UR
776JE
718MA
1440AM
1129RE
1005ME
1 46.6 Y G D D F I S C M P T N L Y G
Y G D D F I S C M P
I S C M P T N L Y G
2 46.6 Y G T D Y I S V M P T N L Y G
Y G T D Y I S V M P
I S V M P T N L Y G
3 53.3 Y G A N Y I A V M P T N L Y G
Y G A N Y I A V M P
I A V M P T N L Y G
4 53.3 Y G T N Y I A V M P T N L Y G
Y G T N Y I A V M P
I A V M P T N L Y G
5 40 Y G L A W I S A M P T N L Y G
Y G L A W I S A M P
I S A M P T N L Y G
6 46.6 Y G R D Y R S V M P T N L Y G
Y G R D Y R S V M P
R S V M P T N L Y G
7 40 H G R D Y R S V M P T N L Y G
H G R D Y R S V M P
R S V M P T N L Y G
8 46.6 Y G R D Y R T V M P T N L Y G
Y G R D Y R T V M P
R T V M P T N L Y G
0 2 4 6
SI

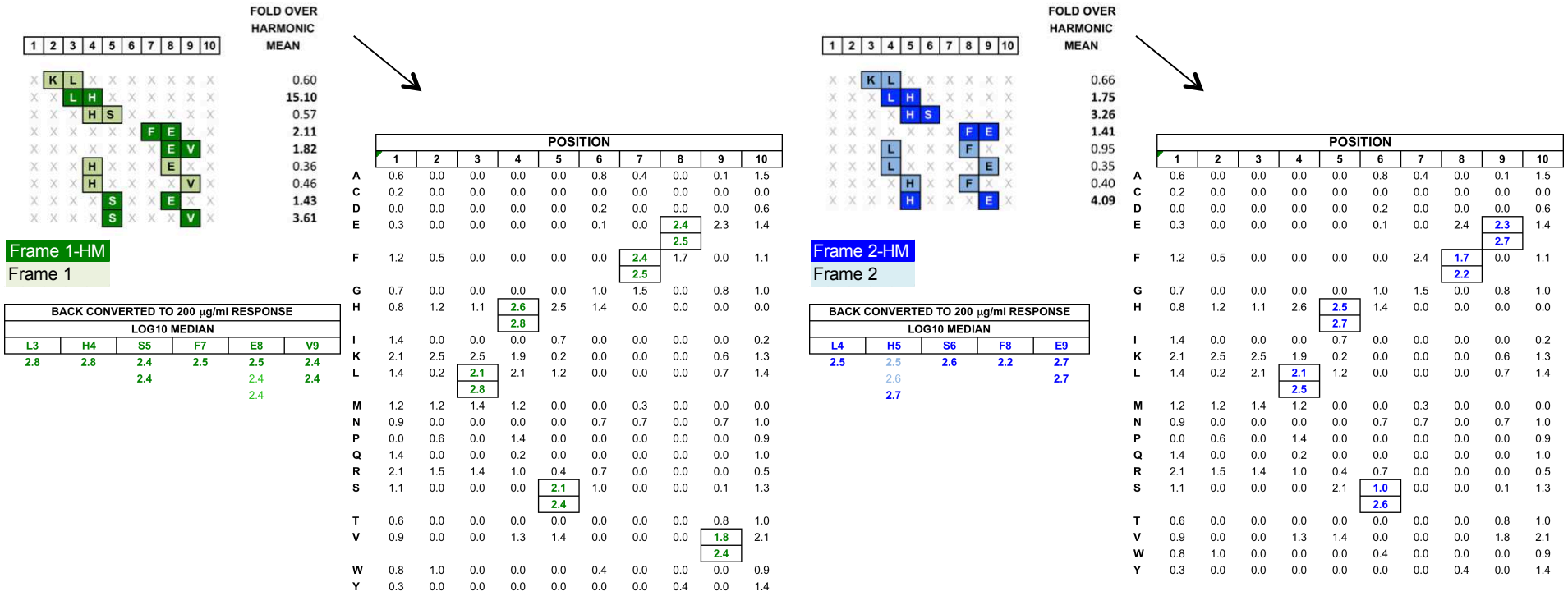

Figure S1. Integration of stimulatory response from testing dual-defined mixtures into the original scoring matrix using the harmonic mean model. In order to integrate the responses from testing dual-defined mixtures into the original scoring matrix using the harmonic mean model, we first retested single defined mixtures along with the dual defined mixtures and used them to normalize all activity values to a single scale using linear regression. Then, all GM-CSF (pg/ml) values for all single defined and dual defined at all doses were converted to *Approximate EC50* values using the formula:
Approximate EC50= [Tested Concentration] * (MaximumGMCSF / GMCSF-1)
Next, the harmonic mean was taken of each pair of single-defined *Approximate EC50* that had a corresponding dual defined mixture, and the value was compared to that of the dual defined mixture. For example, the *Approximate EC50* of the dual defined mixture with L defined in the fourth position and H defined in the fifth position was compared to the harmonic mean of the *Approximate EC50* values of the two corresponding single defined mixtures: the first with L defined in the fourth position, and the second with H defined in the fifth position. The harmonic mean model dictates that the dual defined mixture contains more active individual peptides than either of the single defined mixtures only if its activity is greater than the harmonic mean of the two single defined mixtures[27] (i.e., when the fold over the harmonic mean is greater than one). In total, five dual defined mixtures in Frame 1 (Green) and four in Frame 2 (Blue) exhibited this property (the dual-defined mixtures in darker colors and bolded Fold Over Harmonic Mean). All *Approximate EC50* values were converted back to GM-CSF (pg/ml) values at 200 ug/ml, and then those amino acids and position corresponding to the five dual defined mixtures in Frame 1 had added to them the log base 10 of the highest activity value among the dual defined mixtures with that position defined (Fig. S1, bold values in Log10 median table, as opposed to the lower numerical values in grey). For example, both the dual defined mixture with F defined in position seven and E in position eight, and the dual defined mixture with E in position eight and V in position nine, had activity values greater than their associated harmonic means. The value added to E in the eighth position of the matrix was the activity value for the dual defined mixture with F defined in position seven and E in position eight, because it was the higher of the two (2.5 versus 2.4). Frame 2 was treated the same way, creating the two “updated” matrices shown that were then used to score peptides in the standard Biometrical Analysis fashion.

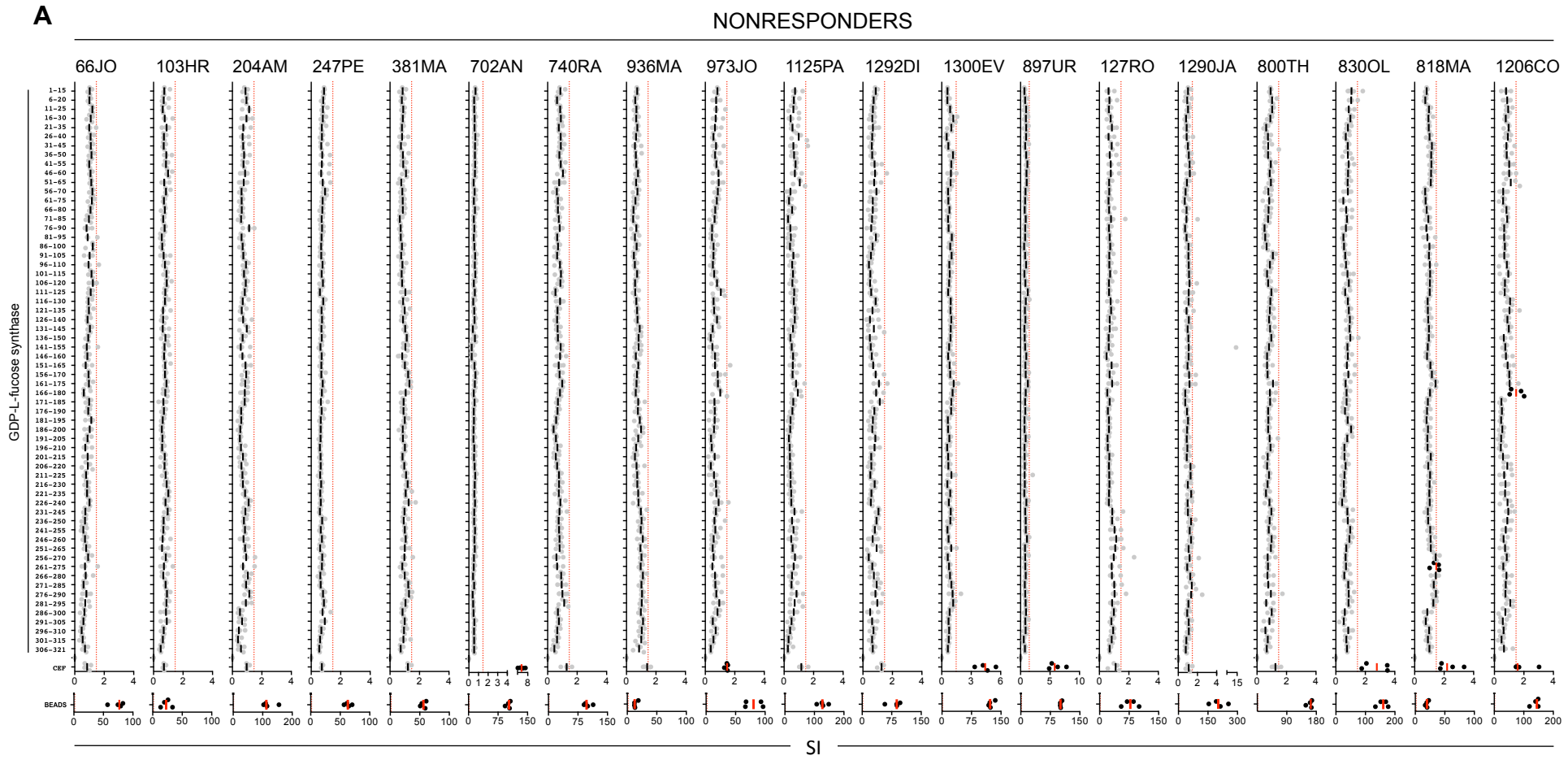

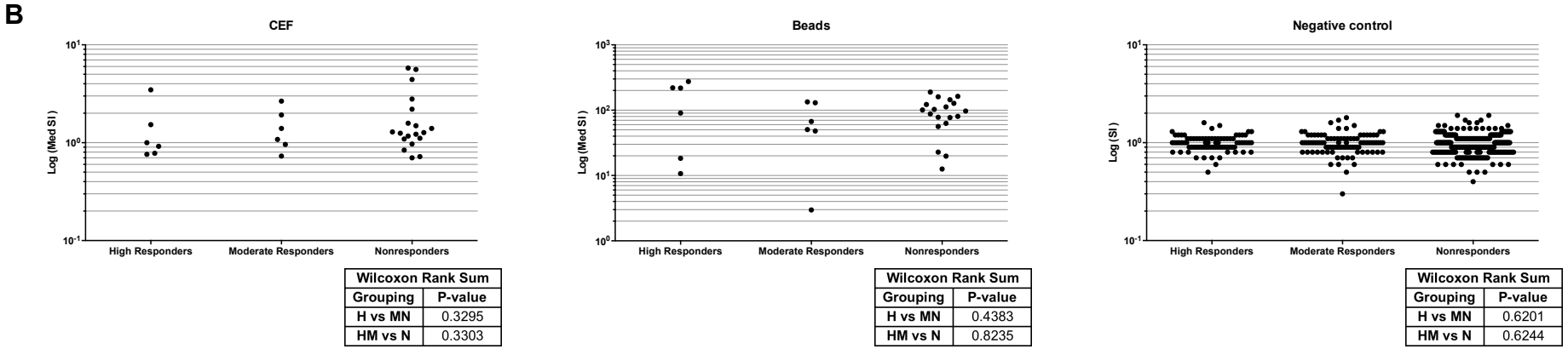

Wilcoxon Rank Sum	
Grouping	P-value
H vs MN	0.3295
HM vs N	0.3303

Wilcoxon Rank Sum	
Grouping	P-value
H vs MN	0.4383
HM vs N	0.8235

Wilcoxon Rank Sum	
Grouping	P-value
H vs MN	0.6201
HM vs N	0.6244

Figure S2

Figure S2. Response of CSF-infiltrating CD4$^+$ T cells. A. Response of CSF-infiltrating CD4$^+$ T cells from nonresponder CIS/MS patients to GDP-L-fucose synthase peptides. Proliferative responses expressed as stimulation indexes (SI) of CSF-infiltrating CD4$^+$ T cells (single round of PHA expansion) to GDP-L-fucose synthase and CEF peptides presented by autologous PBMCs as well as to control beads. Each dot represents one replicate well and median SIs are shown as solid lines. Positive peptides (black dots and red line) are peptides with median of SIs > 1.455 (dotted red line). All peptides have been tested in four replicate wells. **B.** Graphs comparing the proliferative responses of CSF-infiltrating CD4$^+$ T cells to CEF peptides, control beads and only medium (negative control) for the different responder groups. In the CEF peptide pool and control beads graphs, each dot represents the median SIs of four wells for one individual patient. In the negative control graph, each dot represents the SI of one individual well and it has been calculated as: cpm in one individual well without peptide / Median (all replicates cpm without peptide in the patient). Willcoxon statistical analysis and p values are shown for the three comparisons.

A

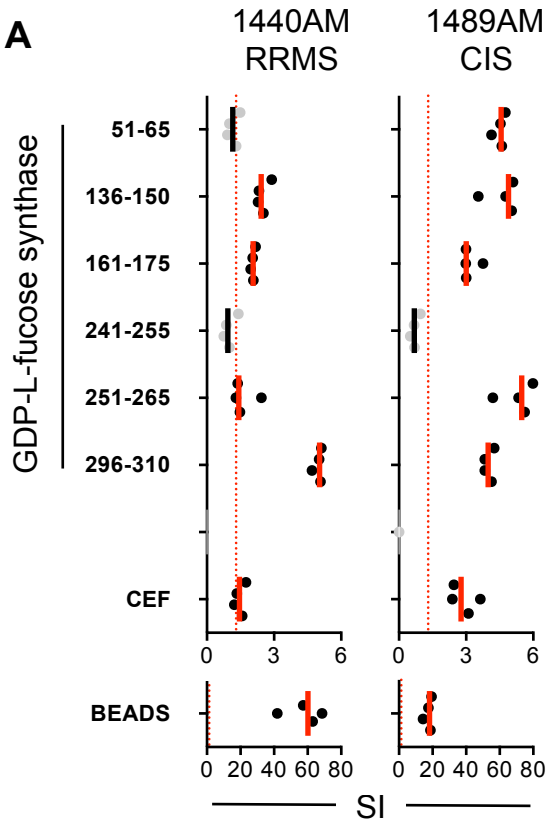

B

HLA CLASS II	1440AM	1489HE
DRB1*	08:01	10:01
DRB1*	13:02	12:01
DRB3*	03:01	**02:02**
DRB3*		
DRB4*		
DRB4*		
DRB5*		
DRB5*		
DQA1*	01:02	01:01
DQA1*	04:01	05:01
DQB1*	04:02	03:01
DQB1*	06:04	05:01

C

					PEPTIDE							
					1	2	3	4	5	6	7	8
				HOMOLOGY HUMAN %	46.6	46.6	53.3	53.3	40	46.6	40	46.6
PHYLUM	CLASS	ORDER	FAMILY	GENUS								
FIRMICUTES	Clostridia	Clostridiales	Lachnospiraceae	Eisenbergiella								
				Roseburia								
				Fusicatenibacter								
				Anaerostipes								
				Butyrivibrio								
				(Clostridium]								
				Blautia								
				Pseudobutyrivibrio								
				Oribacterium								
			Clostridiaceae	Clostridium								
			Ruminococcaceae	Gemmiger								
				Ruminococcus								
				Subdoligranulum								
			Peptococcaceae	Desulfosporosinus								
			Eubacteriaceae	Eubacterium								
	Bacilli	Lactobacillales	Enterococcaceae	Enterococcus								
			Lactobacillaceae	Lactobacillus								
	Negativicutes	Selenomonadales	Selenomonadaceae	Anaerovibrio								
				Selenomonas								
BACTEROIDETES	Bacteroidia	Bacteroidales	Prevotellaceae	Prevotella								
				Alloprevotella								
				Prevotellamassilia								
			Porphyromonadaceae	Gabonia								
				Coprobacter								
				Parabacteroides								
			Bacteroidaceae	Bacteroides								
				Mediterranea								
			Rikenellaceae	Alistipes								
ACTINOBACTERIA	Actinobacteria	Corynebacteriales	Mycobacteriaceae	Mycobacterium								
		Micrococcales	Microbacteriaceae	Leifsonia								
PROTEOBACTERIA	Gammaproteobacteria	Enterobacterales	Enterobacteriaceae	Escherichia								
				Salmonella								
				Shigella								
				Atlantibacter								
				Leclercia								
			Morganellaceae	Photorhabdus								
		Pseudomonadales	Pseudomonadaceae	Pseudomonas								
			Moraxellaceae	Acinetobacter								
		Chromatiales	Ectothiorhodospiraceae	Nitrococcus								
				Thioalkalivibrio								
		Aeromonadales	Aeromonadaceae	Aeromonas								
		Alteromonadales	Alteromonadaceae	Alteromonas								
				Marinobacter								
			Pseudoalteromonadaceae	Pseudoalteromonas								
			Colwelliaceae	Colwellia								
			Psychromonadaceae	Psychromonas								
			Shewanellaceae	Shewanella								
		Methylococcales	Methylococcaceae	Methylobacter								
				Methylomicrobium								
		Cellvibrionales	Microbulbiferaceae	Microbulbifer								
			Cellvibrionaceae	Teredinibacter								
			Halieaceae	Pseudohaliea								
		Vibrionales	Vibrionaceae	Photobacterium								
				Vibrio								
		Thiotrichales	Piscirickettsiaceae	Thiomicrospira								
		Oceanospirillales	Halomonadaceae	Halomonas								
	Betaproteobacteria	Rhodocyclales	Rhodocyclaceae	Azonexus								
		Burkholderiales	Comamonadaceae	Candidatus								
				Comamonas								
			Alcaligenaceae	Bordetella								
		Neisseriales	Chromobacteriaceae	Pseudogulbenkiania								
	Alphaproteobacteria	Rhodobacterales	Rhodobacteraceae	Phaeobacter								
				Tropicibacter								
				Loktanella								
				Nautella								
				Rubellimicrobium								
				Salipiger								
				Thalassobium								
			Hyphomonadaceae	Hyphomonas								
		Rhodospirillales	Rhodospirillaceae	Thalassospira								
VERRUCOMICROBIA	Verrucomicrobiae	Verrucomicrobiales	Akkermansiaceae	Akkermansia								

Figure S3. **New patients and phylogeny of bacterial species sharing GDP-L-fucose synthase peptides. A.** Proliferative responses expressed as stimulation indexes (SI) of CSF-infiltrating $CD4^+$ T cells (single round of PHA expansion) to GDP-L-fucose synthase and CEF peptides presented by autologous PBMCs as well as to control beads. Each dot represents one well, and median SIs are shown as solid lines. Positive peptides (black dots and red line) are peptides with median of all SIs > 1.455 (dotted red line). **B.** HLA class II typing. **C.** Phylogeny of bacterial species sharing GDP-L-fucose synthase peptides. In black are represented stimulatory peptides in four patients, in dark grey in one to three patients and in light grey non stimulatory. Genera common in gut microbiota are shown in red.

Table S1. Summary of human decapeptides predicted with the biometrical approached, synthesized and tested for stimulatory capacity

PEPTIDES FROM HUMAN PROTEINS														Peptides tested at 5 mg/ml
Matrix	Uniprot Database	Rank	Score	PercentMax	Matrix	Uniprot Database	Rank	Database	Rank	Score	PercentMax	10mer	Protein	Mean GM-CSF (pg/ml)
Original	**Human**	1	19.79	86.9%	HM Boost Frame 2	Human	4	Brain Lesions	4	27.14	81.0%	RKKLHKFEET	Q96PE3|INP4A_HUMAN Type I inositol 3,4-bisphosphate 4-phosphatase OS=Homo sapiens GN=INPP4A PE=1 SV=1	3
Original	**Human**	2	19.27	84.6%	HM Boost Frame 2	Human	5	Brain Lesions	5	26.96	80.4%	LKKLHDFEEQ	Q9BXB4|TRPM6_HUMAN Transient receptor potential cation channel subfamily M member 6 OS=Homo sapiens GN=TRPM6 PE=1 SV=2	9
Original	**Human**	3	19.21	84.3%	HM Boost Frame 2	Human	7	Brain Lesions	7	26.90	80.3%	QKKLHDFEEQ	Q96QT4|TRPM7_HUMAN Transient receptor potential cation channel subfamily M member 7 OS=Homo sapiens GN=TRPM7 PE=1 SV=1	9
Original	**Human**	4	18.99	83.4%	HM Boost Frame 2	Human	8	Brain Lesions	8	26.90	80.3%	QKKLSSGEEK	Q15858|SCN9A_HUMAN Sodium channel protein type 9 subunit alpha OS=Homo sapiens GN=SCN9A PE=1 SV=3	4
Original	**Human**	5	18.89	82.9%	HM Boost Frame 1	Human	45			26.35	72.1%	RKLLHRFETE	O15327|INP4B_HUMAN Type II inositol 3,4-bisphosphate 4-phosphatase OS=Homo sapiens GN=INPP4B PE=2 SV=4	14
Original	**Human**	6	18.78	82.4%	HM Boost Frame 2	Human	1	Brain Lesions	1	28.47	84.9%	RRKLHSFYEV	Q5VST9|OBSCN_HUMAN Obscurin OS=Homo sapiens GN=OBSCN PE=1 SV=3	13
Original	**Human**	7	18.71	82.1%								KKKKVAGEEE	I3L1I4|I3L1I4_HUMAN Chromodomain-helicase-DNA-binding protein 3 (Fragment) OS=Homo sapiens GN=CHD3 PE=4 SV=1	0
Original	**Human**	8	18.54	81.4%								LKKVHDFEEQ	Q9HCF6|TRPM3_HUMAN Transient receptor potential cation channel subfamily M member 3 OS=Homo sapiens GN=TRPM3 PE=2 SV=4	49
Original	**Human**	9	18.19	79.9%								KKLLLHVEEV	Q8N8V2|GBP7_HUMAN Guanylate-binding protein 7 OS=Homo sapiens GN=GBP7 PE=2 SV=2	64
Original	**Human**	10	18.18	79.8%	HM Boost Frame 1	Human	4	Brain Lesions	4	28.28	77.3%	QKKHSGFEDE	P10645|CMGA_HUMAN Chromogranin-A OS=Homo sapiens GN=CHGA PE=1 SV=7	9
Original	**Human**	11	18.12	79.5%								LKKKSHMEEK	Q49MG5|MAP9_HUMAN Microtubule-associated protein 9 OS=Homo sapiens GN=MAP9 PE=1 SV=3	6
Original	**Human**	12	18.01	79.1%								KKKKSALFEV	Q9GZU0|CF062_HUMAN Uncharacterized protein C6orf62 OS=Homo sapiens GN=C6orf62 PE=2 SV=1	4
Original	**Human**	13	18.01	79.1%								RKKKSALFEV	Q9GZU0-2|CF062_HUMAN Isoform 2 of Uncharacterized protein C6orf62 OS=Homo sapiens GN=C6orf62	0
Original	**Human**	14	18.00	79.0%								IWKKLSFEEV	Q96JI7|SPTCS_HUMAN Spatacsin OS=Homo sapiens GN=SPG11 PE=1 SV=3	8
Original	**Human**	15	18.00	79.0%	HM Boost Frame 2	Human	13	Brain Lesions	13	25.87	77.2%	LKRLHEFEEQ	Q724N2|TRPM1_HUMAN Transient receptor potential cation channel subfamily M member 1 OS=Homo sapiens GN=TRPM1 PE=1 SV=2	6
Original	**Human**	16	17.97	78.9%	HM Boost Frame 1	Human	3	Brain Lesions	3	28.40	77.7%	LKLHSRFYEL	O75838|CIB2_HUMAN Calcium and integrin-binding family member 2 OS=Homo sapiens GN=CIB2 PE=1 SV=1	55
Original	**Human**	17	17.89	78.5%								QKKLHKFELA	O15514|RPB4_HUMAN DNA-directed RNA polymerase II subunit RPB4 OS=Homo sapiens GN=POLR2D PE=1 SV=1	27
Original	**Human**	18	17.74	77.9%								LGLHHHGEEA	Q9BWH6|RPAP1_HUMAN RNA polymerase II-associated protein 1 OS=Homo sapiens GN=RPAP1 PE=1 SV=3	7
Original	**Human**	19	17.74	77.9%	HM Boost Frame 1	Human	12	Brain Lesions	11	27.63	75.6%	RRLHLHFERV	Q6UXD5|SE6L2_HUMAN Seizure 6-like protein 2 OS=Homo sapiens GN=SEZ6L2 PE=1 SV=2	3
Original	**Human**	20	17.72	77.8%	HM Boost Frame 2	Human	3	Brain Lesions	3	27.26	81.3%	RRLLSSGFEE	O60518|RNBP6_HUMAN Ran-binding protein 6 OS=Homo sapiens GN=RANBP6 PE=1 SV=2	3
Original	**Human**	21	17.70	77.7%								KKKKHSTEGV	P51003|PAPOA_HUMAN Poly(A) polymerase alpha OS=Homo sapiens GN=PAPOLA PE=1 SV=4	6
Original	**Human**	22	17.66	77.5%	HM Boost Frame 1	Human	9	Brain Lesions	8	27.89	76.3%	QRLHLHFEKV	Q53EL9|SEZ6_HUMAN Seizure protein 6 homolog OS=Homo sapiens GN=SEZ6 PE=1 SV=2	5
Original	**Human**	23	17.58	77.2%								SKKHHRGEVC	Q8N7U6|EFHB_HUMAN EF-hand domain-containing family member B OS=Homo sapiens GN=EFHB PE=2 SV=4	0
Original	**Human**	24	17.56	77.1%	HM Boost Frame 2	Human	2	Brain Lesions	2	27.46	81.9%	RKLLSSGFEI	Q8N8A2|ANR44_HUMAN Serine/threonine-protein phosphatase 6 regulatory ankyrin repeat subunit B OS=Homo sapiens GN=ANKRD44 PE=1 SV=3	5
Original	**Human**	25	17.54	77.0%								IKKKHLFENS	Q8N8U5|ATAD1_HUMAN ATPase family AAA domain-containing protein 1 OS=Homo sapiens GN=ATAD1 PE=1 SV=1	0
Original	**Human**	26	17.53	77.0%	HM Boost Frame 2	Human	31	Brain Lesions	28	24.72	73.7%	QKKLHHFFIG	Q8IWB1|IPRI_HUMAN Inositol 1,4,5-trisphosphate receptor-interacting protein OS=Homo sapiens GN=ITPRIP PE=1 SV=1	0
Original	**Human**	27	17.52	76.9%								AKLHHGFGEA	Q9P2P6|STAR9_HUMAN StAR-related lipid transfer protein 9 OS=Homo sapiens GN=STARD9 PE=1 SV=3	1
Original	**Human**	28	17.46	76.6%								LKHVSHGEEL	Q9NZ53|PDXL2_HUMAN Podocalyxin-like protein 2 OS=Homo sapiens GN=PODXL2 PE=1 SV=1	0
Original	**Human**	29	17.46	76.6%								QKKIHKFEEA	Q8N8E3|CE112_HUMAN Centrosomal protein of 112 kDa OS=Homo sapiens GN=CEP112 PE=1 SV=2	0
Original	**Human**	30	17.45	76.6%								LHKKHYFEVL	Q96JI7|SPTCS_HUMAN Spatacsin OS=Homo sapiens GN=SPG11 PE=1 SV=3	1
Original	**Human**	31	17.42	76.5%								LKKHLSGEEH	Q96EU6|RRP36_HUMAN Ribosomal RNA processing protein 36 homolog OS=Homo sapiens GN=RRP36 PE=1 SV=1	24
Original	**Human**	32	17.40	76.4%	HM Boost Frame 1	Human	8	Brain Lesions	7	27.99	76.5%	QKLHLHFERL	Q9BYH1|SE6L1_HUMAN Seizure 6-like protein OS=Homo sapiens GN=SEZ6L PE=1 SV=1	10
Original	**Human**	33	17.37	76.3%	HM Boost Frame 1	Human	24	Brain Lesions	18	27.05	74.0%	RKLKASFEVS	Q8TDX9|PK1L1_HUMAN Polycystic kidney disease protein 1-like 1 OS=Homo sapiens GN=PKD1L1 PE=1 SV=1	338
Original	**Human**	34	17.35	76.2%	HM Boost Frame 2	Human	25			25.03	74.7%	FSKLHTFEEV	Q96JB1|DYH8_HUMAN Dynein heavy chain 8, axonemal OS=Homo sapiens GN=DNAH8 PE=1 SV=2	0
Original	**Human**	35	17.32	76.0%								RKKLSLDEES	Q60296|TRAK2_HUMAN Trafficking kinesin-binding protein 2 OS=Homo sapiens GN=TRAK2 PE=1 SV=2	0
Original	**Human**	36	17.31	76.0%	HM Boost Frame 1	Human	17			27.23	74.5%	EKKVSSFEVF	Q9UHG0|DCDC2_HUMAN Doublecortin domain-containing protein 2 OS=Homo sapiens GN=DCDC2 PE=1 SV=2	0
Original	**Human**	37	17.24	75.7%	HM Boost Frame 1	Human	29	Brain Lesions	22	26.98	73.8%	RKLLSSDFPV	Q4LDE5|SVEP1_HUMAN Sushi, von Willebrand factor type A, EGF and pentraxin domain-containing protein 1 OS=Homo sapiens GN=SVEP1 PE=1 SV=3	7
Original	**Human**	38	17.23	75.6%								MKKKSLGEVL	O94827|PKHG5_HUMAN Pleckstrin homology domain-containing family G member 5 OS=Homo sapiens GN=PLEKHG5 PE=1 SV=3	124
Original	**Human**	39	17.23	75.6%								RKKLVEAEEL	O14578|CTRO_HUMAN Citron Rho-interacting kinase OS=Homo sapiens GN=CIT PE=1 SV=2	0
Original	**Human**	40	17.22	75.6%								RHKKSHTEEK	Q03923|ZNF85_HUMAN Zinc finger protein 85 OS=Homo sapiens GN=ZNF85 PE=2 SV=3	20
Original	**Human**	41	17.20	75.5%								IRKLSSGETV	Q70EL2|UBP45_HUMAN Ubiquitin carboxyl-terminal hydrolase 45 OS=Homo sapiens GN=USP45 PE=1 SV=3	7
Original	**Human**	42	17.20	75.5%								KEKMHHFTEE	Q6ZWH5|NEK10_HUMAN Serine/threonine-protein kinase Nek10 OS=Homo sapiens GN=NEK10 PE=2 SV=3	0
Original	**Human**	43	17.20	75.5%								KKRRHSFEHV	Q9NR48|ASH1L_HUMAN Histone-lysine N-methyltransferase ASH1L OS=Homo sapiens GN=ASH1L PE=1 SV=2	0
Original	**Human**	44	17.16	75.3%								QKRMDDFEEV	O60229|KALRN_HUMAN Kalirin OS=Homo sapiens GN=KALRN PE=1 SV=2	0
Original	**Human**	45	17.16	75.3%								QKRMEDFEEV	O75962|TRIO_HUMAN Triple functional domain protein OS=Homo sapiens GN=TRIO PE=1 SV=2	0
Original	**Human**	46	17.15	75.3%								RKKQAHFEEE	O95544|NADK_HUMAN NAD kinase OS=Homo sapiens GN=NADK PE=1 SV=1	0
Original	**Human**	47	17.13	75.2%	HM Boost Frame 2	Human	26	Brain Lesions	23	24.91	74.3%	QAKLSSFEET	Q5T880|CE162_HUMAN Centrosomal protein of 162 kDa OS=Homo sapiens GN=KIAA1009 PE=1 SV=2	0
Original	**Human**	48	17.08	75.0%								KKMLIDGEEV	Q6PP77|XKR2_HUMAN XK-related protein 2 OS=Homo sapiens GN=XKR2 PE=2 SV=2	0
Original	**Human**	49	17.07	74.9%								KKKLVRSEEN	Q8N157|AHI1_HUMAN Jouberin OS=Homo sapiens GN=AHI1 PE=1 SV=1	0
Original	**Human**	50	17.05	74.8%								KKKQVHFFVN	Q96JY4|CBPB2_HUMAN Carboxypeptidase B2 OS=Homo sapiens GN=CPB2 PE=1 SV=2	0
					HM Boost Frame 1	**Human**	1	**Brain Lesions**	1	31.42	85.9%	NVLHSAFEVG	Q13630|FCL_HUMAN GDP-L-fucose synthase OS=Homo sapiens GN=TSTA3 PE=1 SV=1	12,111
					HM Boost Frame 1	**Human**	2	**Brain Lesions**	2	29.53	80.7%	RKLHSFYEVK	Q5VST9|OBSCN_HUMAN Obscurin OS=Homo sapiens GN=OBSCN PE=1 SV=3	56
Original	Human	16	17.97	78.9%	**HM Boost Frame 1**	**Human**	3	**Brain Lesions**	3	28.40	77.7%	LKLHSRFYEL	O75838|CIB2_HUMAN Calcium and integrin-binding family member 2 OS=Homo sapiens GN=CIB2 PE=1 SV=1	55
Original	Human	10	18.18	79.8%	**HM Boost Frame 1**	**Human**	4	**Brain Lesions**	4	28.28	77.3%	QKKHSGFEDE	P10645|CMGA_HUMAN Chromogranin-A OS=Homo sapiens GN=CHGA PE=1 SV=7	9
					HM Boost Frame 1	**Human**	5	**Brain Lesions**	5	28.22	77.2%	LALHSVFEGL	Q9NY26|S39A1_HUMAN Zinc transporter ZIP1 OS=Homo sapiens GN=SLC39A1 PE=1 SV=1	0
					HM Boost Frame 1	**Human**	6			28.22	77.2%	RRLHSPPEVE	A8MT33|SYC1L_HUMAN Synaptonemal complex central element protein 1-like OS=Homo sapiens GN=SYCE1L PE=2 SV=3	0
					HM Boost Frame 1	**Human**	7	**Brain Lesions**	6	28.12	76.9%	LSLHRMFEVV	Q8WXF8|DEDD2_HUMAN DNA-binding death effector domain-containing protein 2 OS=Homo sapiens GN=DEDD2 PE=1 SV=1	0
Original	Human	32	17.40	76.4%	**HM Boost Frame 1**	**Human**	8	**Brain Lesions**	7	27.99	76.5%	QKLHLHFERL	Q9BYH1|SE6L1_HUMAN Seizure 6-like protein OS=Homo sapiens GN=SEZ6L PE=1 SV=1	10
Original	Human	22	17.66	77.5%	**HM Boost Frame 1**	**Human**	9	**Brain Lesions**	8	27.89	76.3%	QRLHLHFEKV	Q53EL9|SEZ6_HUMAN Seizure protein 6 homolog OS=Homo sapiens GN=SEZ6 PE=1 SV=2	5
					HM Boost Frame 1	**Human**	10	**Brain Lesions**	9	27.86	76.2%	LLLHSIFELN	H7C3K9|H7C3K9_HUMAN Melanophilin (Fragment) OS=Homo sapiens GN=MLPH PE=2 SV=1	0
					HM Boost Frame 1	**Human**	11	**Brain Lesions**	10	27.72	75.8%	NGLHSHSEVL	Q9HCH5|SYTL2_HUMAN Synaptotagmin-like protein 2 OS=Homo sapiens GN=SYTL2 PE=1 SV=3	0
Original	Human	19	17.74	77.9%	**HM Boost Frame 1**	**Human**	12	**Brain Lesions**	11	27.63	75.6%	RRLHLHFERV	Q6UXD5|SE6L2_HUMAN Seizure 6-like protein 2 OS=Homo sapiens GN=SEZ6L2 PE=1 SV=2	3
					HM Boost Frame 1	**Human**	13			27.59	75.4%	LRLHSPPEVT	Q9NZ20|PA2G3_HUMAN Group 3 secretory phospholipase A2 OS=Homo sapiens GN=PLA2G3 PE=1 SV=2	0
					HM Boost Frame 1	**Human**	14			27.55	75.3%	SHLHSLFRVL	Q8NGR2|OR116_HUMAN Olfactory receptor 1L6 OS=Homo sapiens GN=OR1L6 PE=2 SV=2	0
					HM Boost Frame 1	**Human**	15	**Brain Lesions**	12	27.27	74.6%	VELHSHSEVP	Q92551|IPGK1_HUMAN Inositol hexakisphosphate kinase 1 OS=Homo sapiens GN=IP6K1 PE=1 SV=3	0
					HM Boost Frame 1	**Human**	16			27.25	74.5%	GHLHSQLEVS	Q6ZTK2|YPO15_HUMAN Putative uncharacterized protein LOC400499 OS=Homo sapiens PE=2 SV=1	0
Original	Human	36	17.31	76.0%	**HM Boost Frame 1**	**Human**	17			27.23	74.5%	EKKVSSFEVF	Q9UHG0|DCDC2_HUMAN Doublecortin domain-containing protein 2 OS=Homo sapiens GN=DCDC2 PE=1 SV=2	0
					HM Boost Frame 1	**Human**	18			27.22	74.4%	DGLHSSSNEVL	Q5TDP6|LGSN_HUMAN Lengsin OS=Homo sapiens GN=LGSN PE=1 SV=1	0
					HM Boost Frame 1	**Human**	19	**Brain Lesions**	13	27.19	74.4%	LSLHSLFELR	Q6U841|S4A10_HUMAN Sodium-driven chloride bicarbonate exchanger OS=Homo sapiens GN=SLC4A10 PE=2 SV=1	0
					HM Boost Frame 1	**Human**	14	**Brain Lesions**	14	27.17	74.3%	FTPHSRFEVL	Q9P2E5|CHPF2_HUMAN Chondroitin sulfate glucuronyltransferase OS=Homo sapiens GN=CHPF2 PE=2 SV=2	0
					HM Boost Frame 1	**Human**	21	**Brain Lesions**	15	27.15	74.2%	IKLPSSFEKW	Q0P6D6|CCD15_HUMAN Coiled-coil domain-containing protein 15 OS=Homo sapiens GN=CCDC15 PE=2 SV=2	54
					HM Boost Frame 1	**Human**	22	**Brain Lesions**	16	27.08	74.0%	VMLLSLFEEE	Q9P2P5|HECW2_HUMAN E3 ubiquitin-protein ligase HECW2 OS=Homo sapiens GN=HECW2 PE=1 SV=2	0
					HM Boost Frame 1	**Human**	23	**Brain Lesions**	17	27.07	74.0%	FALHSLFEAK	Q96PN7|TREF1_HUMAN Transcriptional-regulating factor 1 OS=Homo sapiens GN=TRERF1 PE=1 SV=1	0
Original	Human	33	17.37	76.3%	**HM Boost Frame 1**	**Human**	24	**Brain Lesions**	18	27.05	74.0%	RKLKASFEVS	Q8TDX9|PK1L1_HUMAN Polycystic kidney disease protein 1-like 1 OS=Homo sapiens GN=PKD1L1 PE=1 SV=1	338
					HM Boost Frame 1	**Human**	25	**Brain Lesions**	19	27.04	73.9%	KALHSDFIVK	P52333|JAK3_HUMAN Tyrosine-protein kinase JAK3 OS=Homo sapiens GN=JAK3 PE=1 SV=2	0
					HM Boost Frame 1	**Human**	26	**Brain Lesions**	20	27.01	73.9%	KKLRSSFESS	Q5JTJ3|COA6_HUMAN Cytochrome c oxidase assembly factor 6 homolog OS=Homo sapiens GN=COA6 PE=1 SV=1	23
					HM Boost Frame 1	**Human**	27			27.00	73.8%	LQLHSPSFERG	Q8TDY3|ACTT2_HUMAN Actin-related protein T2 OS=Homo sapiens GN=ACTRT2 PE=2 SV=2	0
					HM Boost Frame 1	**Human**	28	**Brain Lesions**	21	26.98	73.8%	RKCHSSGEVQ	Q8N5D0|WDTC1_HUMAN WD and tetratricopeptide repeats protein 1 OS=Homo sapiens GN=WDTC1 PE=1 SV=2	4
Original	Human	37	17.24	75.7%	**HM Boost Frame 1**	**Human**	29	**Brain Lesions**	22	26.98	73.8%	RKLLSDFPVV	Q4LDE5|SVEP1_HUMAN Sushi, von Willebrand factor type A, EGF and pentraxin domain-containing protein 1 OS=Homo sapiens GN=SVEP1 PE=1 SV=3	7
					HM Boost Frame 1	**Human**	30	**Brain Lesions**	23	26.95	73.7%	KKRHSYFEKP	Q13123|RED_HUMAN Protein Red OS=Homo sapiens GN=IK PE=1 SV=3	11
					HM Boost Frame 1	**Human**	31			26.94	73.7%	VHLHSFFAVG	Q86VW1|S22AG_HUMAN Solute carrier family 22 member 16 OS=Homo sapiens GN=SLC22A16 PE=1 SV=1	0
					HM Boost Frame 1	**Human**	32	**Brain Lesions**	24	26.89	73.5%	EALLSGFEVI	O60503|ADCY9_HUMAN Adenylate cyclase type 9 OS=Homo sapiens GN=ADCY9 PE=1 SV=4	0
					HM Boost Frame 1	**Human**	33	**Brain Lesions**	25	26.80	73.3%	EKLFSQFEVD	Q9NXB0|MKS1_HUMAN Meckel syndrome type 1 protein OS=Homo sapiens GN=MKS1 PE=1 SV=2	0
					HM Boost Frame 1	**Human**	34	**Brain Lesions**	26	26.75	73.1%	GDLKSGFEEV	Q1XH10|SKDA1_HUMAN SKI/DACH domain-containing protein 1 OS=Homo sapiens GN=SKIDA1 PE=2 SV=1	0
					HM Boost Frame 1	**Human**	35	**Brain Lesions**	27	26.69	73.0%	KGLHSKKEVP	Q7KZF4|SND1_HUMAN Staphylococcal nuclease domain-containing protein 1 OS=Homo sapiens GN=SND1 PE=1 SV=1	0
					HM Boost Frame 1	**Human**	36	**Brain Lesions**	28	26.61	72.8%	EFLASSFEVS	Q15269|PWP2_HUMAN Periodic tryptophan protein 2 homolog OS=Homo sapiens GN=PWP2 PE=1 SV=2	0
					HM Boost Frame 1	**Human**	37	**Brain Lesions**	29	26.57	72.7%	GVLHSKFWVV	Q96BZ4|PLD4_HUMAN Phospholipase D4 OS=Homo sapiens GN=PLD4 PE=2 SV=2	0
					HM Boost Frame 1	**Human**	38			26.51	72.5%	KQLVHHFEVD	F8WAS2|F8WAS2_HUMAN Inter-alpha-trypsin inhibitor heavy chain H1 OS=Homo sapiens GN=ITIH1 PE=2 SV=1	0
					HM Boost Frame 1	**Human**	39			26.50	72.5%	RHLHSVLEEL	A1L168|CT202_HUMAN Uncharacterized protein C20orf202 OS=Homo sapiens GN=C20orf202 PE=2 SV=2	0
					HM Boost Frame 1	**Human**	40	**Brain Lesions**	30	26.45	72.3%	RLLSSGFEEV	O60518|RNBP6_HUMAN Ran-binding protein 6 OS=Homo sapiens GN=RANBP6 PE=1 SV=2	24
					HM Boost Frame 1	**Human**	41	**Brain Lesions**	31	26.45	72.3%	QMLHPIFEEA	Q9BS26|ERP44_HUMAN Endoplasmic reticulum resident protein 44 OS=Homo sapiens GN=ERP44 PE=1 SV=1	0
					HM Boost Frame 1	**Human**	42	**Brain Lesions**	32	26.42	72.2%	RRLHSTHEEL	Q03001|DYST_HUMAN Dystonin OS=Homo sapiens GN=DST PE=1 SV=4	7
					HM Boost Frame 1	**Human**	43	**Brain Lesions**	33	26.40	72.2%	RKLHWLFELL	Q14997|PSME4_HUMAN Proteasome activator complex subunit 4 OS=Homo sapiens GN=PSME4 PE=1 SV=2	116
					HM Boost Frame 1	**Human**	44	**Brain Lesions**	34	26.40	72.2%	VELHSDMEVT	P04275|VWF_HUMAN von Willebrand factor OS=Homo sapiens GN=VWF PE=1 SV=4	0
Original	Human	5	18.89	82.9%	**HM Boost Frame 1**	**Human**	45			26.35	72.1%	RKLLHRFETE	O15327|INP4B_HUMAN Type II inositol 3,4-bisphosphate 4-phosphatase OS=Homo sapiens GN=INPP4B PE=2 SV=4	14
					HM Boost Frame 1	**Human**	46			26.31	71.9%	NKLISEFEEE	Q8NE09|RGS22_HUMAN Regulator of G-protein signaling 22 OS=Homo sapiens GN=RGS22 PE=1 SV=3	357
					HM Boost Frame 1	**Human**	47	**Brain Lesions**	35	26.30	71.9%	SKLVSNKEVV	Q15751|HERC1_HUMAN Probable E3 ubiquitin-protein ligase HERC1 OS=Homo sapiens GN=HERC1 PE=1 SV=2	171

					HM Boost Frame 1	**Human**	48	**Brain Lesions**	36	26.29	71.9%	LLLHSLFPVP	|Q9UJ68|MSRA_HUMAN Mitochondrial peptide methionine sulfoxide reductase OS=Homo sapiens GN=MSRA PE=1 SV=1	0
					HM Boost Frame 1	**Human**	49	**Brain Lesions**	37	26.28	71.9%	RKLDSVFEER	|P14780|MMP9_HUMAN Matrix metalloproteinase-9 OS=Homo sapiens GN=MMP9 PE=1 SV=3	0
					HM Boost Frame 1	**Human**	50	**Brain Lesions**	38	26.25	71.8%	RFKHSSTEVL	|A7KAX9|RHG32_HUMAN Rho GTPase-activating protein 32 OS=Homo sapiens GN=ARHGAP32 PE=1 SV=1 EXP=0.271770	0
								Brain Lesions	39	26.25	71.8%	QSVHHGFEVV	|O15198|SMAD9_HUMAN Mothers against decapentaplegic homolog 9 OS=Homo sapiens GN=SMAD9 PE=1 SV=1	0
								Brain Lesions	40	26.23	71.7%	HLLNSGFEVP	|A7KAX9|RHG32_HUMAN Rho GTPase-activating protein 32 OS=Homo sapiens GN=ARHGAP32 PE=1 SV=1 EXP=0.271770	0
					HM Boost Frame 2	**Human**	1	**Brain Lesions**	1	28.47	84.9%	RRKLHSFYEV	|Q5VST9|OBSCN_HUMAN Obscurin OS=Homo sapiens GN=OBSCN PE=1 SV=3	13
Original	Human	24	17.56	77.1%	**HM Boost Frame 2**	**Human**	2	**Brain Lesions**	2	27.46	81.9%	RKLLSSGFEI	|Q8N8A2|ANR44_HUMAN Serine/threonine-protein phosphatase 6 regulatory ankyrin repeat subunit B OS=Homo sapiens GN=ANKRD44 PE=1 SV=3	5
Original	Human	20	17.72	77.8%	**HM Boost Frame 2**	**Human**	3	**Brain Lesions**	3	27.26	81.3%	RRLLSSGFEE	|O60518|RNBP6_HUMAN Ran-binding protein 6 OS=Homo sapiens GN=RANBP6 PE=1 SV=2	3
Original	Human	1	19.79	86.9%	**HM Boost Frame 2**	**Human**	4	**Brain Lesions**	4	27.14	81.0%	RKKLHKFEET	|Q96PE3|INP4A_HUMAN Type I inositol 3,4-bisphosphate 4-phosphatase OS=Homo sapiens GN=INPP4A PE=1 SV=1	3
Original	Human	2	19.27	84.6%	**HM Boost Frame 2**	**Human**	5	**Brain Lesions**	5	26.96	80.4%	LKKLHDFEEQ	|Q9BXB4|TRPM6_HUMAN Transient receptor potential cation channel subfamily M member 6 OS=Homo sapiens GN=TRPM6 PE=1 SV=2	9
					HM Boost Frame 2	**Human**	6	**Brain Lesions**	6	26.91	80.3%	GLLLHSIFEL	|H7C3K9|H7C3K9_HUMAN Melanophilin (Fragment) OS=Homo sapiens GN=MLPH PE=2 SV=1	0
Original	Human	3	19.21	84.3%	**HM Boost Frame 2**	**Human**	7	**Brain Lesions**	7	26.90	80.3%	QKKLHDFEEQ	|Q96QT4|TRPM7_HUMAN Transient receptor potential cation channel subfamily M member 7 OS=Homo sapiens GN=TRPM7 PE=1 SV=1	9
Original	Human	4	18.99	83.4%	**HM Boost Frame 2**	**Human**	8	**Brain Lesions**	8	26.90	80.3%	QKKLSSGEEK	|Q15858|SCN9A_HUMAN Sodium channel protein type 9 subunit alpha OS=Homo sapiens GN=SCN9A PE=1 SV=3	4
					HM Boost Frame 2	**Human**	9	**Brain Lesions**	9	26.85	80.1%	RKHLHSGQEA	|Q5JTD0|TJAP1_HUMAN Tight junction-associated protein 1 OS=Homo sapiens GN=TJAP1 PE=1 SV=1	0
					HM Boost Frame 2	**Human**	10	**Brain Lesions**	10	26.60	79.4%	QKLVHSLFES	|O15067|PUR4_HUMAN Phosphoribosylformylglycinamidine synthase OS=Homo sapiens GN=PFAS PE=1 SV=4	0
					HM Boost Frame 2	**Human**	11	**Brain Lesions**	11	26.51	79.1%	CYLLHSFEEF	|Q4LDE5|SVEP1_HUMAN Sushi, von Willebrand factor type A, EGF and pentraxin domain-containing protein 1 OS=Homo sapiens GN=SVEP1 PE=1 SV=3	0
					HM Boost Frame 2	**Human**	12	**Brain Lesions**	12	25.89	77.2%	SKTLHSVEEK	|Q8TB20|CC110_HUMAN Coiled-coil domain-containing protein 110 OS=Homo sapiens GN=CCDC110 PE=2 SV=1	0
Original	Human	15	18.00	79.0%	**HM Boost Frame 2**	**Human**	13	**Brain Lesions**	13	25.87	77.2%	LKRLHEFEEQ	|Q724N2|TRPM1_HUMAN Transient receptor potential cation channel subfamily M member 1 OS=Homo sapiens GN=TRPM1 PE=1 SV=2	6
					HM Boost Frame 2	**Human**	14	**Brain Lesions**	14	25.86	77.1%	VKELHSAEEG	|O60941|DTNB_HUMAN Dystrobrevin beta OS=Homo sapiens GN=DTNB PE=1 SV=1	0
					HM Boost Frame 2	**Human**	15	**Brain Lesions**	15	25.59	76.3%	SLLLHSQEEK	|Q8IWZ3|ANKH1_HUMAN Ankyrin repeat and KH domain-containing protein 1 OS=Homo sapiens GN=ANKHD1 PE=1 SV=1	0
					HM Boost Frame 2	**Human**	16	**Brain Lesions**	16	25.55	76.2%	AVHLHSGEEL	|Q92519|TRIB2_HUMAN Tribbles homolog 2 OS=Homo sapiens GN=TRIB2 PE=2 SV=1	0
					HM Boost Frame 2	**Human**	17	**Brain Lesions**	17	25.55	76.2%	HTRLHSGEEP	|Q6IV72|ZN425_HUMAN Zinc finger protein 425 OS=Homo sapiens GN=ZNF425 PE=2 SV=1	0
					HM Boost Frame 2	**Human**	18	**Brain Lesions**	18	25.51	76.1%	MPLLHAIFEV	|O43592|XPOT_HUMAN Exportin-T OS=Homo sapiens GN=XPOT PE=1 SV=2	1
					HM Boost Frame 2	**Human**	19	**Brain Lesions**	19	25.38	75.7%	EKKRHSYFEK	|Q13123|RED_HUMAN Protein Red OS=Homo sapiens GN=IK PE=1 SV=3	0
					HM Boost Frame 2	**Human**	20			25.32	75.5%	QAKLHSQEED	|Q4V328|GRAP1_HUMAN GRIP1-associated protein 1 OS=Homo sapiens GN=GRIPAP1 PE=1 SV=1	0
					HM Boost Frame 2	**Human**	21	**Brain Lesions**	20	25.27	75.4%	QQKKHSGFED	|P10645|CMGA_HUMAN Chromogranin-A OS=Homo sapiens GN=CHGA PE=1 SV=7	2
					HM Boost Frame 2	**Human**	22	**Brain Lesions**	21	25.12	74.9%	LKKLHQQFEM	|Q9UQ26-8|RIMS2_HUMAN Isoform 8 of Regulating synaptic membrane exocytosis protein 2 OS=Homo sapiens GN=RIMS2	0
					HM Boost Frame 2	**Human**	23			25.05	74.7%	KLLLHSGVEN	|Q8N1W0|YF005_HUMAN Transmembrane protein FLJ37396 OS=Homo sapiens PE=2 SV=2	2,779
					HM Boost Frame 2	**Human**	24	**Brain Lesions**	22	25.04	74.7%	DNVLHSAFEV	|Q13630|FCL_HUMAN GDP-L-fucose synthase OS=Homo sapiens GN=TSTA3 PE=1 SV=1	7,817
Original	Human	34	17.35	76.2%	**HM Boost Frame 2**	**Human**	25			25.03	74.7%	FSKLHTFEEV	|Q96JB1|DYH8_HUMAN Dynein heavy chain 8, axonemal OS=Homo sapiens GN=DNAH8 PE=1 SV=2	0
Original	Human	47	17.13	75.2%	**HM Boost Frame 2**	**Human**	26	**Brain Lesions**	23	24.91	74.3%	QAKLSSFEET	|Q5TB80|CE162_HUMAN Centrosomal protein of 162 kDa OS=Homo sapiens GN=KIAA1009 PE=1 SV=2	0
					HM Boost Frame 2	**Human**	27	**Brain Lesions**	24	24.82	74.0%	SLALHSVFEG	|Q9NYZ6|S39A1_HUMAN Zinc transporter ZIP1 OS=Homo sapiens GN=SLC39A1 PE=1 SV=1	0
					HM Boost Frame 2	**Human**	28	**Brain Lesions**	25	24.82	74.0%	EFALHSLEEA	|Q96PN7|TREF1_HUMAN Transcriptional-regulating factor 1 OS=Homo sapiens GN=TRERF1 PE=1 SV=1	0
					HM Boost Frame 2	**Human**	29	**Brain Lesions**	26	24.75	73.8%	MRHLKSFFEA	|Q7Z7H5|TMED4_HUMAN Transmembrane emp24 domain-containing protein 4 OS=Homo sapiens GN=TMED4 PE=1 SV=1	0
					HM Boost Frame 2	**Human**	30	**Brain Lesions**	27	24.74	73.8%	QKKRHSFLES	|Q49MG5|MAP9_HUMAN Microtubule-associated protein 9 OS=Homo sapiens GN=MAP9 PE=1 SV=3	0
Original	Human	26	17.53	77.0%	**HM Boost Frame 2**	**Human**	31	**Brain Lesions**	28	24.72	73.7%	QKKLHHFFIG	|Q8IWB1|IPRI_HUMAN Inositol 1,4,5-trisphosphate receptor-interacting protein OS=Homo sapiens GN=ITPRIP PE=1 SV=1	0
					HM Boost Frame 2	**Human**	32	**Brain Lesions**	29	24.72	73.7%	TLSLHSLFEL	|Q6U841|S4A10_HUMAN Sodium-driven chloride bicarbonate exchanger OS=Homo sapiens GN=SLC4A10 PE=2 SV=1	0
					HM Boost Frame 2	**Human**	33	**Brain Lesions**	30	24.69	73.7%	LRLFHSFEEL	|Q9UIY3|RWD2A_HUMAN RWD domain-containing protein 2A OS=Homo sapiens GN=RWDD2A PE=1 SV=1	0
					HM Boost Frame 2	**Human**	34			24.67	73.6%	QKFLHSSFVA	|Q9UIV8|SPB13_HUMAN Serpin B13 OS=Homo sapiens GN=SERPINB13 PE=1 SV=2	0
					HM Boost Frame 2	**Human**	35	**Brain Lesions**	31	24.66	73.6%	AWLLHSGPEG	|O43299|AP5Z1_HUMAN AP-5 complex subunit zeta-1 OS=Homo sapiens GN=AP5Z1 PE=1 SV=2	0
					HM Boost Frame 2	**Human**	36			24.57	73.3%	TKLLHRTEEL	|Q68CJ6|SLIP_HUMAN Nuclear GTPase SLIP-GC OS=Homo sapiens GN=NUGGC PE=2 SV=3	0
					HM Boost Frame 2	**Human**	37	**Brain Lesions**	32	24.56	73.3%	FKTLSSKFEL	|Q8WWM7|ATX2L_HUMAN Ataxin-2-like protein OS=Homo sapiens GN=ATXN2L PE=1 SV=2	0
					HM Boost Frame 2	**Human**	38	**Brain Lesions**	33	24.50	73.1%	KRRLHLVFEY	|Q00532|CDKL1_HUMAN Cyclin-dependent kinase-like 1 OS=Homo sapiens GN=CDKL1 PE=1 SV=5	0
					HM Boost Frame 2	**Human**	39	**Brain Lesions**	34	24.47	73.0%	EHLLNSGFEV	|A7KAX9|RHG32_HUMAN Rho GTPase-activating protein 32 OS=Homo sapiens GN=ARHGAP32 PE=1 SV=1	0
					HM Boost Frame 2	**Human**	40			24.42	72.9%	VMKLLSIFES	|Q3B7T1|EDRF1_HUMAN Erythroid differentiation-related factor 1 OS=Homo sapiens GN=EDRF1 PE=1 SV=1	0
					HM Boost Frame 2	**Human**	41	**Brain Lesions**	35	24.41	72.8%	KLELHSSEEA	|Q6TFL3|CC171_HUMAN Coiled-coil domain-containing protein 171 OS=Homo sapiens GN=CCDC171 PE=2 SV=1	0
					HM Boost Frame 2	**Human**	42			24.41	72.8%	KLPLHSSEEA	|P57721|PCBP3_HUMAN Poly(rC)-binding protein 3 OS=Homo sapiens GN=PCBP3 PE=2 SV=2	0
					HM Boost Frame 2	**Human**	43	**Brain Lesions**	36	24.37	72.7%	LKRLLSNEEE	|O14976|GAK_HUMAN Cyclin-G-associated kinase OS=Homo sapiens GN=GAK PE=1 SV=2	0
					HM Boost Frame 2	**Human**	44			24.24	72.3%	TTRLHSLEEK	|Q7Z3Z0|K1C25_HUMAN Keratin, type I cytoskeletal 25 OS=Homo sapiens GN=KRT25 PE=1 SV=1	0
					HM Boost Frame 2	**Human**	45	**Brain Lesions**	37	24.20	72.2%	HARLHSLEET	|Q5T160|SYRM_HUMAN Probable arginine--tRNA ligase, mitochondrial OS=Homo sapiens GN=RARS2 PE=1 SV=1	0
					HM Boost Frame 2	**Human**	46	**Brain Lesions**	38	24.20	72.2%	LPRLHGHFEQ	|Q9UPU7|TBD2B_HUMAN TBC1 domain family member 2B OS=Homo sapiens GN=TBC1D2B PE=1 SV=2	0
					HM Boost Frame 2	**Human**	47	**Brain Lesions**	39	24.18	72.1%	VKTLHHKEEV	|Q6ZMW2|ZN782_HUMAN Zinc finger protein 782 OS=Homo sapiens GN=ZNF782 PE=2 SV=1	0
					HM Boost Frame 2	**Human**	48	**Brain Lesions**	40	24.17	72.1%	SPSLHSREEA	|B7Z7H5|B7Z7H5_HUMAN Coiled-coil domain-containing protein 116 OS=Homo sapiens GN=CCDC116 PE=2 SV=1	0
					HM Boost Frame 2	**Human**	49	**Brain Lesions**	41	24.16	72.1%	PRKLHWLFEL	|Q14997|PSME4_HUMAN Proteasome activator complex subunit 4 OS=Homo sapiens GN=PSME4 PE=1 SV=2	0
					HM Boost Frame 2	**Human**	50			24.14	72.0%	LKKLLSFAEN	|Q5W041|ARMC3_HUMAN Armadillo repeat-containing protein 3 OS=Homo sapiens GN=ARMC3 PE=2 SV=2	0

Table S2. GDP-L-fucose synthase, Myelin and CEF Peptides

GDP-L-fucose synthase	
GDP-L-fucose synthase 1-15	MGEPQGSMRILVTGG
GDP-L-fucose synthase 6-20	GSMRILVTGGSGLVG
GDP-L-fucose synthase 11-25	LVTGGSGLVGKAIQK
GDP-L-fucose synthase 16-30	SGLVGKAIQKVVADG
GDP-L-fucose synthase 21-35	KAIQKVVADGAGLPG
GDP-L-fucose synthase 26-40	VVADGAGLPGEDWVF
GDP-L-fucose synthase 31-45	AGLPGEDWVFVSSKD
GDP-L-fucose synthase 36-50	EDWVFVSSKDADLTD
GDP-L-fucose synthase 41-55	VSSKDADLTDTAQTR
GDP-L-fucose synthase 46-60	ADLTDTAQTRALFEK
GDP-L-fucose synthase 51-65	TAQTRALFEKVQPTH
GDP-L-fucose synthase 56-70	ALFEKVQPTHVIHLA
GDP-L-fucose synthase 61-75	VQPTHVIHLAAMVGG
GDP-L-fucose synthase 66-80	VIHLAAMVGGLFRNI
GDP-L-fucose synthase 71-85	AMVGGLFRNIKYNLD
GDP-L-fucose synthase 76-90	LFRNIKYNLDFWRKN
GDP-L-fucose synthase 81-95	KYNLDFWRKNVHMND
GDP-L-fucose synthase 86-100	FWRKNVHMNDNVLHS
GDP-L-fucose synthase 91-105	VHMNDNVLHSAFEVG
GDP-L-fucose synthase 96-110	NVLHSAFEVGARKVV
GDP-L-fucose synthase 101-115	AFEVGARKVVSCLST
GDP-L-fucose synthase 106-120	ARKVVSCLSTCIFPD
GDP-L-fucose synthase 111-125	SCLSTCIFPDKTTYP
GDP-L-fucose synthase 116-130	CIFPDKTTYPIDETM
GDP-L-fucose synthase 121-135	KTTYPIDETMIHNGP
GDP-L-fucose synthase 126-140	IDETMIHNGPPHNSN
GDP-L-fucose synthase 131-145	IHNGPPHNSNFGYSY
GDP-L-fucose synthase 136-150	PHNSNFGYSYAKRMI
GDP-L-fucose synthase 141-155	FGYSYAKRMIDVQNR
GDP-L-fucose synthase 146-160	AKRMIDVQNRAYFQQ
GDP-L-fucose synthase 151-165	DVQNRAYFQQYGCTF
GDP-L-fucose synthase 156-170	AYFQQYGCTFTAVIP
GDP-L-fucose synthase 161-175	YGCTFTAVIPTNVFG
GDP-L-fucose synthase 166-180	TAVIPTNVFGPHDNF
GDP-L-fucose synthase 171-185	TNVFGPHDNFNIEDG
GDP-L-fucose synthase 176-190	PHDNFNIEDGHVLPG
GDP-L-fucose synthase 181-195	NIEDGHVLPGLIHKV
GDP-L-fucose synthase 186-200	HVLPGLIHKVHLAKS
GDP-L-fucose synthase 191-205	LIHKVHLAKSSGSAL
GDP-L-fucose synthase 196-210	HLAKSSGSALTVWGT
GDP-L-fucose synthase 201-215	SGSALTVWGTGNPRR
GDP-L-fucose synthase 206-220	TVWGTGNPRRQFIYS
GDP-L-fucose synthase 211-225	GNPRRQFIYSLDLAQ
GDP-L-fucose synthase 216-230	QFIYSLDLAQLFIWV
GDP-L-fucose synthase 221-235	LDLAQLFIWVLREYN
GDP-L-fucose synthase 226-240	LFIWVLREYNEVEPI
GDP-L-fucose synthase 231-245	LREYNEVEPIILSVG
GDP-L-fucose synthase 236-250	EVEPIILSVGEEDEV
GDP-L-fucose synthase 241-255	ILSVGEEDEVSIKEA
GDP-L-fucose synthase 246-260	EEDEVSIKEAAEAVV
GDP-L-fucose synthase 251-265	SIKEAAEAVVEAMDF
GDP-L-fucose synthase 256-270	AEAVVEAMDFHGEVT
GDP-L-fucose synthase 261-275	EAMDFHGEVTFDTTK

GDP-L-fucose synthase 266-280	HGEVTFDTTKSDGQF
GDP-L-fucose synthase 271-285	FDTTKSDGQFKKTAS
GDP-L-fucose synthase 276-290	SDGQFKKTASNSKLR
GDP-L-fucose synthase 281-295	KKTASNSKLRTYLPD
GDP-L-fucose synthase 286-300	NSKLRTYLPDFRFTP
GDP-L-fucose synthase 291-305	TYLPDFRFTPFKQAV
GDP-L-fucose synthase 296-310	FRFTPFKQAVKETCA
GDP-L-fucose synthase 301-315	FKQAVKETCAWFTDN
GDP-L-fucose synthase 306-321	KETCAWFTDNYEQARK
Myelin	
MOG 1-20	GQFRVIGPRHPIRALVGDEV
MOG 35-55	MEVGWYRPPFSRVVHLYRNGK
MBP 13-32	KYLATASTMDHARHGFLPRH
MBP 83-99	ENPVVHFFKNIVTPRT
MBP 111-129	LSRFSWGAEGQRPGFGYGG
MBP 146-170	AQGTLSKIFKLGGRDSRSGSPMARR
PLP 139-154	HCLGKWLGHPDKFVGI
CEFT2 Mix (CEF)	
Influenza A	FVFTLTVPSER
Influenza A	SGPLKAEIAQRLEDV
Influenza A	YDVPDYASLRSLVASS
Influenza B	PYYTGEHAKAIGN
Tetanus	GQIGNDPNRDIL
Influenza A	PKYVKQNTLKLA
Influenza A	PKYVKQNTLKLAT
Influenza A	DRLRRDQKS
EBV	AGLTLSLLVICSYLFISRG
Tetanus	QYIKANSKFIGITEL
Tetanus	QYIKANSKFIGITE
Tetanus	FNNFTVSFWLRVPKVSASHLE
EBV	TSLYNLRRGTALA
Tetanus	KFIIKRYTPNNEIDSF
Tetanus	VSIDKFRIFCKALNPK
EBV	VPGLYSPCRAFFNKEELL
HCMV	DKREMWMACIKELH
EBV	TGHGARTSTEPTTDY
EBV	KELKRQYEKKLRQ
Influenza A	RGYFKMRTGKSSIMRS
EBV	TVFYNIPPMPL
EBV	AEGLRALLARSHVER
EBV	PGPLRESIVCYFMVFLQTHI

Table S3. Peptides from brain proteins identified by proteomic analysis in brain tissue.

Protein	UniProt	Peptide Sequence	Residues	MS WM	MS GM	HD WM	HD GM
Myelin basic protein	P02686	ASTNSETNRGESEK	15 - 28	14	14	-	14
		NLGELSR	31 - 37	-	3	-	-
		NAWQDAHPADPGSRPHLIR	75 - 93	-	2	-	2
		DAPGREDNTFK	98 - 108	4	4	-	4
		DRPSESDELQTIQEDSAATSESLDVMASQK	109 - 138	-	6	-	6
		HGSKYLATASTMDHAR	144 - 159	18	18	18	-
		YLATASTMDHAR	148 - 159	35	35	35	35
		YLATASTMDHARHGFLPR	148 - 165	46	46	46	46
		YLATASTMDHARHGFLPRHR	148 - 167	11	11	11	11
		YLATASTMDHARHGFLPRHRDTGILDSIGR	148 - 177	9	-	9	-
		HGFLPR	160 - 165	12	12	12	12
		HGFLPRHR	160 - 167	13	13	13	13
		HGFLPRHRDTGILDSIGR	160 - 177	16	-	16	16
		HGFLPRHRDTGILDSIGRFFGGDR	160 - 187	-	-	1	-
		HGFLPRHRDTGILDSIGRFFGGDRGAPK	160 - 191	4	-	4	-
		HRDTGILDSIGR	166 - 177	29	29	29	29
		HRDTGILDSIGRFFGGDR	166 - 187	20	20	20	20
		HRDTGILDSIGRFFGGDRGAPK	166 - 191	25	25	25	25
		HRDTGILDSIGRFFGGDRGAPKR	166 - 192	-	-	2	-
		DTGILDSIGR	168 - 177	14	14	14	14
		DTGILDSIGRFFGGDR	168 - 183	21	21	21	21
		DTGILDSIGRFFGGDRGAPK	168 - 187	21	21	21	21
		DTGILDSIGRFFGGDRGAPKR	168 - 188	2	-	2	-
		DTGILDSIGRFFGGDRGAPKRGSGK	168 - 192	2	-	2	-
		FFGGDR	178 - 183	8	8	8	8
		FFGGDRGAPK	178 - 187	24	24	24	24
		FFGGDRGAPKR	178 - 188	5	-	5	-
		FFGGDRGAPKRGSGK	178 - 192	2	-	2	-
		FFGGDRGAPKRGSGKDSHHPAR	178 - 199	-	-	2	-
		RGSGKDSHHPAR	188 - 199	2	-	-	-
		RGSGKDSHHPARTAHYGSLPQK	188 - 209	9	9	9	9
		GSGKDSHHPARTAHYGSLPQK	189 - 209	2	-	2	-
		DSHHPARTAHYGSLPQK	193 - 209	28	28	28	28
		DSHHPARTAHYGSLPQKSHGR	193 - 213	3	-	3	-
		DSHHPARTAHYGSLPQKSHGRTQDENPVVHFFK	193 - 225	1	-	-	-
		TAHYGSLPQK	200 - 209	21	21	21	21
		TAHYGSLPQKSHGR	200 - 213	21	21	21	21
		TAHYGSLPQKSHGRTQDENPVVHFFK	200 - 225	11	-	11	11
		SHGRTQDENPVVHFFK	210 - 225	37	37	37	37
		SHGRTQDENPVVHFFKNIVTPR	210 - 231	4	-	4	-
		SHGRTQDENPVVHFFKNIVTPRTPPPSQGK	210 - 239	-	-	1	-
		TQDENPVVHFFK	214 - 225	34	34	34	34
		TQDENPVVHFFKNIVTPR	214 - 231	27	27	27	27
		TQDENPVVHFFKNIVTPRTPPPSQGK	214 - 239	9	9	9	9
		NIVTPR	226 - 231	10	10	10	10
		NIVTPRTPPPSQGK	226 - 239	62	62	62	62
		NIVTPRTPPPSQGKGRGLSLSR	226 - 247	-	-	1	-
		TPPPSQGK	232 - 239	3	-	-	-
		TPPPSQGKGR	232 - 241	-	-	3	-
		TPPPSQGKGRGLSLSR	232 - 247	-	-	1	-
		GRGLSLSR	240 - 247	12	12	12	-
		GRGLSLSRFSWGAEGQRPGFGYGGR	240 - 264	13	13	13	-
		GRGLSLSRFSWGAEGQRPGFGYGGRASDYK	240 - 269	10	-	10	-
		GLSLSRFSWGAEGQRPGFGYGGR	242 -264	14	14	14	14
		GLSLSRFSWGAEGQRPGFGYGGRASDYK	242 - 269	6	6	6	-
		FSWGAEGQRPGFGYGGR	248 - 264	35	35	35	35
		FSWGAEGQRPGFGYGGRASDYK	248 - 269	35	35	35	35
		FSWGAEGQRPGFGYGGRASDYKSAHK	248 - 273	7	-	7	-
		ASDYKSAHKGFK	265 - 276	3	-	3	-
		ASDYKSAHKGFKGVDAQGTLSK	265 - 286	2	-	2	-
		SAHKGFKGVDAQGTLSK	270 - 286	6	-	6	-
		SAHKGFKGVDAQGTLSKIFK	270 - 289	-	-	1	-
		GFKGVDAQGTLSK	274 - 286	18	18	18	18
		GFKGVDAQGTLSKIFK	274 - 289	-	-	2	-
		GFKGVDAQGTLSKIFKLGGRDSR	274 - 296	-	-	1	-
		GVDAQGTLSK	277 - 286	24	24	24	24
		GVDAQGTLSKIFK	277 - 289	9	-	9	9
		GVDAQGTLSKIFKLGGR	277 - 293	-	-	1	-
		GVDAQGTLSKIFKLGGRDSR	277 - 296	3	-	3	-

		IFKLGGR	287 - 293	5	-	5	-
		IFKLGGRDSR	287 - 296	4	-	4	-
		IFKLGGRDSRSGSPMAR	287 - 303	3	-	3	-
		IFKLGGRDSRSGSPMARR	287 - 304	3	-	3	-
		LGGRDSR	292 - 296	2	-	2	-
		LGGRDSRSGSPMAR	292 - 303	45	45	45	45
		LGGRDSRSGSPMARR	292 - 304	10	-	10	10
		DSRSGSPMAR	294 - 303	41	41	41	41
		DSRSGSPMARR	294 - 304	11	11	11	11
		SGSPMAR	297 - 303	24	24	24	24
		SGSPMARR	297 - 304	9	9	9	9
				993	871	985	865
Myelin proteolipid protein	P60201	LIETYFSK	46 - 53	12	12	12	12
		QIFGDYK	99 - 105	15	15	15	15
		GLSATVTGGQK	112 - 122	24	24	24	24
		GLSATVTGGQKGR	112 - 124	14	14	14	14
		GLSATVTGGQKGRGSR	112 - 127	4	-	4	-
		GRGSRGQHQAHSLER	123 - 137	4	4	-	4
		GSRGQHQAHSLER	125 - 137	-	9	-	9
		GQHQAHSLER	128 - 137	15	15	-	15
		VCHCLGK	138 - 144	-	-	-	3
		TSASIGSLCADAR	193 - 205	12	12	12	12
		TSASIGSLCADARMYGVLPWNAFPGK	193 - 218	-	-	-	1
		MYGVLPWNAFPGK	206 - 218	48	48	48	48
		VCGSNLLSICK	219 - 229	-	9	-	9
				148	153	129	157
Myelin-oligodendrocyte glycoprotein	Q16653	VIGPRHPIR	34 - 42	3	-	3	3
		VIGPRHPIRALVGDEVELPCR	34 - 54	1	-	-	-
		HPIRALVGDEVELPCR	39 - 54	-	-	-	3
		ALVGDEVELPCR	43 - 54	12	12	12	12
		ALVGDEVELPCRISPGK	43 - 59	-	-	-	1
		VVHLYR	76 - 81	11	11	11	11
		VVHLYRNGK	76 - 84	12	12	12	12
		VVHLYRNGKDQDGDQAPEYR	76 - 95	15	15	15	15
		VVHLYRNGKDQDGDQAPEYRGRTELLK	76 - 102	5	-	5	5
		NGKDQDGDQAPEYR	82 - 95	31	31	31	31
		NGKDQDGDQAPEYRGR	82 - 97	4	-	4	-
		NGKDQDGDQAPEYRGRTELLK	82 - 102	2	-	2	-
		DQDGDQAPEYR	85 - 95	12	12	12	12
		DQDGDQAPEYRGR	85 - 97	9	-	9	9
		DQDGDQAPEYRGRTELLK	85 - 102	4	-	4	4
		GRTELLKDAIGEGK	96 - 109	-	2	-	-
		GRTELLKDAIGEGKVTLR	96 - 113	-	-	1	-
		DAIGEGKVTLR	103 - 113	9	9	9	-
		DAIGEGKVTLRIR	103 - 115	-	-	2	-
		FSDEGGFTCFFR	119 - 130	12	12	12	12
		DHSYQEEAAMELK	131 - 143	24	24	24	24
		LRAEIENLHR	186 - 195	13	13	13	13
		AEIENLHR	188 - 195	12	12	12	12
		TFDPHFLR	196 - 203	5	5	-	5
		RLAGQFLEELR	234 - 244	-	-	-	3
		RLAGQFLEELRNPF	234 - 247	8	8	8	8
		LAGQFLEELR	235 - 244	-	9	9	9
		LAGQFLEELRNPF	235 - 247	12	12	12	12
				216	199	222	216
Myelin-associated glycoprotein	P20916	FDFPDELRPAVVHGVWYFNSPYPK	44 - 67	12	12	12	12
		NYPPVVFK	68 - 75	12	12	12	12
		SRTQVVHESFQGR	76 - 88	10	10	10	10
		SRTQVVHESFQGRSR	76 - 90	1	-	-	-
		TQVVHESFQGR	78 - 88	12	12	12	12

		LLGDLGLR	91 - 98	12	12	12	12
		LREDEGTWVQVSLLHFVPTR	189 - 208	13	13	13	13
		EDEGTWVQVSLLHFVPTR	191 - 208	-	6	-	6
		DGTVLR	276 - 281	4	4	4	4
		DTVQCLCVVK	426 - 435	-	6	-	6
		SNPEPSVAFELPSR	436 - 449	9	9	-	9
		EFVYSER	459 - 465	8	8	8	8
		SGLVLTSILTLR	466 - 477	12	12	12	12
		SGLVLTSILTLRGQAQAPPR	466 - 485	3	-	-	-
		GQAQAPPR	478 - 485	12	12	12	12
		VICTAR	486 - 491	-	-	-	2
		NLYGAK	492 - 497	2	-	2	-
		SLELPFQGAHR	498 - 508	12	12	12	12
		NVTESPSFSAGDNPPVLFSSDFR	541 - 563	12	12	12	12
		NVTESPSFSAGDNPPVLFSSDFRISGAPEK	541 - 570	7	7	7	7
		ISGAPEK	564 - 570	3	-	-	-
		ISGAPEKYESER	564 - 575	12	12	12	12
		ISGAPEKYESERR	564 - 576	2	-	2	-
		ISGAPEKYESERRLGSER	564 - 581	-	-	2	-
		YESERRLGSER	571 - 581	6	6	6	6
		YESERRLGSERR	571 - 582	-	-	-	1
		RLGSERRLLGLR	576 - 587	2	-	2	-
		RLLGLR	582 - 587	9	9	9	9
		RLLGLRGEPPELDLSYSHSDLGK	582 - 604	12	12	12	12
		LLGLRGEPPELDLSYSHSDLGK	583 - 604	10	10	10	10
		LLGLRGEPPELDLSYSHSDLGKRPTK	583 - 608	2	-	2	-
		GEPPELDLSYSHSDLGK	588 - 604	12	12	12	12
		DSYTLTEELAEYAEIR	609 - 624	12	12	12	12
		DSYTLTEELAEYAEIRVK	609 - 626	8	-	-	8
				243	232	221	243
Myelin-associated oligodendrocyte basic protein	Q13875	QQPAAPPAVVR	82 - 92	12	12	12	12
		QQPAAPPAVVRAPAKPR	82 - 98	-	-	3	-
		QPRPRPEVRPPPAK	136 - 149	-	-	2	2
		SSPLRGPGASR	162 - 172	2	-	2	-
		SSPLRGPGASRGGSPVK	162 - 178	6	-	6	-
		GPGASRGGSPVK	167 - 178	-	-	2	-
				20	12	27	14
Oligodendrocyte myelin glycoprotein	P23515	TLDISNNR	82 - 90	12	12	12	12
		TLDISNNRLESLPAHLPR	82 - 99	18	18	18	18
		LESLPAHLPR	91 - 99	12	12	12	12
		SDTAYQWNLK	117 - 126	12	12	12	12
		YLDVSK	127 - 132	8	8	8	8
		VVLIKNTLR	138 - 146	-	9	9	9
		SLEVLNLSSNK	147 - 157	12	12	12	12
		LWTVPTNMPSK	158 - 168	22	22	22	22
		FTFIPDQSFDQLFQLQEITLYNNR	203 - 226	14	14	14	14
		WSCDHK	227 - 232	-	2	-	2
		WMMETK	241 - 246	17	17	17	17
		AHVIGTPCSTQISSLK	247 - 262	9	9	-	9
		ETTFGATLSK	311 - 320	8	8	-	8
				144	155	136	155

Proteome data correspond to white matter (WM) and grey matter (GM) from multiple sclerosis patients (MS, n=15) and healthy donors (HD, n=9). In bold are GDP-L-fucose synthase values.

Table S4. Patient Classification and HLA binding

A

Peptide	161-175	51-65	136-150	251-265	241-255	246-260	26-40	226-240	236-250	256-270	296-310	1-15	76-90	156-170	121-135	131-145	166-180	231-245	261-275	271-285	Log10 SI Wsum	
66JO	0.96	1.12	0.92	0.78	0.59	0.70	1.08	1.00	0.69	0.91	0.47	1.02	0.81	0.94	0.96	1.03	0.61	0.73	0.70	0.60	0.00	Nonresponder
103FH	0.87	0.73	0.80	0.58	0.67	0.61	0.70	0.81	0.68	0.83	0.69	0.73	0.75	0.78	0.64	0.62	0.79	0.96	0.70	0.82	0.00	Nonresponder
204AM	0.87	0.77	0.69	0.87	0.86	0.76	0.70	1.10	0.79	0.94	0.44	0.89	1.14	0.94	0.64	0.97	0.84	0.89	0.72	0.93	0.00	Nonresponder
247PE	0.78	0.78	0.72	0.61	0.65	0.73	0.73	0.65	0.74	0.75	0.69	0.87	0.74	0.69	0.70	0.70	0.72	0.59	0.73	0.65	0.00	Nonresponder
381MA	1.31	0.76	1.13	1.00	1.00	1.06	0.82	1.27	0.93	0.98	0.95	0.85	0.72	1.23	1.00	1.03	1.06	0.99	0.84	1.24	0.00	Nonresponder
702AN	0.62	0.50	0.63	0.61	0.64	0.58	0.68	0.64	0.55	0.53	0.54	0.69	0.57	0.69	0.56	0.41	0.51	0.56	0.51	0.55	0.00	Nonresponder
740RA	0.99	0.78	0.70	0.81	0.77	0.80	0.89	0.86	0.75	0.59	0.66	0.86	0.82	0.81	0.67	0.68	0.84	0.81	0.64	0.95	0.00	Nonresponder
936MA	0.68	0.66	0.83	0.95	0.97	1.11	0.65	0.82	1.03	1.01	1.04	0.73	0.67	0.72	0.72	0.90	0.63	0.98	0.96	1.02	0.00	Nonresponder
973JO	0.85	0.91	0.37	0.50	0.68	0.57	0.56	0.90	0.62	0.56	0.70	0.83	0.47	0.85	0.61	0.50	1.02	0.72	0.49	0.69	0.00	Nonresponder
1125PA	0.81	1.07	0.43	0.57	0.63	0.49	0.99	0.49	0.54	0.73	0.41	0.74	0.43	0.58	0.74	0.61	0.93	0.71	0.65	0.50	0.00	Nonresponder
1292DI	1.09	0.76	0.47	0.93	0.81	0.66	0.63	0.54	0.92	0.40	0.72	0.87	0.57	0.86	0.65	0.75	0.90	1.06	0.64	0.93	0.00	Nonresponder
1300EV	1.21	0.90	0.89	0.97	0.59	0.70	0.51	0.73	0.88	0.61	0.75	0.59	0.70	0.86	0.90	0.91	1.11	0.92	0.74	0.98	0.00	Nonresponder
897UR	1.25	1.05	0.70	0.76	0.89	1.10	0.95	0.99	0.87	0.79	0.86	0.66	0.79	0.88	0.74	0.65	0.88	0.79	0.81	0.72	0.00	Nonresponder
127RO	0.86	0.67	0.63	1.08	1.03	1.15	0.62	0.65	0.86	0.98	0.94	0.62	0.65	0.70	0.80	0.70	0.54	0.88	0.84	1.01	0.00	Nonresponder
1290JA	1.17	0.91	1.06	1.08	1.19	1.34	0.88	0.98	1.34	1.18	1.10	1.02	0.72	1.13	0.87	0.98	0.74	1.01	0.94	1.41	0.00	Nonresponder
800TH	1.08	0.94	0.97	0.94	0.80	0.99	0.74	0.84	0.86	0.72	0.57	0.92	0.51	0.72	0.88	0.89	0.88	0.98	0.74	0.76	0.00	Nonresponder
830OL	0.67	0.81	0.99	0.71	0.98	0.93	0.68	0.43	0.81	0.67	0.85	1.06	0.69	0.85	0.89	0.93	0.73	0.79	0.69	0.84	0.00	Nonresponder
818MA	1.42	1.10	0.96	1.10	1.06	1.09	1.01	1.03	0.92	1.43	0.99	0.82	0.80	1.17	0.90	0.97	1.05	0.90	1.47	1.30	0.17	Nonresponder
1206CO	1.03	1.11	0.64	0.72	0.77	0.62	0.91	0.89	0.87	0.84	0.62	0.79	0.67	1.01	1.03	0.98	1.47	0.94	0.60	0.77	0.17	Nonresponder
780UR	1.09	0.84	0.90	0.76	0.88	0.76	1.11	1.54	0.91	0.91	0.68	1.05	0.78	0.94	0.90	0.90	0.85	0.76	0.84	0.82	0.79	Moderate Responder
866JE	1.32	0.87	1.03	1.60	0.87	0.81	0.97	0.97	1.03	1.11	0.79	0.80	0.68	0.98	0.92	0.92	0.93	0.93	0.92	1.12	0.98	Moderate Responder
748UR	1.48	0.83	1.11	1.42	0.94	1.01	0.80	1.02	0.88	0.98	0.92	0.83	0.89	1.24	0.87	1.05	0.97	0.83	1.10	1.13	1.01	Moderate Responder
1346JU	1.44	0.88	1.49	0.73	0.86	0.79	1.13	1.01	0.93	0.67	0.95	1.04	0.46	1.26	1.12	1.47	0.97	0.68	0.74	0.94	1.02	Moderate Responder
1081SA	1.63	0.81	1.32	1.10	1.30	1.45	1.01	0.95	1.47	1.30	1.09	1.25	0.95	1.25	1.48	1.28	1.27	1.63	1.38	1.47	1.34	Moderate Responder
817JD	1.53	1.31	1.12	1.09	0.06	1.01	4.09	0.98	0.95	1.23	1.05	0.97	0.87	1.25	1.10	1.06	0.97	0.82	0.84	0.82	1.43	Moderate Responder
1129RE	1.47	1.55	1.70	1.65	1.55	1.47	1.09	1.10	1.26	1.30	1.90	1.33	0.93	1.12	0.88	0.78	0.92	0.98	0.78	1.05	1.81	High Responder
1005ME	1.20	1.87	1.91	1.95	1.83	2.04	1.57	1.30	1.78	2.85	1.95	1.02	2.14	0.97	0.77	0.88	0.76	0.82	1.24	0.93	2.00	High Responder
1173DI	2.30	1.81	2.42	2.63	2.09	2.27	1.34	0.56	1.39	1.96	1.39	1.67	0.82	1.64	0.74	0.92	0.91	0.78	0.57	0.69	2.09	High Responder
718MA	4.57	1.56	0.89	0.79	0.80	0.95	0.69	25.93	0.73	0.65	0.91	1.22	0.69	0.75	1.03	1.14	1.25	0.80	0.62	0.90	2.16	High Responder
816DA	3.50	4.77	8.21	4.27	2.03	3.76	3.04	1.59	1.49	4.65	1.99	1.70	1.62	5.21	0.80	0.94	0.88	0.56	1.16	0.89	2.38	High Responder
776JE	2.35	4.37	7.40	6.99	6.24	7.04	4.76	2.44	4.52	6.41	4.81	2.50	1.53	4.55	1.01	0.95	0.93	0.93	1.01	1.05	2.50	High Responder
Peptide Sum	8	6	6	6	5	5	4	4	4	4	4	3	3	3	1	1	1	1	1	1		

Immunodominant Peptides

B

Binding Affinity (percentile-rank)*																					
DRB3*0101	37.47	13.48	29.81	68.2	29.81	75.22	16.25	21.74	39.16	43.26	39.06	61.74	4.67	10.49	2.79	11.29	60.77	33.2	20.11	41.85	
DRB3*0202	8.36	2.14	74.35	61.77	74.52	94.52	83.08	91.67	19.12	86.02	43.48	77.96	10.58	51.08	65.44	93.75	86.86	19.8	70.27	82.89	

Red cells med SI > 1.455.

* A lower number indicates higher binding affinity (http://tools.immuneepitope.org/mhcii/).

Table S5. Bacteria selected for GDP-L-fucose synthase comparison

Bacterial species		Relevance in MS	Reference	GDP fucose synthase sequences analyzed (NCBI)
Acinetobacter calcoaceticus	Gut microbiota	Increased in MS patients	Cekanaviciute E, Proceedings of ECTRIMS, 2016	Not found
Adlercreutzia	Gut microbiota	Decreased in RRMS patients	Chen J, Sci Rep, 2016	Not found
Akkermansia muciniphila	**Gut microbiota**	**Increased in MS patients**	**Jangi S, Nat Comm, 2016**	**Akkermansia KLE1798, 1797, 1605, CAG:304 (present in gut)**
Anaerostipes hadrus	Gut microbiota	Decreased in Japanese RRMS patients	Miyake S, Plos one, 2015	Not found
Bacteroides coprocola	Gut microbiota	Decreased in Japanese RRMS patients	Miyake S, Plos one, 2015	Not found
Bacteroides coprophilus	Gut microbiota	Decreased in Japanese RRMS patients	Miyake S, Plos one, 2015	Not found
Bacteroides fragilis	**Gut microbiota**	**Oral administration lowers clinical score in EAE by polysaccharide A**	**Ochoa-Reparaz J, J Immunol 2010**	**Bacteroides fragilis**
Bacteroides stercoris	**Gut microbiota**	**Decreased in Japanese RRMS patients**	**Miyake S, Plos one, 2015**	**Bacteroides stercoris**
Bifidobacterium	Gut microbiota	Increased in pediatric MS patients	Tremlett H, Eur J Neurol, 2016	Not found
Bilophilia	Gut microbiota	Increased in pediatric MS patients	Tremlett H, Eur J Neurol, 2016	Not found
Blautia	Gut microbiota	**Increased in RRMS patients**	**Chen J, Sci Rep, 2016**	**Blautia obeum and Blautia wexlerae (present in gut)**
butyrate-producing bacterium A2-175	Gut microbiota	Decreased in Japanese RRMS patients	Miyake S, Plos one, 2015	Not found
butyrate-producing bacterium SL7/1	Gut microbiota	Decreased in Japanese RRMS patients	Miyake S, Plos one, 2015	Not found
Butyricimonas synergistica	Gut microbiota	Decreased in MS patients	Jangi S, Nat Comm, 2016	Not found
Christensenellaceae	Gut microbiota	Increased in pediatric MS patients	Tremlett H, Eur J Neurol, 2016	Not found
Clostridiaceae bacterium SH032	Gut microbiota	Decreased in Japanese RRMS patients	Miyake S, Plos one, 2015	Not found
Clostridium perfringens type A	Gut microbiota	Decreased in MS patients	Rumah KR, Plos one 2013	Not found
Clostridium perfringens type B	Gut microbiota	Found in human for the first time in a MS patient at the disease onset	Rumah KR, Plos one 2013	Not found
Clostridium sp.	**Gut microbiota**	**Decreased in Japanese RRMS patients**	**Miyake S, Plos one, 2015**	**Clostridium strain KLE1755 (present in gut)**
Clostridium sp. ID5	Gut microbiota	Decreased in Japanese RRMS patients	Miyake S, Plos one, 2015	Not found
Clostridium sp. RT8	Gut microbiota	Decreased in Japanese RRMS patients	Miyake S, Plos one, 2015	Not found
Collinsella aerofaciens	Gut microbiota	Decreased in MS patients untreated	Jangi S, Nat Comm, 2016	Not found
Desulfotomaculum sp. CYP1	Gut microbiota	Decreased in Japanese RRMS patients	Miyake S, Plos one, 2015	Not found
Desulfovibrio	Gut microbiota	Increased in pediatric MS patients	Tremlett H, Eur J Neurol, 2016	Several strains
Dorea	Gut microbiota	Increased in RRMS patients	Chen J, Sci Rep, 2016	Not found
Eubacterium rectale ATCC 33656	Gut microbiota	Decreased in Japanese RRMS patients	Miyake S, Plos one, 2015	Not found
Faecalibacterium prausnitzii	Gut microbiota	Decreased in Japanese RRMS patients	Miyake S, Plos one, 2015	Not found
Fusobacterium	Gut microbiota	Absence associated to shorter time to relapse in pediatric MS	Tremlett H, J Neurol Sci, 2016	Not found
Haemophilus	Gut microbiota	Increased in RRMS patients	Chen J, Sci Rep, 2016	Not found
Lachnospira pectinoschiza	Gut microbiota	Decreased in Japanese RRMS patients	Miyake S, Plos one, 2015	Not found
Lachnospiraceae	**Gut microbiota**	**Decreased in pediatric MS patients**	**Tremlett H, Eur J Neurol, 2016**	**Lachnospiraceae bacterium 3-1 (present in gut)**
Lactobacillus rogosae	Gut microbiota	Decreased in Japanese RRMS patients	Miyake S, Plos one, 2015	Not found
Lepotrichia	Gut microbiota	Absence associated to shorter time to relapse in pediatric MS	Tremlett H, J Neurol Sci, 2016	Not found
Megamonas funiformis YIT 11815	Gut microbiota	Decreased in Japanese RRMS patients	Miyake S, Plos one, 2015	Not found
Methanobrevibacter smithii	Gut microbiota	Increased in MS patients	Jangi S, Nat Comm, 2016	Not found
Mycoplana	Gut microbiota	Increased in RRMS patients	Chen J, Sci Rep, 2016	Not found
Parabacteroides	**Gut microbiota**	**Decreased in RRMS patients**	**Chen J, Sci Rep, 2016**	**Parabacteroides distastonis**
Parabacteroides distasonis	**Gut microbiota**	**Decreased in MS patients**	**Baranzini S data**	**Parabacteroides distastonis**
Prevotella	Gut microbiota	Decreased in RRMS patients	Chen J, Sci Rep, 2016	Several strains
Prevotella copri DSM 18205	Gut microbiota	Decreased in Japanese RRMS patients	Miyake S, Plos one, 2015	Not found
Prevotella stercorea	Gut microbiota	Decreased in MS patients untreated	Jangi S, Nat Comm, 2016	Not found
Pseudomonas	Gut microbiota	Increased in RRMS patients	Chen J, Sci Rep, 2016	Several strains
Roseburia sp.1120	Gut microbiota	Decreased in Japanese RRMS patients	Miyake S, Plos one, 2015	Not found
Ruminococcaceae	Gut microbiota	Decreased in pediatric MS patients	Tremlett H, Eur J Neurol, 2016	Not found
Sarcina ventriculi	Gut microbiota	Decreased in treated vs untreaded MS patients	Jangi S, Nat Comm, 2016	Not found
Slackia isoflavoniconvertens	Gut microbiota	Decreased in MS patients untreated	Jangi S, Nat Comm, 2016	Not found
Streptococcus thermophiles/salivarius	Gut microbiota	Increased in Japanese RRMS patients	Miyake S, Plos one, 2015	Not found
Sutterella stercoricanis	Gut microbiota	Increased in treated vs untreated MS patients	Jangi S, Nat Comm, 2016	Not found
Sutterella wadsworthensis	Gut microbiota	Increased in treated vs untreated MS patients	Jangi S, Nat Comm, 2016	Not found
Sutterella wadsworthensis 2_1_59BFAA	Gut microbiota	Decreased in Japanese RRMS patients	Miyake S, Plos one, 2015	Not found
Enterococcus faecium	**Gut microbiota (Pathogen)**			**Enterococcus faecalis**
Escherichia coli	**Gut microbiota (Pathogen)**			**Escherichia coli**
Helicobacter pylori	**Gut microbiota (Pathogen)**			**Helicobacter pylori**
Klebsiella pneumoniae	**Gut microbiota (Pathogen)**			**Klebsiella pneumoniae**
Campylobacter jejuni	**Pathogen**			**Campylobacter jejuni**
Mycobacterium avium	**Pathogen**			**Mycobacterium avium**
Mycobacterium tuberculosis	**Pathogen**			**Mycobacterium tuberculosis**
Porphyromonas gingivalis	**Pathogen**			**Porphyromonas gingivalis**
Pseudomonas sp	**Pathogen**			**Pseudomonas sp**
Salmonella enterica	**Pathogen**			**Salmonella enterica**
Shigella flexneri	**Pathogen**			**Shigella flexneri**
Shigella sonnei	**Pathogen**			**Shigella sonnei**
Vibrio cholerae	**Pathogen**			**Vibrio cholerae**
Yersinia pestis	**Pathogen**			**Yersinia pestis**

In red bacteria from which GDP-L-synthase sequence has been compared with the human homologous.

Table S6. Sequence homology between human and bacterial GDP-L-fucose synthase peptides

A

GUT MICROBIOTA (MS)		51- TAQTRALFEKVQPTH -65	%	136- PHNSNFGYSYAKRMI -150	%	161- YGCTFTAVIPTNVFG -175	%	251- EEDEVSIKEAAEAVV -265	%
Blautia	Blautia obeum	QDAVEKFFATEKPEY	13.33	LEKTNEAYALAKISG	26.67	YGDDFISCMPTNLYG	46.67	TGKELTIKELTELVA	40.00
Clostridium sp.	Clostriudium sp. KLE1755	QAQVRDFFEKERPDV	46.67	LEETNEAYAIAKIAG	26.67	YGDDFISCMPTNLYG	46.67	TGKEITIKELAETVR	46.67
Lachnospiraceae	Lachnospiraceae bacterium 3-1	QAQVTAFFEDEKPDV	33.33	LEATNEAYAIAKIAG	26.67	YGDDFISCMPTNLYG	46.67	TGKEVTIRQLAETVQ	40.00
Blautia	Blautia wexlerae	QDAVEKFFATEKPEY	13.33	LEKTNEAYALAKISG	26.67	YGTDYISVMPTNLYG	46.67	TGKELTIKELTELVA	40.00
Akkermansia muciniphila	Akkermansia sp KLE 1798	PAAVREFFDREKPEY	26.67	LEYTNEPYAIAKIAG	26.67	YGANYIAVMPTNLYG	53.33	TGKEISIRGLAELIA	33.33
	Akkermansia sp KLE 1797	PAAVREFFDREKPEY	26.67	LEYTNEPYAIAKIAG	26.67	YGANYIAVMPTNLYG	53.33	TGKEISIRGLAELIA	33.33
	Akkermansia sp KLE 1605	PAAVREFFDREKPEY	26.67	LEYTNEPYAIAKIAG	26.67	YGANYIAVMPTNLYG	53.33	TGKEISIRGLAELIA	33.33
	Akkermansia sp CAG:344	PAAVREFFDREKPEY	26.67	LEYTNEPYAIAKIAG	26.67	YGTNYIAVMPTNLYG	53.33	TGKEISIGDLARLIA	26.67
Bacteroides fragilis		GAAVKQFFDEEMPEY	20.00	LEYTNEPYAIAKIAG	26.67	YGTNYIAVMPTNLYG	53.33	TGKEITIRELAGLIV	33.33
Bacteroides stercoris		GVAVRRFFDEEQPEY	26.67	LEYTNEPYAIAKIAG	26.67	YGTNYIAVMPTNLYG	53.33	TGKEITIRRLAELIV	33.33
Parabacteroides distasonis	Parabacteroides distasonis	QAAVNEFFAAERPDY	20.00	LEYSNEPYAIAKIAG	33.33	YGTNYIAVMPTNLYG	53.33	TGIELSIREVAELIR	40.00

PATHOGENS

GUT MICROBIOTA (NO MS)									
Enterococcus faecium		QDAVEAFFAQEKPDY	20.00	LEKTNEAYALAKISG	26.67	YGTDYISVMPTNLYG	46.67	TGKELSIKELTEMVA	46.67
Escherichia coli		SRAVHDFFASERIDQ	6.67	LEPTNEPYAIAKIAG	26.67	YGRDYRSVMPTNLYG	46.67	TGVDCTIRELAQTIA	20.00
Helicobacter pylori		KDNVQAYLKEYKPTG	20.00	LELTNEGYALAKLSV	33.33	KGVFYKTLVPCNLYG	26.67	SGVDYSIEEYYEKVA	33.33
Klebsiella pneumoniae		AQDVNNFFANERIDE	6.67	LESTNEPYAIAKIAG	26.67	YNRDYRSVMPTNLYG	40.00	TGVDCSIKELAETIS	40.00
NO GUT MICROBIOTA									
Campylobacter jejuni		QQAVIEFFKNEQPEY	20.00	LEYNATSFGVAKISG	13.33	YGTNFITLALNNLYG	33.33	TGIDYSIAEVAQMVK	33.33
Mycobacterium avium		RAKTFDFVLESRPQV	20.00	LESTNDAYAIAKIAG	26.67	YGLAWISAMPTNLYG	40.00	TGVDHTIREIAEMVA	33.33
Mycobacterium tuberculosis		RAATFDFVLESRPQV	20.00	LEPTNDAYAIAKIAG	26.67	HGLPWISAMPTNLYG	33.33	TGIDHTIGEIAEMVA	33.33
Porphyromonas gingivalis		AVAVREFFDKEEPQY	26.67	LEYTNEPYAIAKIAG	26.67	YGTNYIAVMPTNLYG	53.33	TGEEISIRDLASLIA	26.67
Pseudomonas sp		PAAVQAYFARHRVDQ	20.00	LEPTNEPYAVAKIAG	26.67	HGRDYRSVMPTNLYG	40.00	TGVDCTIAELAQALV	33.33
Salmonella enterica		GRAVQAFFAGAGIDQ	13.33	LEPTNEPYAIAKIAG	26.67	YGRDYRSVMPTNLYG	46.67	TGVDCTIRELAQTIA	20.00
Shigella sonnei		SRAVHDFFASERIDQ	6.67	LEPTNEPYAIAKIAG	26.67	YGRDYRSVMPTNLYG	46.67	TGVDCTIRELAQTIA	20.00
Vibrio cholerae		QKAVNAFFATERIDE	13.33	LEATNEPYAIAKIAG	26.67	YGRDYRSVMPTNLYG	46.67	TGVDCTIREMAETMA	26.67
Yersinia pestis		QSAVQKFFATEKIDE	6.67	LEPTNEPYAIAKIAG	26.67	YGRDYRSVMPTNLYG	46.67	TGVDCTIRELAETMA	26.67
Shigella flexneri		SRAVHDFFASERIDQ	6.67	LEPTNEPYAIAKIAG	26.67	YGRDYRTVMPTNLYG	46.67	TGVDCTIRELAQTIA	20.00

% - percentage of identidal amino acids. In red are identical amino acids. Identical peptide shared by different bacteria has the same cell color.

B

PEPTIDE 1	YGDDFISCMPTNLYG
PEPTIDE 2	YGTDYISVMPTNLYG
PEPTIDE 3	YGANYIAVMPTNLYG
PEPTIDE 4	YGTNYIAVMPTNLYG
PEPTIDE 5	YGLAWISAMPTNLYG
PEPTIDE 6	YGRDYRSVMPTNLYG
PEPTIDE 7	HGRDYRSVMPTNLYG
PEPTIDE 8	YGRDYRTVMPTNLYG

Table S7. Demographical and clinical characteristics of MS patients and non-MS controls

	sex	age	cause of death	Post-mortem time (h)	MS type	Disease Duration (years)	Brain Tissue Block	Brain Tissue Type
MS Patients								
MS 1	F	56	Breast carcinoma, Pneumothorax	8	SPMS	31	6	GM
MS 2	F	58	Peritonitis, inflamed caecal diverticulum	16	PPMS	22	9	WM
MS 3	F	78	Myocardial infection, acute abdomen	18	SPMS	33	1	WM
MS 6	F	58	Bronchopneumonia	6	PPMS	21	7	WM
MS 8	M	40	Dehydration / Multiple Sclerosis	18	SPMS	23	1	WM
							3	WM
MS 14	F	78	Lung infection	9	PPMS	47	2	GM
MS 15	F	51	Multiple Sclerosis	15	SPMS	21	2	WM
MS 23	F	78	Metastatic carcinoma of bronchus	5	SPMS	42	1	WM
							5	GM
MS 28	F	54	Bronchopneumonia	22	SPMS	20	1	WM
MS 32	F	39	Bronchopneumonia	18	PRMS	21	3	GM
MS 40	M	40	Respiratory failure, sepsis	10	SPMS	9	5	GM
MS 47	M	37	Intestinal obstruction	12	PPMS	27	2	GM
MS 51	F	49	Bronchopneumonia	12	PPMS	27	2	WM
Non-MS Controls								
Non-MS 15	M	64	Cardiac failure	18			5	WM
Non-MS 18	M	35	Carcinoma of the tongue	22			3	GM
Non-MS 21	M	75	Aspiration pneumonia	17			1	GM
							2	WM
Non-MS 28	F	60	heart failure, heart mestastasis	21			2	GM
							1	WM
Non-MS 39	M	na.	Acute cardial death	10			5	GM
Non-MS 46	M	68	Metastatic colon cancer	10			1	GM
Non-MS 30	M	69	pericardial tamponade	7			1	GM